ANALYSIS AND CONTROL OF QUASI DISTRIBUTED PARAMETER SYSTEMS

Thesis by

Chuen Jin Goh

In Partial Fulfillment of the Requirements

for the Degree of

Doctor of Philosophy

California Institute of Technology

Pasadena, California

1983

(Submitted November 15, 1982)

ACKNOWLEDGEMENTS

I am much indebted to the following:

To Professor T. K. Caughey, who has generously and patiently spent countless hours discussing everything from heteroclinic oscillation to catamaran sailing; whose lofty brilliance I have much aspired, whose student I may boast to have been.

To Caltech, Jet Propulsion Laboratory and National University of Singapore for all the TV dinners I had these past two years.

To Dr. Lincoln Wood, Dr. Carl Chen, Dr. Tom Bauer, Dr. Tim O'Sullivan, Keith Zondervan, the raiders, and the blokes of the society of professional students, who have helped and uphold me in various ways.

To Marta Nyiri, Rennie Dudek and Cecilia Lin who did a marvelous job in typing this thesis and preparing the figures.

Lastly, to my parents and heavenly father, without whom all these would have been but a dream.

ABSTRACT

As engineering systems become larger and more flexible, serious consideration must be given to the very high order, and consequently very high bandwidth, of these so called quasi-distributed parameter systems. In particular, as practical active control devices such as sensors and actuators have finite bandwidth, great care must be exercised so that control of low frequency modes does not cause instability of intermediate and high frequency modes. In this report, the nature of these stability problems is investigated in the context of direct velocity feedback control, and approximate bounds on the diagonal elements of the modal gain matrix are derived. Two velocity feedback techniques are proposed to alleviate potential instability, but these are dependent on the natural damping of the system, which remains uncertain in practice. Another technique using position feedback is considered. Despite certain additional complications, position feedback control proves to be more advantageous in many ways than velocity feedback. Some preliminary analyses on a quasi-linear vibration suppression technique via damping matrix modification are also presented. The feasibility of these theoretical techniques are confirmed by means of a numerical simulation on a simply supported discrete shear beam.

ACRONYMS

DPS	Distributed Parameter System
QDPS	Quasi-Distributed Parameter System
LSS	Large Space Structures
LAS	Liapunov Asymptotic Stable
iff	If and only If
PDE	Partial Differential Equation
ODE	Ordinary Differential Equation
DOFB	Direct Output Feedback
TF	Tuning Filter
WLOG	Without Loss of Generality
S/A	Sensor / Actuator

LIST OF SYMBOLS

The following are symbols that frequently appear throughout the thesis. * denotes variable dimensionality.

Symbols	Dimension	
A	*	State matrix of 1^{st} order system
$\mathcal{B}$	N x N	Modal gain matrix
C	N_A x N_A	Control gain matrix
D	N x N	Natural viscous damping matrix
$\mathcal{D}$	N x N	Modal damping matrix
F(t)	N	Control force vector
I	*	Identity matrix
i	scalar	$\sqrt{-1}$
K	N x N	Stiffness matrix
M	N x N	Inertia (Mass) matrix
N	scalar	Number of modelled system states
$\mathbb{N}$	-	The Natural Number System
N_A	scalar	Number of S/A pairs = number of controlled modes
N_f	scalar	Number of Tuning Filters
$\mathbb{R}$	-	The Real Number System
S	N_A x N	S/A location matrix
s	scalar	Laplace transform variable
T_1, T_2	scalar	Lead compensator time constants
u	N_A	Actuator state vector
V	scalar	Liapunov function
y	N	System state vector
Z_i	N_A	State vector of the i^{th} tuning filter

Symbols	Dimension	
β_i	scalar	Twice the open loop damping of the i^{th} mode
β_a	scalar	Twice the open loop damping of the actuator
β_{f_i}	scalar	Twice the open loop damping of the i^{th} tuning filter
γ_i	scalar	Scalar gain for the i^{th} mode
δ_{mn}	scalar	Kronecker Delta Tensor
ϵ	scalar	Small parameter
ζ_n	scalar	Natural damping ratio of system
ζ_a	scalar	Natural damping ratio of actuator
ζ_{f_i}	scalar	Natural damping ratio of the i^{th} TF
η	*	Canonical actuator state vector
Θ	$N_A \times N$	$S\Phi$
λ_i	scalar	i^{th} eigenvalue of relevant system
ξ	N	Modal state vector
ρ	*	Compensator state vector (only in Chapter 3)
Φ	N x N	Modal matrix
Ω	N x N	Canonical stiffness matrix
ω_i	scalar	Natural frequency of the i^{th} mode
ω_a	scalar	Natural frequency of the actuator
ω_{f_i}	scalar	Natural frequency of the i^{th} TF
$\square$	-	End of Proof

CONTENTS

Chapter 1

INTRODUCTION

1.1 MATHEMATICAL FORMULATION

By definition, a Distributed Parameter System (or a continuous system) is a dynamical system whose state is continuous in both the temporal and spatial domains. Consequently the dynamics of such a system is described by partial differential equations. For the purpose of application to vibratory systems such as large flexible space structures, we shall only concern ourselves with the class of hyperbolic systems described by the generalized wave equation:

$$m(x)\frac{\partial^2 y(x,t)}{\partial t^2} + D_o\frac{\partial y(x,t)}{\partial t} + K_o y(x,t) = F_C(x,t) \qquad (1.1.1)$$

where $y(x,t)$ represents the system's physical state relative to equilibrium, defined continuously in the spatial domain T and temporal domain $[0,\infty)$. The forcing terms on the right hand side are excited by the external transient disturbance and the distributed control $F_C(x,t)$. At any instant, all sufficiently smooth and square integrable $y(x,t)$ satisfying the appropriate boundary conditions

$$L_i y(x,t) = 0 \quad , \quad i = 1,2,\ldots,p \qquad (1.1.2)$$

(where L_i are linear operators) together with the inner product defined by

$$< y(x,t),\ z(x,t) > = \int_T y \cdot z\, m(x)dx \qquad (1.1.3)$$

and the associated norm

$$||y|| = < y \cdot y >^{\frac{1}{2}}$$

constitute an infinite dimensional Hilbert space $H_o = L^2(T)$. The mass

density $m(x)$ is a positive and bounded function defined on T. K_o is a linear, self-adjoint, time-invariant and positive semi-definite operator of order 2p representing the internal stiffness of the system; the spectrum of K_o is discrete and by virtue of its self-adjointness, the eigenfunctions form a complete orthonormal set $\{\phi_n(x),\ n = 1,..,\infty\}$ such that

$$K_o\phi_n(x) = \omega_n^2\, m(x)\phi_n(x), \quad n = 1,2,\ldots,\infty \tag{1.1.4}$$

and

$$< \phi_n(x),\ \phi_m(x) > = \delta_{mn} \tag{1.1.5}$$

where ω_n is the modal frequency corresponding to the n^{th} modal state $\phi_n(x)$. $D_o \frac{\partial y}{\partial t}$ denotes the natural linear viscous damping of the system; its magnitude is usually small, but rather uncertain, in practice [1].

The research on control of distributed parameter systems in general has only been recent. Some rigorous mathematical treatment can be found in [2]-[4], where advanced functional analysis and other abstract mathematical tools have been used to derive complicated adjoint equations which, if ever solved, will yield an optimal control system. Such theories are rigorous and stimulating, but one may raise the question as to whether these theories can be applied to the physical realm without major modifications. This was the major issue raised in a recent conference on the application of distributed systems theory to the control of large space structures held at the Jet Propulsion Laboratory where two schools of thought were in direct conflict. The first school, led by BALAKRISHNAN, insisted that the PDE approach is the better way and should be adhered to until such time as it is deemed absolutely

necessary to discretize. The other school, led by HUGHES [5] and being more pragmatic, favored the approach of finite discretization throughout the entire design process. We tend to favor the second school for the following reasons:

(i) Even though the PDE approach may be feasible in some extremely simple system such as the Euler-Bernoulli beam, most engineering systems are extremely complex; and it is most difficult, if not impossible, to find a suitable PDE that will accurately describe a complex system together with all its boundary conditions.

(ii) In the event that such a complex PDE can be found, there is no guarantee that it will be easy to analyze and to derive conditions for optimality.

(iii) With the present technological know-how, it is not quite possible yet to exercise distributed control. In other words, we are faced with the ultimate problem of controlling an infinite dimensional DPS with a finite dimensional controller.

In view of the mathematical and technical difficulties involved in the PDE approach, it is imperative to seek a finite truncation of the infinite dimensional system. One way of doing so mathematically is to truncate the eigenfunction expansion solution to (1.1.1). Applying the principle of separation of variables, we approximate the solution to (1.1.1) by

$$y(x,t) \simeq \sum_{n=1}^{N} \xi_n(t)\, \phi_n(x), \tag{1.1.6}$$

The exact solution can be realized in the limit as $N \to \infty$. Substituting (1.1.6) into (1.1.1), multiplying by $\phi_m(x)$ and integrating over the spatial domain Γ, we obtain

$$\ddot{\xi}_m(t) + \sum_{n=1}^{N} \mathcal{D}_{mn}\dot{\xi}_n(t) + \omega_m^2\xi_m(t) = f_m(t), \quad m = 1,\ldots,N \tag{1.1.7}$$

where $$\mathcal{D}_{mn} = \int_T \phi_m(x) D_o(\phi_n(x))\, dx \tag{1.1.8}$$

and $$f_m(t) = \int_T [F_C(x,t) + F_D(x,t)]\, \phi_m(x)\, dx \tag{1.1.9}$$

(1.1.7) is essentially a system of ODE's governing the first N modal states of the infinite dimensional system of (1.1.1), and can be conveniently expressed in the matrix notation

$$\ddot{\xi} + \mathcal{D}\,\dot{\xi} + \Omega\xi = f(t) \tag{1.1.10}$$

where $\xi, f \in \mathbb{R}^N$, $\mathcal{D}, \Omega \in \mathbb{R}^{N\times N}$, $\Omega = \text{diag}\,(\omega_n^2)$. This approach however, serves only as a mathematical guideline since firstly the PDE (1.1.1) is difficult to find and secondly it is difficult to know what the $\phi_n(x)$ are, especially as continuous functions of x.

In practice, it is much easier and more practical to model a DPS as an approximation to a discrete system and regard it as a discrete system throughout. Such an approach has become standard engineering practice through the powerful use of finite element analysis. In theory this differs from the eigenfunction expansion truncation method but in practice, they both result in an equivalent set of equations (1.1.10). At least the approximation by finite truncation is usually good for the lower order modes. As control theorists we are not so concerned about how a discrete model of a continuous system can be obtained by finite element analysis--this is an independent subject in its own right and the job of structural engineers. We shall conveniently assume that it is possible to carry out such analysis so as to model the continu-

ous system by the following set of ordinary differential equations:

$$M\ddot{y} + D\dot{y} + Ky = F_C(t) \tag{1.1.11}$$

where M is an NxN positive definite inertia matrix, D an NxN positive semi-definite viscous damping matrix, and K an NxN positive semi-definite stiffness matrix. These matrices are system parameters to be identified from finite element analysis. $y(t)$ is a real N-dimensional state vector and $F_C(t)$ a real N-dimensional control vector. As the external disturbances are assumed to be in the form of initial conditions, we shall regard the control problem as a regulator problem. The dimension of the system has thus been reduced from infinity to a finite N. (In other words, the spectrum of the DPS has been reduced from one with infinite bandwidth to one with finite bandwidth.) The larger N is, the better will (1.1.11) approximate the DPS (1.1.1). One can also visualize the discrete system (1.1.11) as a distribution of mass elements connected by springs (which may have negative spring constants) and dashpots. For our present purposes, we shall henceforth refer to the system (1.1.11), with N large, as a "Quasi-Distributed Parameter System." The QDPS (1.1.11) is characterized by the matrices M and K and can be analyzed in the modal (or eigen, or canonical) form via the congruent transformation Φ which simultaneously diagonalizes M and K, such that

$$\Phi^T M \Phi = I_N \tag{1.1.12}$$

$$\Phi^T D \Phi = \mathcal{D} \tag{1.1.13}$$

$$\Phi^T K \Phi = \Omega = \mathrm{diag}(\omega_n^2) \tag{1.1.14}$$

The n^{th} column of Φ is the eigenvector corresponding to the n^{th} mode, with frequency ω_n. The modal state vector ξ is given by

$$y = \Phi \xi \tag{1.1.15}$$

The modal damping matrix $\mathcal{D}$ is non-diagonal in general unless classical normal modes exist, but it is nevertheless assumed diagonally dominant. Under the transformation (1.1.12)-(1.1.15), (1.1.1) is reduced to the modal equation

$$\ddot{\xi} + \mathcal{D}\,\dot{\xi} + \Omega\xi = \Phi^{T}F(t) \tag{1.1.16}$$

which is equivalent to what we had before (c.f. (1.1.10)) by truncation of the eigenfunction expansion.

Throughout this report, the analysis is carried out in the context of LSS control although it can be applied, with some modification perhaps, to other large scale vibratory systems, such as seismic structures, large scale social-economic systems, or biological systems.

1.2 REVIEW OF ACTIVE CONTROL TECHNIQUES

The central problem in active control of QDPS is vibration suppression. To be exact, given a finite number of resources such as sensors, actuators and controllers, how can the control F(t) be constructed to steer the QDPS from a non-null state to its null state in some optimal way and at the same time preserve global asymptotic stability. There has been a proliferation of the theory of LSS control in the recent literature, and these are well reviewed in [6] and [7]. A large proportion of all active control techniques proposed to date are of optimal control type [8]-[12]. However, in addition to being complicated, difficult to implement, and requiring large on-board computer capacity, etc., optimal control techniques inevitably encounter

the notorious problem of "Control and Observation Spillover", which is likely to render the system unstable. What happens physically is that due to the high dimensionality of the problem, the energy used in controlling the lower order modes spills into some of the uncontrolled modes through the coupling,and destabilizes the latter modes. These spillover effects are both predicted by theory [8] and demonstrated by hardware experiments [13]; and despite efforts in overcoming them [14,15], remain stubborn. It is one of the usual difficulties in engineering control problems where optimal performance is frequently in conflict with stability.

Another much simpler technique is known as the Direct Output Feedback Control [16]. Not only is the use of collocated (sensors and actuators) velocity feedback [17] - [19] easier to implement, it also guarantees global stability. Spillover still exists, but rather than being detrimental, it stabilizes the uncontrolled and unmodelled modes.

Whether by using optimal control techniques with state estimator or by DOFB control, the control F(t) in (1.1.11) essentially takes the form

$$F(t) = - B_1 y - B_2 \dot{y} \qquad (1.2.1)$$

In the case of optimal control, the NxN gain matrices B_1 and B_2 are time dependent and related to the solution of a pertinent matrix Ricatti differential equation. In the case of DOFB, B_1 and B_2 are time invariant. In particular if collocated velocity feedback were used, so that $B_1 \equiv 0$ and B_2 is positive semi-definite, then it is quite obvious that the resulting control system is globally stable. With N_A pairs of collocated sensors and actuators available, DOFB allows the eigenvalues of the first N_A

fundamental modes of the system to be approximately assigned. Thus DOFB can be conceived as a version of the pole placement technique [20]. In view of the fact that stability is the most important requirement of real LSS, collocated velocity feedback control seems to be potentially a more important technique than optimal control.

However, there still remains one crucial problem, yet unfortunately ignored by most, namely, the interaction of actuator dynamics with the structural dynamics. Under certain easily attainable conditions it can be shown that intermediate modes of frequency close to the actuator's frequency can become unstable [21][22]. A thorough investigation into the nature of this instability is presented in the next chapter. To avoid these instability problems is a non-trivial task if velocity feedback is used. Two methods are suggested in Chapters 3 and 4 respectively. The first method generalizes the lead compensation technique commonly used in classical single-input-single-output control system design and applies it to the control of QDPS. Under careful design of compensation parameters, the overall system can be rendered stable. The second method simply suppresses the feedback of all the modes which are likely to become unstable. Both these methods suffer from the lack of robustness as they require extensive knowledge about the system modal structure and natural damping. A much superior, though not quite conventional, technique--positive position feedback control [23]--will be presented in Chapter 5. It is shown that the scheme does more than guarantee global stability, it also has numerous advantages over velocity feedback control schemes. In Chapter 6, we deviate from the conventional method of control actuation and

seek the alternative use of electronic damping by stiffness modification [24]. A coherent juxtaposition of these theories is presented in Chapter 7 through the numerical simulation of a simply supported discrete shear beam.

Throughout this report, two crucial assumptions are made.

Assumption I. The rigid body mode can always be decoupled from the vibrational modes. Thus the two major aspects of LSS control, namely: attitude pointing and vibration suppression, can be considered separately. The decoupling can be achieved either by proper design of the feedback gain matrix or by using relative sensing and actuation. In this report we shall only concentrate on the problem of vibration suppression.

Assumption II. The dynamics of the actuators is assumed to be second order. Higher order dynamics can always be assumed, but will give rise to more complicated algebra without necessarily deducing further instructive information, as the second order assumption is believed to be the most realistic choice.

Needless to say, the practical situation could deviate significantly from the theoretical prediction if these assumptions do not hold.

Chapter 2

STABILITY ANALYSIS OF COUPLED SYSTEM AND ACTUATOR DYNAMICS

2.1 ASYMPTOTIC STABILITY OF A SINGULARLY PERTURBED SYSTEM

All actuators used in practice inevitably possess some inertia and hence must be regarded as finite bandwidth dynamical systems. Collocated rate feedback control (and expectedly, optimal control with spillover eliminated) may work fine if the actuators are assumed to have no dynamics but this is unfortunately not so. BALAS [25] shows that with fast modes truncated, neglecting of actuator dynamics is justifiable (i.e. does not destabilize the system), if these dynamics are sufficiently fast. This claim is obviously false due to conflicting assumptions. No matter how fast the actuator dynamics may be, they must have finite bandwidth, whereas the flexible system is one of infinite bandwidth (or at least very large--in any case, larger than that of the actuator) whether one would like to model it as such or not. Note in passing that sensor dynamics are not so important, as the sensor bandwidth is usually much higher than the actuator bandwith.

Without actuator dynamics, the equation governing the collocated velocity feedback control of a QDPS (from (1.2.1))

$$M\ddot{y} + D\dot{y} + Ky = F(t) = -S^{T}CS\dot{y} \tag{2.1.1}$$

where S is a N_AxN integer valued matrix referred to as the sensor/actuator location matrix [18], with individual entries defined by

$$[S]_{ij} = \begin{cases} 1 & \text{if S/A pair i is located at element j} \\ 0 & \text{otherwise} \end{cases} \tag{2.1.2}$$

Sometimes S is written as a set of integers denoting the set of elements

at which the S/A are located. C is a $N_A \times N_A$ time-invariant gain matrix. It is easy to see that if C is positive definite then the feedback essentially adds a positive semi-definite passive damping to the existing natural damping D; hence, the resulting system must be globally stable.

With the inclusion of actuator dynamics (assumed 2nd order), however, (2.1.1) is modified to be

$$M \ddot{y} + D \dot{y} + K y = -S^T C u \tag{2.1.3}$$

$$\ddot{u} + 2\zeta_a \omega_a \dot{u} + \omega_a^2 (u - S\dot{y}) = 0 \tag{2.1.4}$$

where u is an N_A dimensional real vector representing the state of the N_A actuators which have identical damping ratios ζ_a and natural frequencies ω_a. Applying the following transformation:

$$y = \Phi \xi \tag{2.1.5}$$

$$u = S \Phi \eta \tag{2.1.6}$$

where Φ is the modal matrix defined in 1.1, the equations of motion in the modal space are

$$\ddot{\xi} + \mathcal{D}\dot{\xi} + \Omega\xi = - \Phi^T S^T C S \Phi \eta = - \mathcal{B}\eta \tag{2.1.7}$$

$$\ddot{\eta} + 2\zeta_a \omega_a \dot{\eta} + \omega_a^2 (\eta - \dot{\xi}) = 0 \tag{2.1.8}$$

The transformation (2.1.6) introduces $N-N_A$ degrees of redundancy into (2.1.8). Though quite unnecessary, it yields symmetry in (2.1.7), so that subsequent analysis is simplified.

Let us assume for the moment that we are dealing with a finite discrete system rather than a QDPS, i.e., N is sufficiently small such that actuator bandwidth can indeed exceed that of the system, then the

following theorem is apparent.

Theorem 2.1

If $\omega_a >> \max_{i=1,\ldots N} \omega_i$, then the coupled system (2.1.7) and (2.1.8) is stable.

The proof of theorem 2.1 requires the use of the well-known Klimushchev and Krasovskii lemma [26] which we shall state without proof here.

K-K Lemma

Given the linear system of differential equations

$$\dot{x}_1 = A_{11}\, x_1 + A_{12}\, x_2 \tag{2.1.9}$$

$$\varepsilon \dot{x}_2 = A_{21}\, x_1 + A_{22}\, x_2 \tag{2.1.10}$$

where ε is a small positive parameter, x_i's and A_{ij}'s are vectors and matrices of appropriate dimension, with A_{22} invertible, the corresponding degenerate (or reduced) system is defined by setting $\varepsilon = 0$, so that

$$\bar{x}_2 = - A_{22}^{-1}\, A_{21}\, \bar{x}_1 \tag{2.1.11}$$

$$\dot{\bar{x}}_1 = (A_{11} - A_{12}\, A_{22}^{-1}\, A_{21})\, \bar{x}_1 \tag{2.1.12}$$

Thus if $A_{11} - A_{12}\, A_{22}^{-1}\, A_{21}$ and A_{22} are both stable matrices and if ε is sufficiently small, (i.e. $\exists\ \varepsilon_1 \ni \forall\ \varepsilon < \varepsilon_1$) then the system (2.1.9) and (2.1.10) is Liapunov Asymptotically stable, and furthermore the trajectories of the original system converge uniformly to the trajectories of the reduced system.

The proof of this lemma is non-trivial but theorem (2.1) can be deduced readily from it. Set $\varepsilon = \frac{1}{\omega_a}$ to be the perturbation parameter and rewrite (2.1.7) and (2.1.8) in the form of (2.1.9) and (2.1.10), i.e.,

$$\frac{d}{dt}\begin{bmatrix}\xi\\ \dot{\xi}\end{bmatrix} = \underbrace{\begin{bmatrix}0 & I\\ -\Omega & -\mathcal{D}\end{bmatrix}}_{A_{11}}\begin{bmatrix}\xi\\ \dot{\xi}\end{bmatrix} + \underbrace{\begin{bmatrix}0 & 0\\ -\mathcal{B} & 0\end{bmatrix}}_{A_{12}}\begin{bmatrix}\eta\\ \varepsilon\dot{\eta}\end{bmatrix} \tag{2.1.13}$$

$$\varepsilon\frac{d}{dt}\begin{bmatrix}\eta\\ \varepsilon\dot{\eta}\end{bmatrix} = \underbrace{\begin{bmatrix}0 & 0\\ 0 & I\end{bmatrix}}_{A_{21}}\begin{bmatrix}\xi\\ \dot{\xi}\end{bmatrix} + \underbrace{\begin{bmatrix}0 & I\\ -I & -2\zeta_a I\end{bmatrix}}_{A_{22}}\begin{bmatrix}\eta\\ \varepsilon\dot{\eta}\end{bmatrix} \tag{2.1.14}$$

Note that the A_{ij}'s are independent of the perturbation parameter ε. Note that A_{11} and A_{22} are known to be stable with A_{22} non-singular, and

$$A_{11} - A_{12}\,A_{22}^{-1}\,A_{21} = \begin{bmatrix}0 & I\\ -\Omega & -\mathcal{D}-\mathcal{B}\end{bmatrix} \tag{2.1.15}$$

which is exactly the stable state matrix of the reduced system obtained by ignoring actuator dynamics. Hence, by increasing ω_a, ε can be made sufficiently small, and consequently the theorem follows directly from the K-K lemma. □

We have intentionally proved a false statement as our initial assumption is wrong. BALAS [25] did essentially the same thing though he did not suspect the fallacy. As a real continuous system has infinite bandwidth, the threshold bound ε_1 in the K-K lemma, in effect, reduces to zero. Real actuators always have finite bandwidth, and hence the condition in theorem 2.1 can never be realized physically.

2.2 GLOBAL STABILITY ANALYSIS : DECOUPLING OF SYSTEM VIA PERTURBATION THEORY

An exact sufficient and necessary condition for stability of the QDPS with actuator dynamics (2.1.7), (2.1.8) is extremely difficult to obtain indeed. Conventional tools such as the Bellman-Gronswall lemma and

the Liapunov Direct method prove to be futile, due to the high dimensionality and lack of symmetry. We would expect the system to become unstable if the feedback gain matrix $\mathcal{B}$ becomes too "large" (the definition of "large" is not very clear cut here). Global techniques such as those which require a bound on the norm of $\mathcal{B}$ as a sufficient condition for stability tend to destroy much of the fine structure. A typical case is the use of a Vector Liapunov function for an interconnected system [27,28]. It can be shown that the sufficient condition for stability using this method can be hundreds or thousands of times overly restrictive!

What is really needed is a method that will not only predict global stability, but will also predict the stability of individual modes and the stability margin of each mode as well. It turns out that if $\mathcal{B}$ is sufficiently "small", (but is still able to impart up to 20% damping ratio to the controlled modes), then decoupling of the QDPS via perturbation theory enables us to investigate the stability of individual modes.

Even though the actuator system (2.1.8) has vector input and output it is in effect a scalar system since each actuator has identical dynamics. Taking Laplace Transform of (2.1.7) and (2.1.8) and combining, we have

$$\left[s^2 I_N + s\mathcal{D} + \Omega + \frac{\omega_a^2 s}{s^2+2\zeta_a\omega_a s+\omega_a^2}\mathcal{B} \right] \hat{\xi} = \begin{array}{l}\text{Terms governed}\\ \text{by Initial}\\ \text{Conditions}\end{array} \qquad (2.2.1)$$

Thus the stability of the coupled system is determined by the root of the characteristic equation

$$\det\left[\,(s^2 I_N + s\mathcal{D} + \Omega)(s^2 + 2\zeta_a\omega_a s + \omega_a^2) + \omega_a^2 s\mathcal{B}\right] = 0 \qquad (2.2.2)$$

Thus if the elements of $\mathcal{B}$ and $\mathcal{D}$ are sufficiently small, we can attach a small parameter ε to each and let

$$\tilde{\mathcal{B}} = \frac{1}{\varepsilon}\mathcal{B} \qquad (2.2.3)$$

$$\tilde{\mathcal{D}} = \frac{1}{\varepsilon}\mathcal{D} \qquad (2.2.4)$$

and consequently (2.2.2) yields

$$\prod_{i=1}^{N}\left[(s^2 + 2\zeta_a\omega_a s + \omega_a^2)(s^2 + \beta_i s + \omega_i^2) + \omega_a^2 s\gamma_i\right] + O(\varepsilon^2) = 0 \qquad (2.2.5)$$

where $\beta_i = 2\zeta_n\omega_i$ and γ_i are the i^{th} diagonal elements of $\mathcal{D}$ and $\mathcal{B}$ respectively and ζ_a & ζ_n the damping ratios of the actuator and QDPS, respectively. Hence we can regard, to first order accuracy, the dynamics of the coupled system as being governed by N modal subsystems each having a characteristic equation

$$g_i(s) = (s^2 + \beta_a s + \omega_a^2)(s^2 + \beta_i s + \omega_i^2) + \omega_a^2\gamma_i s = 0 \qquad (2.2.6)$$

which represents the dynamics of the scalar system

$$\ddot{\xi}_i + \beta_i\dot{\xi}_i + \omega_i^2\xi_i = -\gamma_i\eta_i \qquad (2.2.7)$$

$$\ddot{\eta}_i + \beta_a\dot{\eta}_i + \omega_a^2(\eta_i - \dot{\xi}_i) = 0 \qquad (2.2.8)$$

It is now easy to analyze the stability of these scalar systems by classical control techniques. Later simulation shows that this approximation is good for closed loop damping up to as high as 30%.

2.3. SCALAR THEORY : DERIVATION OF STABILITY BOUNDARY

Setting $s = i\omega$ in the scalar characteristic equation (2.2.6) and partitioning into real and imaginary parts

$$Re\ g(i\omega) = \omega^4 - \omega^2(\omega_i^2 + \omega_a^2 + \beta_i\beta_a) + \omega_i^2\omega_a^2 \tag{2.3.1}$$

$$Im\ g(i\omega) = -(\beta_i+\beta_a)\omega^3 + (\beta_i\omega_a^2 + \beta_a\omega_i^2 + \omega_a^2\gamma_i)\omega \tag{2.3.2}$$

the first cross-over point of the Nyquist plot with the real axis ($Im\ g(i\omega_c) = 0$) occurs at [the root of $Im\ g(i\omega) = 0$]

$$\omega_c^2 = \frac{(\beta_i\omega_a^2 + \beta_a\omega_i^2 + \omega_a^2\gamma_i)}{\beta_i + \beta_a} \tag{2.3.3}$$

Nyquist's stability criterion states that a sufficient and necessary condition for stability is that the Nyquist plot have zero net encirclements around the origin, which is equivalent to saying that

$$\Delta = Re(i\omega_c) < 0 \tag{2.3.4}$$

We shall examine this stability criterion from two perspectives. Firstly, if we regard γ_i as a fixed parameter, then (2.3.4) can be expressed as a 5^{th} degree polynomial in ω_i, (see Fig. 2.1), i.e.

$$\begin{aligned}\Delta(\omega_i,\gamma_i) = {} & (-2\zeta_n\beta_a)\omega_i^5 + (-4\zeta_n^2\beta_a^2)\omega_i^4 \\ & + (4\zeta_n\beta_a\omega_a^2 - 2\gamma_i\zeta_n\omega_a^2 - 2\zeta_n\beta_a^3 - 8\zeta_n^3\beta_a\omega_a^2)\omega_i^3 \\ & + (\gamma_i\beta_a\omega_a^2 - 4\zeta_n^2\gamma_i\beta_a\omega_a^2 - 4\zeta_n^2\beta_a\omega_a^2)\omega_i^2 \\ & + (2\zeta_n\gamma_i\omega_a^4 - 2\zeta_n\beta_a\omega_a^4 - 2\gamma_i\zeta_n\beta_a^2\omega_a^2)\omega_i \\ & + (-\gamma_i\beta_a\omega_a^4 + \gamma_i^2\omega_a^4) < 0\end{aligned} \tag{2.3.5}$$

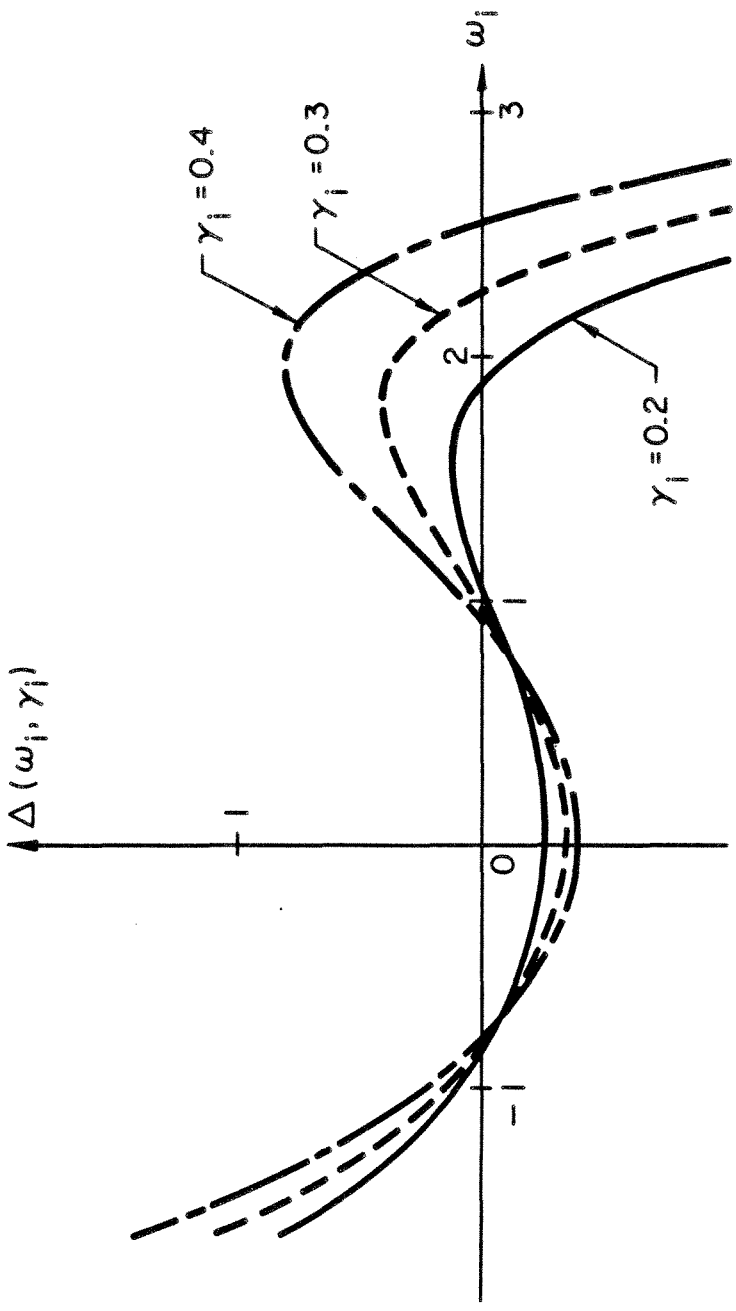

Fig. 2.1 Δ vs. ω_i for Varying γ_i, $\omega_a = 1.0$, $\zeta_a = 0.7$, $\zeta_n = 0.01$.

Depending on γ_i and the rest of the parameters, there exists an unstable frequency range which lies approximately between ω_a and $2\omega_a$. The size of this range increases as γ_i is increased. Hence, to first order accuracy and with γ_i fixed, the mode i is unstable if its frequency lies within this range.

Alternatively, we can examine the stability of all modes from a global perspective. Rearranging (2.3.5) as a quadratic in γ_i yields

$$\Delta(\omega_i,\gamma_i) = (\omega_a^4)\gamma_i^2 + (\beta_a\omega_i^2\omega_a^2 - \beta_i\omega_i^2\omega_a^2 + \beta_i\omega_a^4 - \beta_i^2\beta_a\omega_a^2 - \beta_a\omega_a^4 - \beta_i\beta_a^2\omega_a^2)\,\gamma_i$$
$$+ (-\beta_i\beta_a\omega_i^4 + 2\beta_i\beta_a\omega_i^2\omega_a^2 - \beta_i^2\beta_a^2\omega_i^2 - \beta_i\beta_a^3\omega_i^2 - \beta_a\beta_i^3\omega_a^2 \qquad (2.3.6)$$
$$- \beta_i\beta_a\omega_a^4 - \beta_i^2\beta_a^2\omega_a^2) < 0$$

This condition is satisfied if and only if $\gamma_i \in (\gamma_\ell, \gamma_u)$ where γ_ℓ and γ_u are the roots of the quadratic (2.3.6),

$$\gamma_\ell(\omega_i) = 4\zeta_n\zeta_a(\zeta_n\omega_i + \zeta_n\omega_a)\left(\frac{\omega_i}{\omega_a}\right) + (\zeta_a\omega_a - \zeta_n\omega_i)\left(1 - \left(\frac{\omega_i}{\omega_a}\right)^2\right)$$
$$- (\zeta_n\omega_i + \zeta_a\omega_a)\sqrt{\left(1 - \left(\frac{\omega_i}{\omega_a}\right)^2\right)^2 + 16\zeta_n^2\zeta_a^2\left(\frac{\omega_i}{\omega_a}\right)^2 + 8\zeta_n\zeta_a\left(\frac{\omega_i}{\omega_a}\right)\left(1 + \left(\frac{\omega_i}{\omega_a}\right)^2\right)} \qquad (2.3.7)$$

and

$$\gamma_u(\omega_i) = 4\zeta_n\zeta_a(\zeta_n\omega_i + \zeta_n\omega_a)\left(\frac{\omega_i}{\omega_a}\right) + (\zeta_a\omega_a - \zeta_n\omega_i)\left(1 - \left(\frac{\omega_i}{\omega_a}\right)^2\right)$$
$$+ (\zeta_n\omega_i + \zeta_a\omega_a)\sqrt{\left(1 - \left(\frac{\omega_i}{\omega_a}\right)^2\right)^2 + 16\zeta_n^2\zeta_a^2\left(\frac{\omega_i}{\omega_a}\right)^2 + 8\zeta_n\zeta_a\left(\frac{\omega_i}{\omega_a}\right)\left(1 + \left(\frac{\omega_i}{\omega_a}\right)^2\right)} \qquad (2.3.8)$$

These two curves together define the stability boundary, i.e., sufficient and necessary conditions for stability, as shown in Fig. 2.2. Notice that this stability boundary can also be derived, in a more painstaking manner, by plotting the upper and lower end points for instability in Fig. 2.1 against their corresponding gain γ_i. It is important to know that the stability boundary is highly dependent on the natural damping ζ_n of the system. As ζ_n decreases, the stable region shrinks, and in the limit as $\zeta_n \to 0$, the stability boundary degenerates into the ω_i axis and an asymptote which passes through ω_a (see Fig. 2.3). Consequently, if $\zeta_n = 0$, all modes of frequency greater than ω_a are unstable if positive gain is used. The effects of varying ω_a and ζ_a are also shown in Fig. 2.4 and Fig. 2.5, respectively, although these quantities are not quite as important as ζ_n.

Note that one may desire to compute the unstable frequency range for a given positive γ_1 (i.e., find the inverse function of γ in (2.3.7) and (2.3.8)). The exact inverse expression seems impossible to obtain, but for a sufficiently large or small value of $R = \frac{\omega_i}{\omega_a}$, we can obtain asymptotic expressions of the lower and upper limits $\omega_i^*(\gamma)$ and $\omega_i^{**}(\gamma)$ of the unstable frequency range (see Fig. 2.6) as (suppressing i from γ_i),

$$\text{for } R \ll 1 \quad \omega_i^*(\gamma) = \omega_a \sqrt{1 - \frac{\gamma}{2\zeta_a \omega_a}} \tag{2.3.9}$$

$$\text{for } R \gg 1 \quad \omega_i^{**}(\gamma) = \frac{\omega_a}{2} \left(\frac{\gamma}{2\zeta_n \omega_a}\right)^{1/3} \left[1 + \sqrt{1 - \frac{4(4\zeta_a^2 - 1)}{3} \left(\frac{2\zeta_n \omega_a}{\gamma}\right)^{2/3}}\right] \tag{2.3.10}$$

The derivation of these asymptotic formulae are included in Appendix A.

It is now possible to predict global stability of the ODPS (2.1.7) and (2.1.8) by simply checking the location of the plot of scalar gain vs.

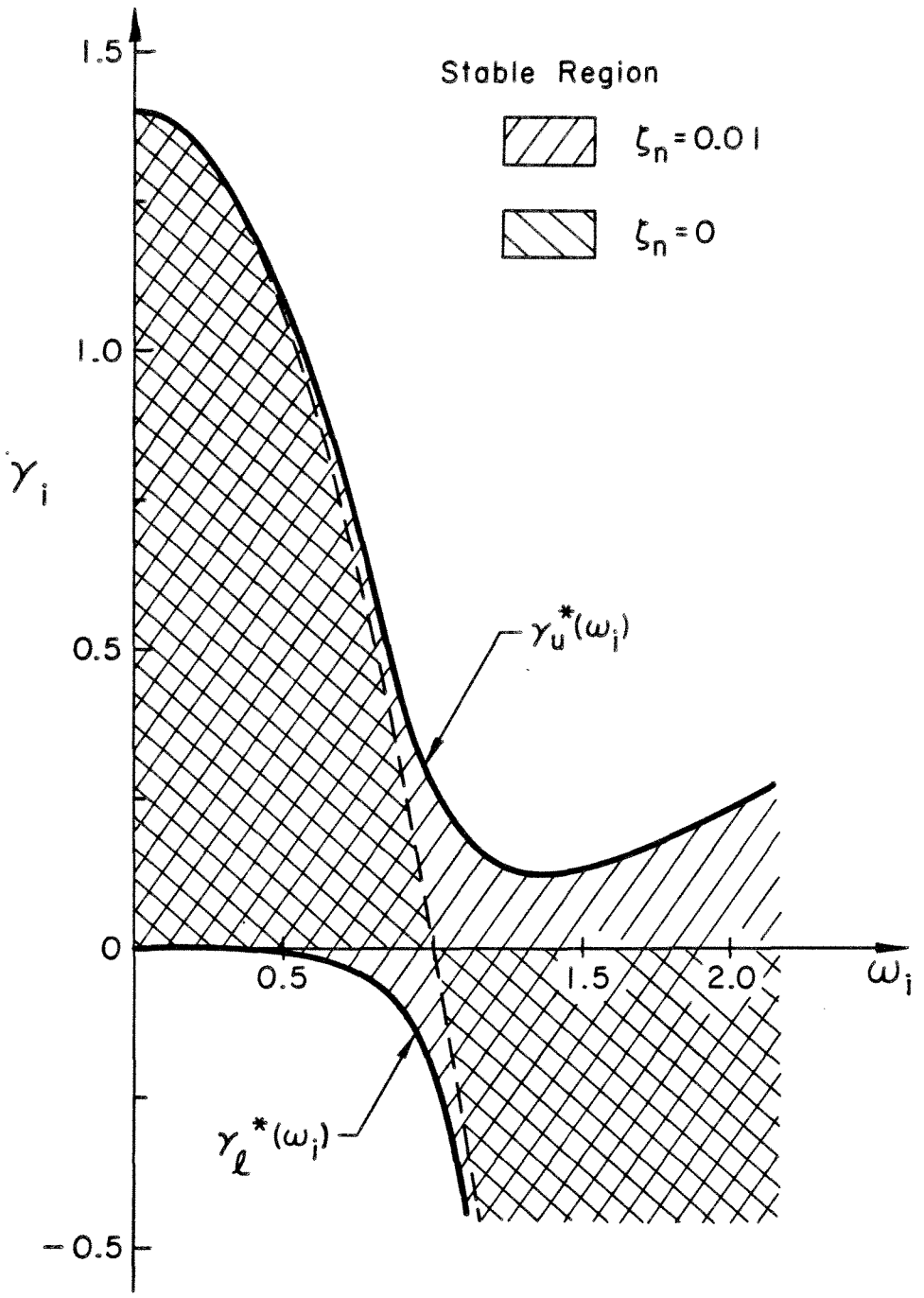

Fig. 2.2 Stability Boundary for Scalar Velocity Feedback System. $\omega_a = 1.0$, $\zeta_a = 0.7$.

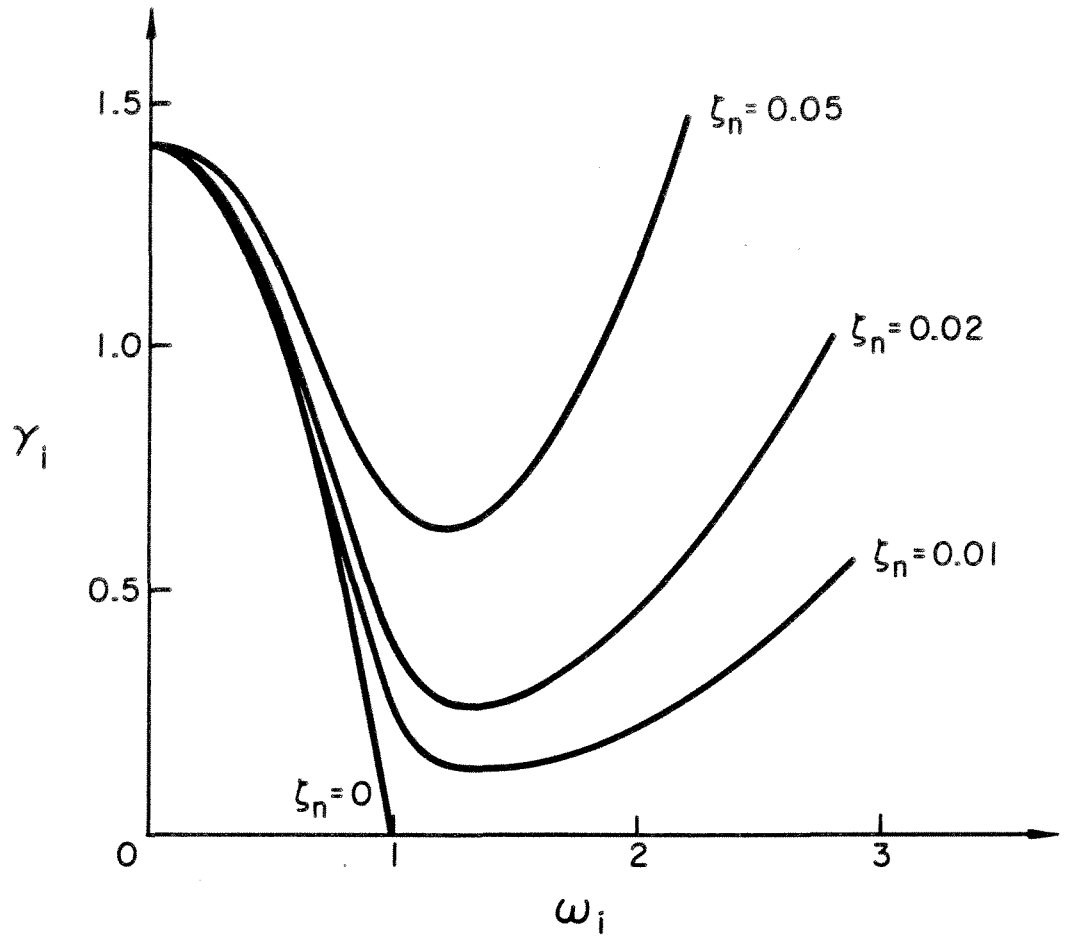

Fig. 2.3 Effect of Varying ζ_n on Stability Boundary

$\omega_a = 1.0$, $\zeta_a = 0.7$

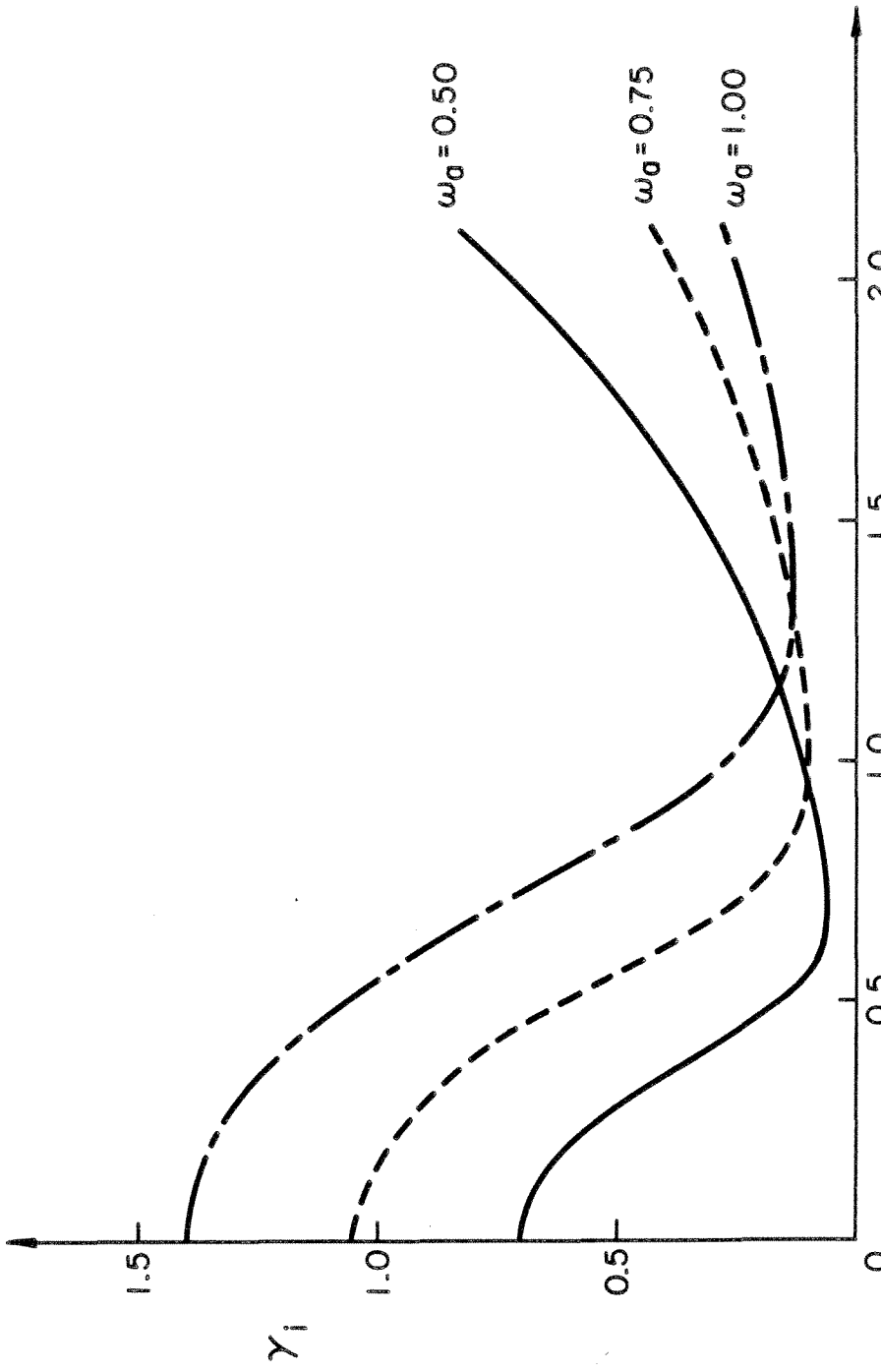

Fig. 2.4 Effect of Varying ω_a on Stability Boundary, $\zeta_a = 0.7$, $\zeta_n = 0.01$

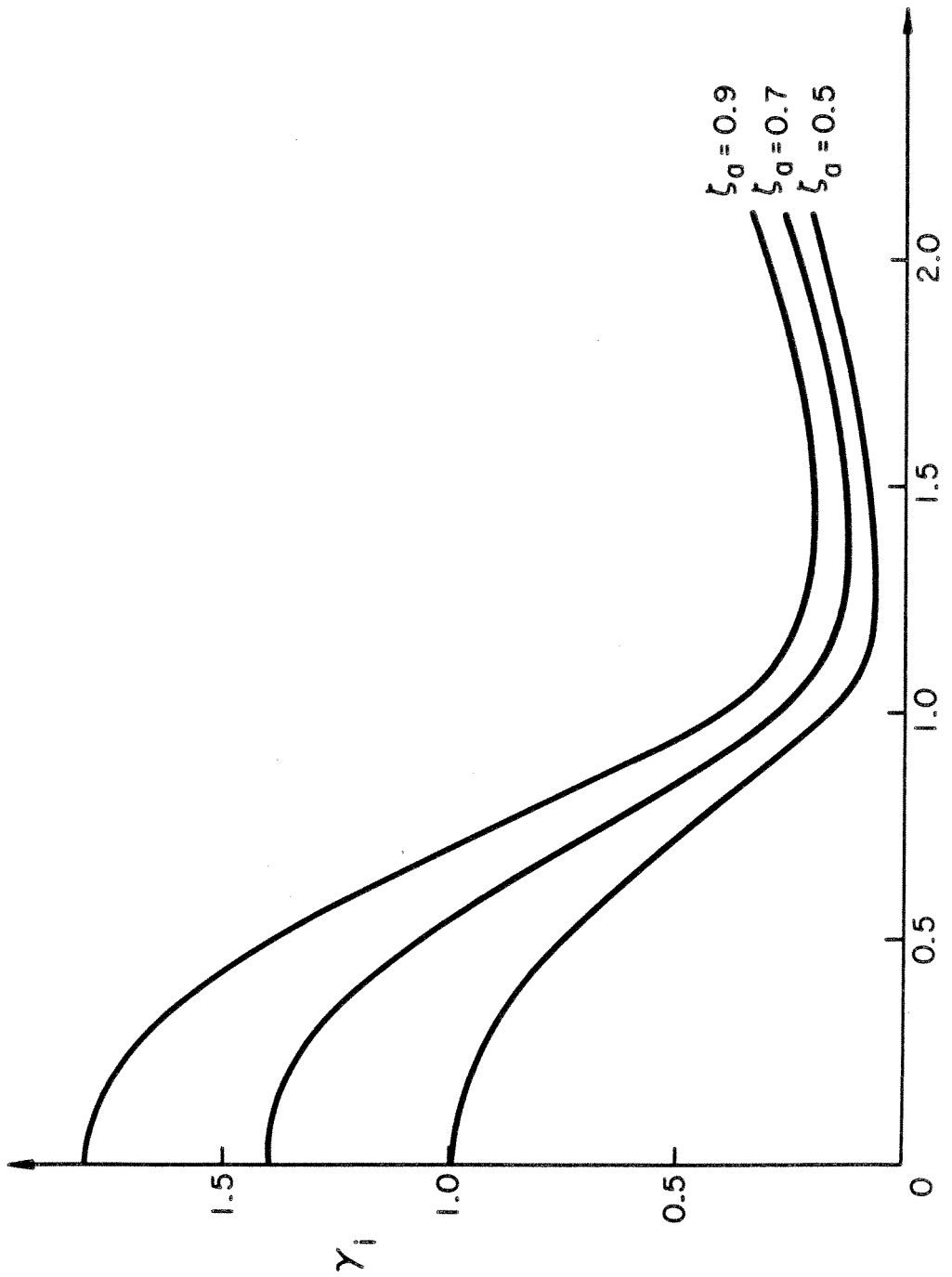

Fig. 2.5 Effect of Varying ζ_a on Stability Boundary, $\zeta_n = 0.01$, $\omega_a = 1.0$

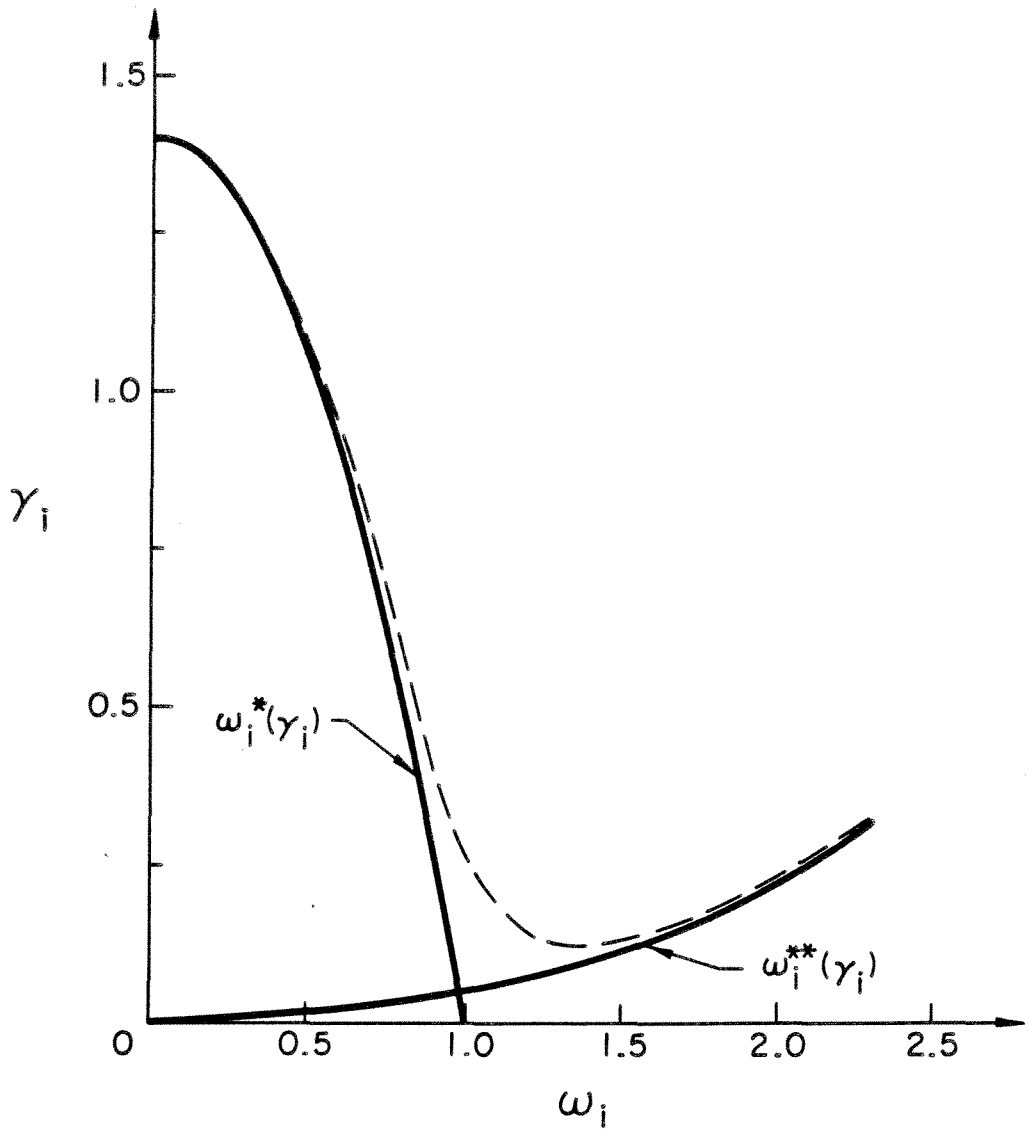

Fig. 2.6 Asymptotic Stability Boundary, $\omega_a = 1.0$, $\zeta_a = 0.7$, $\zeta_n = 0.01$

$$\omega_i^*(\gamma_i) = \frac{\omega_a}{2}\left(\frac{\gamma_i}{2\zeta_n\omega_a}\right)^{\frac{1}{3}}\left(1+\sqrt{1-\frac{4(4\zeta_a^2-1)}{3}\left(\frac{2\zeta_n\omega_a}{\gamma_i}\right)^{2/3}}\right)$$

$$\omega_i^{**}(\gamma_i) = \omega_a\sqrt{1-\frac{\gamma_i}{2\zeta_a\omega_a}}$$

natural frequency for each individual mode in Fig. 2.2. In fact we can go a step further and predict the marginal stability of each mode.

2.4 CLOSED LOOP DAMPING CHARACTERISTICS

In order to obtain a better understanding of the closed loop damping characteristics of the modes in relation to the stability boundary, we shall compare the characteristic equation (2.2.6) with its equivalent closed loop expression.

$$(s^2 + \beta_p s + \omega_p^2)(s^2 + \beta_q s + \omega_q^2) = 0 \tag{2.4.1}$$

For sufficiently small gain, the closed loop modal frequency ω_p is expected to be close to the open loop frequency ω_i, and hence β_p represents the closed loop damping of the mode which can be prescribed a priori by adjusting the gain γ_i. To do so, we expand (2.2.6) and (2.4.1) and equate terms in similar powers of s, i.e.

$$s^3 : \beta_i + \beta_a = \beta_p + \beta_q \tag{2.4.2}$$

$$s^2 : \omega_i^2 + \omega_a^2 + \beta_i\beta_a = \omega_p^2 + \omega_q^2 + \beta_p\beta_q \tag{2.4.3}$$

$$s^1 : \beta_i\omega_a^2 + \beta_a\omega_i^2 + \gamma_i\omega_a^2 = \beta_p\omega_p^2 + \beta_q\omega_q^2 \tag{2.4.4}$$

$$s^0 : \omega_i^2\omega_a^2 = \omega_p^2\omega_q^2 \tag{2.4.5}$$

A priori prescription of β_p will result in 4 simultaneous equations in the 4 unknowns $\gamma_i, \omega_p, \omega_q, \beta_q$. These can be reduced further to a quadratic in just γ_i, whose roots are given by

$$\gamma_i(\omega_i, \beta_p) = \frac{-A_2 \pm \sqrt{A_2^2 - 4A_3A_1}}{2} \tag{2.4.6}$$

where

$$A_1 = \omega_a^4 \tag{2.4.7}$$

$$\beta_q = \beta_i + \beta_a - \beta_p \tag{2.4.8}$$

$$K_1 = \omega_i^2 + \omega_a^2 + \beta_i\beta_a - \beta_p\beta_q \tag{2.4.9}$$

$$K_2 = \beta_i\omega_a^2 + \beta_a\omega_i^2 \tag{2.4.10}$$

$$A_2 = -\omega_a^2(\beta_p K_1 + \beta_q K_1 - 2K_2) \tag{2.4.11}$$

$$A_3 = (\beta_p K_1 - K_2)(\beta_q K_1 - K_2) + (\beta_p - \beta_q)^2\omega_i^2\omega_a^2 \tag{2.4.12}$$

For comparison purposes, it is desirable to prescribe the approximate closed loop damping ratio ζ_p($\ni \beta_p = 2\zeta_p\omega_i$) instead. The resulting plots of γ_i as a function of ω_i for various ζ_p are shown in Fig. 2.7. and Fig. 2.8.

Two interesting cases, both of which can be confirmed theoretically, demand special attention. Firstly, for a non-zero ζ_n the locus of ζ_p = 0 % simply degenerates into the stability boundary, and secondly the locus of $\zeta_p = \zeta_n$ degenerates into the stability boundary of ζ_n = 0 %. These two loci thus partition the stable region of a non-zero ζ_n into four mutually exclusive regions (see fig. 2.7) as follows

$$\text{Region I,} \quad \gamma_i > 0, \quad \zeta_p > \zeta_n \; ; \tag{2.4.13}$$

$$\text{Region II,} \quad \gamma_i > 0, \quad \zeta_p < \zeta_n \; ; \tag{2.4.14}$$

$$\text{Region III,} \quad \gamma_i < 0, \quad \zeta_p < \zeta_n \; ; \tag{2.4.15}$$

$$\text{Region IV,} \quad \gamma_i < 0, \quad \zeta_p > \zeta_n \; ; \tag{2.4.16}$$

The following observations can be made:

(i) For modes of $\omega_i > \omega_a$, higher than natural closed-loop damping is impossible if positive gain is used. Conversely, for modes of $\omega_i < \omega_a$,

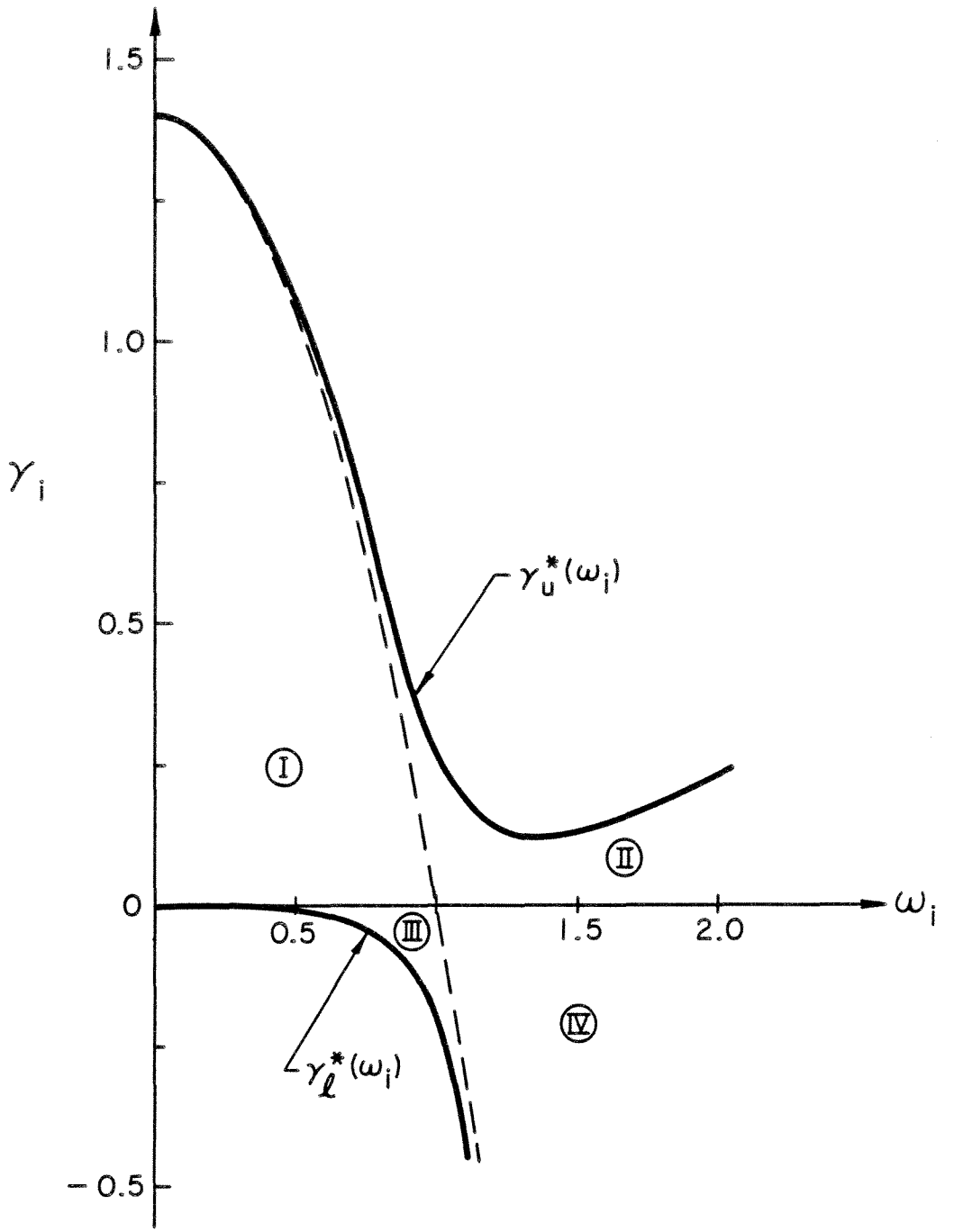

Fig. 2.7 Partition of Stable Region for Non-trivial ζ_n

$\omega_a = 1.0$, $\zeta_a = 0.7$, $\zeta_n = 0.01$

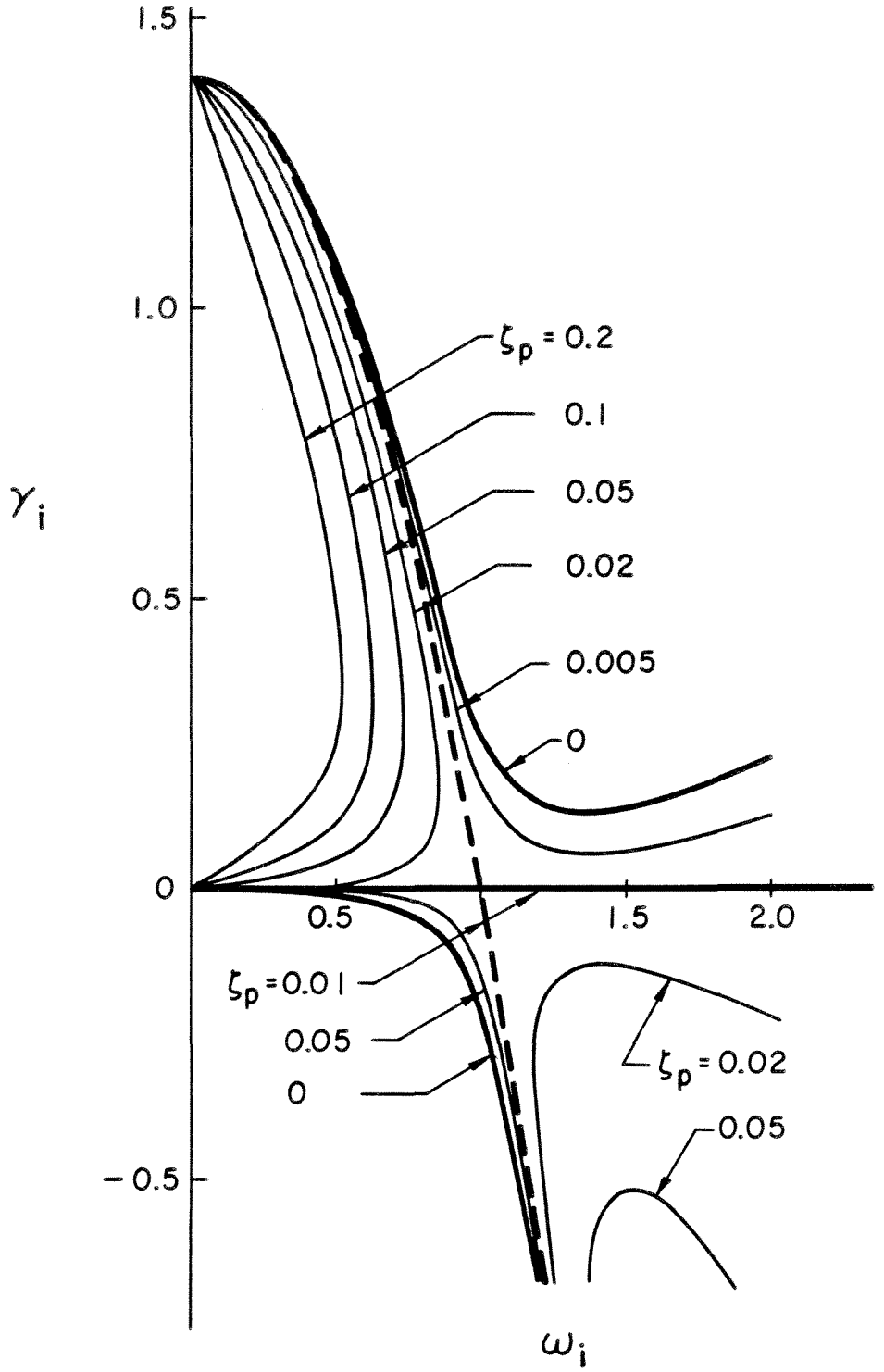

Fig. 2.8 Closed Loop Damping Characteristics

$\omega_a = 1.0$, $\zeta_a = 0.7$, $\zeta_n = 0.01$

higher than natural closed-loop damping is also impossible if negative gain is used.

(ii) $\forall\ \zeta_p > \zeta_n$, $\exists$ a frequency range in which ζ_p cannot be attained no matter how large or how small the gain may be. For example, for $\zeta_p = 5\ \%$ ($\zeta_n = 1\ \%$, $\zeta_a = 70\ \%$), this range is approximately [$0.72\ \omega_a$, $1.37\ \omega_a$].

(iii) As ω_i approaches ω_a from both sides, the maximum attainable closed loop damping becomes very small.

(iv) The iso-ζ_p locus for negative gain seems to lie much further down from the ω_i axis than the case of positive gain. This means that if negative γ_i were to be used for modes of $\omega_i > \omega_a$, much higher gain magnitude is required to attain the same order of damping as for the positive γ_i case.

The above predicted closed loop damping characteristics are confirmed later by numerical simulation (Chapter 7), and the understanding of such is crucial in the design of compensated feedback treated in the next chapter.

Chapter 3

STABLE VELOCITY FEEDBACK CONTROL BY GENERALIZED LEAD COMPENSATION

3.1 SCALAR THEORY: APPLICATION OF CONVENTIONAL LEAD COMPENSATION TECHNIQUE

The problem of overcoming the potential instability discussed previously is, in general, not a trivial one. In particular we would like to increase the stability margin of those potentially unstable modes without upsetting the prescribed stability of the lower controlled modes or causing the higher uncontrolled modes to be unstable. As in most engineering control systems, the design process for a stable system is usually by trial and error, and by sound judgement based on past experience. A theoretically rigorous method that absolutely guarantees stability is unlikely except for simple low order systems. One commonly used technique for stable design of single-input-single-output classical control systems is the lead compensation method. This technique is well known and treated in just about every text book on classical control theory and hence needs no further reiteration here. However, the use of extended lead compensation [or lag, or lead-lag] on multiple-input-multiple-output systems is not as straightforward as the single-input-single-output systems. In this chapter we shall endeavor to generalize the idea of lead-compensation into our very high order QDPS. Later simulation shows that, with appropriate design of the lead compensation network parameters, global stability of the system can indeed be achieved.

To understand the detailed mechanism involved, it is constructive to examine the stability of the pertinent scalar coupled system

$$\ddot{\xi} + \beta_i\dot{\xi} + \omega_i^2\xi = -\gamma_i\eta \tag{3.1.1}$$

$$\ddot{\eta} + \beta_a\dot{\eta} + \omega_a^2(\eta - \dot{\xi}) = 0 \tag{3.1.2}$$

via Bode Diagram analysis. The open loop transfer function of this system is

$$G_{OL}(S) = \frac{\gamma_i\omega_a^2 s}{(s^2+\beta_i s+\omega_i^2)(s^2+\beta_a s+\omega_a^2)} \tag{3.1.3}$$

the Bode plot of which (with typical parameters of ζ_n = 1%, γ_i= 0.2, ζ_a= 0.7, ω_a= 1.0) for various values of ω_i is shown in Fig. 3.1. The upper figure is a magnitude plot of

$$\log |G_{OL}(i\omega)| = \log\gamma_i\omega_a^2 + \log\omega - \log\left[(\omega_i^2-\omega^2)^2+(\beta_i\omega)^2\right]^{\frac{1}{2}} - \log\left[(\omega_a^2-\omega^2)^2+(\beta_a\omega)^2\right]^{\frac{1}{2}} \tag{3.1.4}$$

and the lower figure is a phase plot of

$$\angle G_{OL}(i\omega) = \frac{\pi}{2} - \tan^{-1}\frac{\beta_i\omega}{(\omega_i^2-\omega^2)} - \tan^{-1}\frac{\beta_a\omega}{(\omega_a^2-\omega^2)} \tag{3.1.5}$$

As ω_i increases past ω_a, the phase margin decreases from a positive value [stable] to a negative value [unstable] to non-existence [stable] one as shown by the following table :

Modal Frequency ω_i	Phase Margin	Stability
0.8	16^0	Stable
1.1	0^0	Critical
1.3	-7.3^0	Unstable
1.7	-10^0	Unstable
1.9	0^0	Critical
2.2	no cross over, P.M. does not exist	Stable

Table 3.1 Phase Margin of Different Frequency Modes

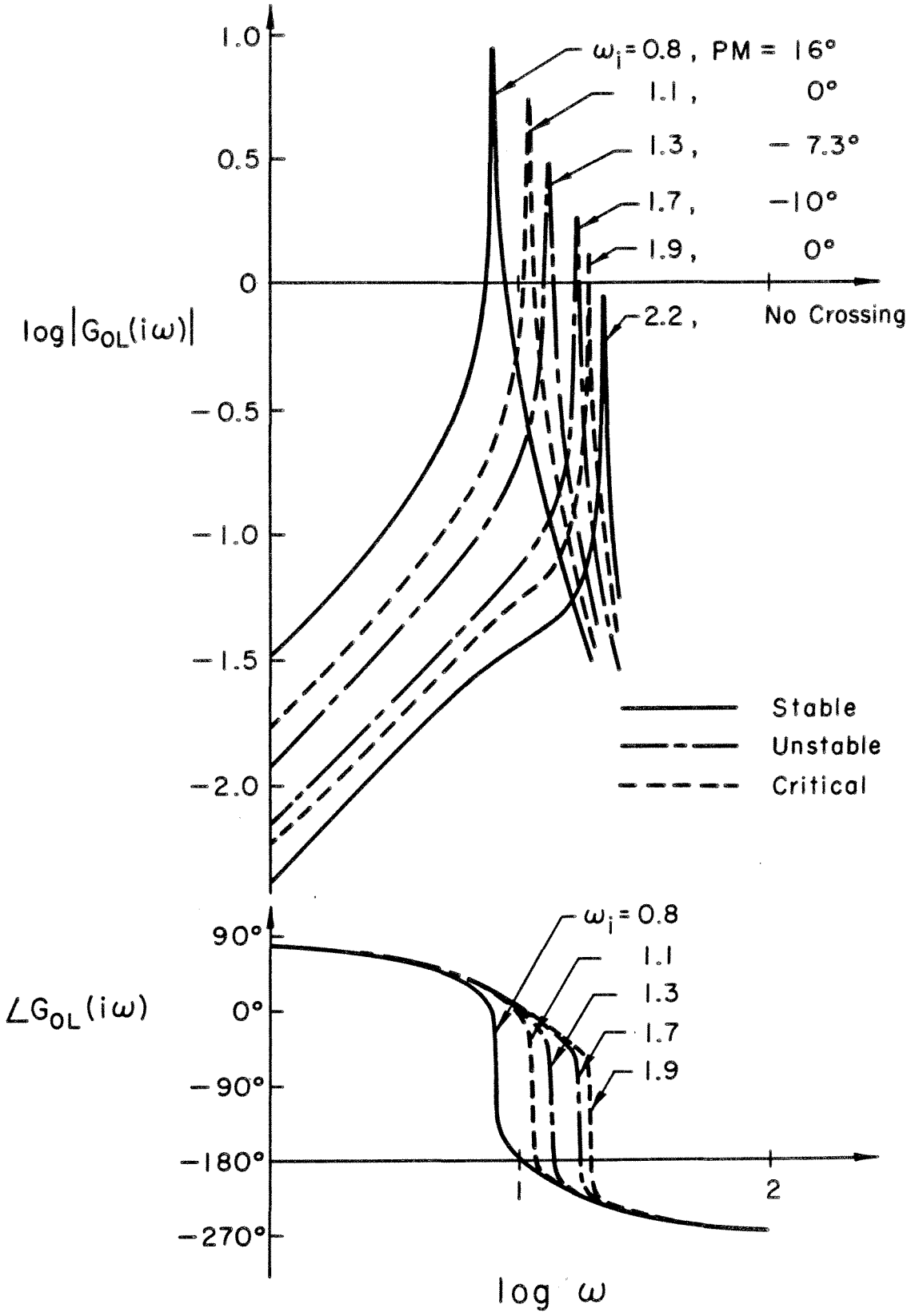

Fig. 3.1 Bode Diagram for Scalar Uncompensated System

$\gamma_i = 0.2$, $\omega_a = 1.0$, $\zeta_n = 0.01$, $\zeta_a = 0.7$

Hence the range $\omega_i \in [1.1, 1.9]$ corresponds to what we have referred to in Chapter 2 as the critical frequency range, and a comparison shows that this is consistent with the stability boundary of Fig. 2.3. The principle of lead compensation is to introduce into the uncompensated system a dynamical system which rectifies the instability by increasing the phase margin. A typical lead network has a transfer function given by

$$G_L(S) = \frac{1+T_2 S}{1+T_1 S}, \quad T_1 < T_2 \tag{3.1.6}$$

The compensated system is now described by

$$\text{system state} \qquad \ddot{\xi} + \beta_i \dot{\xi} + \omega_i^2 \xi = -\gamma_i \eta \tag{3.1.7}$$

$$\text{actuator state} \qquad \ddot{\eta} + \beta_a \dot{\eta} + \omega_a^2 (\eta - \dot{\rho}) = 0 \tag{3.1.8}$$

$$\text{lead compensator} \qquad T_1 \dot{\rho} + \rho = T_2 \dot{\xi} + \xi \tag{3.1.9}$$

with $\xi, \eta, \rho \in \mathbb{R}$. Even though this can be reduced to a 5^{th} order scalar system, and Nyquist plot technique can be used to establish conditions for stability on γ_i, T_1, T_2, the resulting expressions are highly complicated and are not likely to be of practical use. We shall only include them in Appendix B for completeness. The resulting open loop transfer function of the compensated system is now

$$G'_{OL}(S) = \frac{\gamma_i \omega_a^2 s(1+T_2 s)}{(1+T_1 s)(s^2+\beta_i s+\omega_i^2)(s^2+\beta_a s+\omega_a^2)} \tag{3.1.10}$$

As the system is linear, the Bode plot of the compensated system is just the algebraic sum of the Bode plot of the uncompensated system (Fig. 3.1) and the lead network. There remains the question of selecting T_1 and T_2 in (3.1.6) such that the phase margin of the compensated system

results in positive values. The lead network (see Fig. 3.2) has the feature that the magnitude increases at the frequency $1/T_2$ and levels off at $1/T_1$ and the corresponding phase increases below $1/T_2$ to a maximum value at $\omega_m = \sqrt{\frac{1}{T_1 T_2}}$ and reduces to zero again above $1/T_1$. As the unstable frequency range starts at about $\omega = \omega_a$, we note that the effect of setting $T_2 = \frac{1}{\omega_a}$ is to increase the phase of the Bode plot after $\omega = 1/T_2$. Since the system is highly resonant at $\omega = \omega_i$, the increase in magnitude due to lead compensation causes the cross-over frequency to change very little. If T_1 is chosen to be sufficiently small [$\frac{1}{T_1}$ sufficiently large] the phase increase at cross-over is sufficient to create a positive phase margin. To clarify the above argument, we shall present a typical unstable system ($\omega_i = 1.3$), before and after compensation, as shown in Fig 3.2. If the values of T_1 and T_2 are set at 0.1 and 1.0 respectively, the previous phase margin of -7.3^0 is now increased to 32^0. In fact this lead network can even stabilize any mode with frequency in the critical range.

Note in passing that the choice of T_1 and T_2 remains somewhat arbitrary; for example, if $T_1 = 0.2$ is used instead of $T_1 = 0.1$ in the previous case, the resulting phase characteristic is almost as good. Conceivably, an optimal choice of T_1 and T_2 may exist but will not be trivial to determine.

3.2 EXTENSION TO MULTIVARIATE SYSTEM

Since the inclusion of lead compensation in the coupled system/actuator dynamics alters the crossover frequency in the Bode Plot only slightly (due to the high resonance of the system), it essentially just raises the phase of the Bode Plot in the range of frequency between $1/T_1$ and $1/T_2$. If we choose T_1 and T_2 such that this

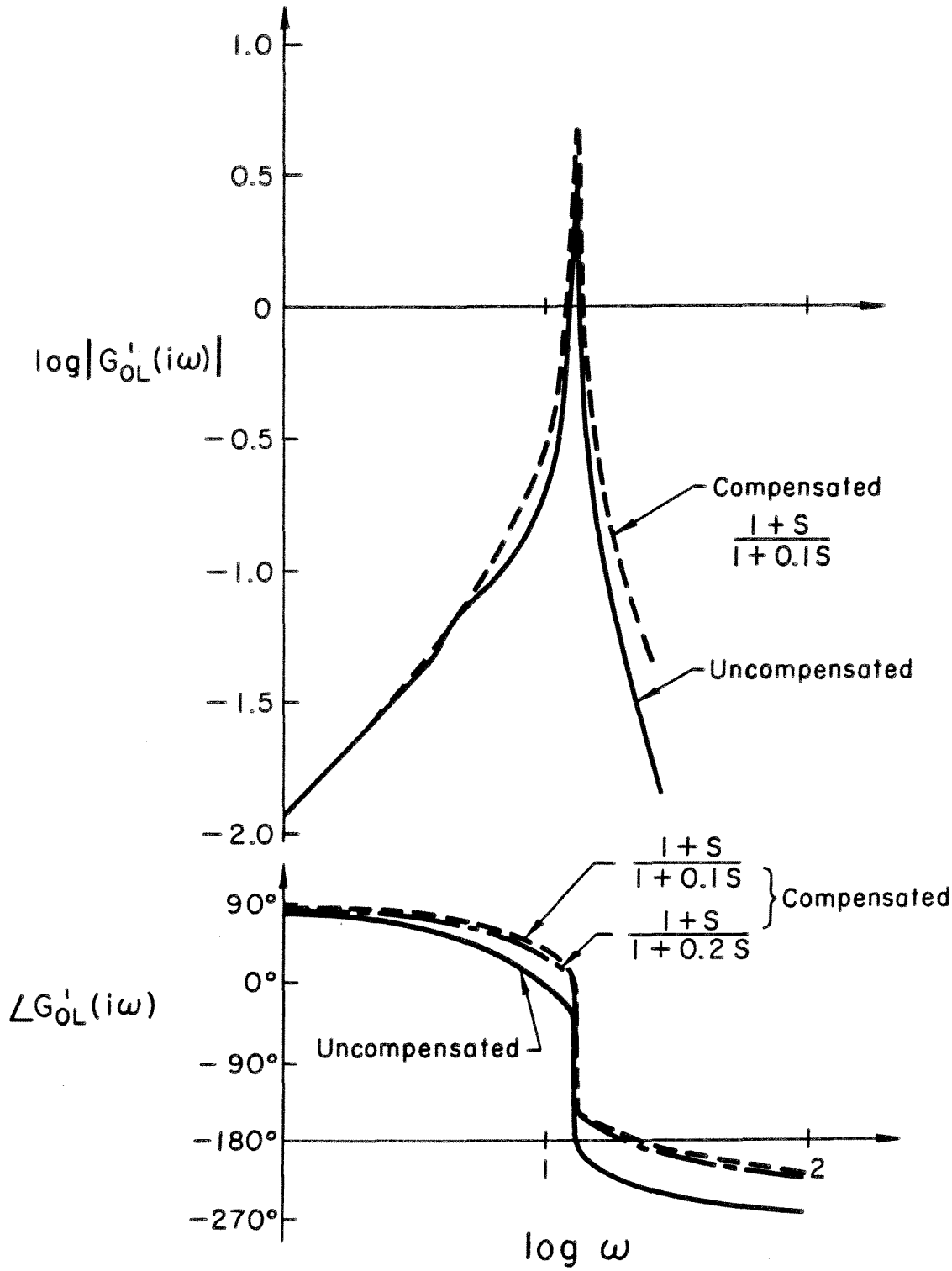

Fig. 3.2 Bode diagram for Scalar Compensated System

$\omega_a = 1.0$, $\zeta_n = 0.01$, $\zeta_a = 0.7$, $\gamma_i = 0.2$, $\omega_i = 1.3$

range covers the critical frequency range as discussed in Chapter 2, then hopefully those potentially unstable modes will be made stable without affecting the other modes very much. This is by no means a rigorous theoretical proof that guarantee stability but rather an educated and logical guess. The feasibility of this approach is confirmed by later simulation.

To generalize the idea of lead compensation into our present multivariate system, we introduce into the system (2.1.3) and (2.1.4) a lead network such that

$$\text{QDPS} \qquad M\ddot{y} + D\dot{y} + Ky = -S^T C u \tag{3.2.1}$$

$$\text{Actuator} \qquad \ddot{u} + \beta_a \dot{u} + \omega_a^2(u - \dot{\rho}) = 0 \tag{3.2.2}$$

$$\text{Lead compensator} \qquad T_1\dot{\rho} + \rho = T_2(S\dot{y}) + (Sy) \tag{3.2.3}$$

where $y \in \mathbb{R}^N$, $u, \rho \in \mathbb{R}^{N_A}$, $T_1, T_2 \in \mathbb{R}$. Equivalently, the modal form is given by ($y = \Phi\xi$)

$$\ddot{\xi} + \mathcal{D}\dot{\xi} + \Omega\xi = -\Phi^T S^T u \tag{3.2.4}$$

$$\ddot{u} + \beta_a \dot{u} + \omega_a^2(u - \dot{\rho}) = 0 \tag{3.2.5}$$

$$T_1\dot{\rho} + \rho = T_2(S\Phi\dot{\xi}) + (S\Phi\xi) \tag{3.2.6}$$

Note that even though the lead compensator has multiple inputs and multiple outputs, it is actually a system of identical systems since T_1 and T_2 are scalar. Conceivably, better performance can be achieved if T_1 and T_2 are extended to matrices. This again is not a trivial problem and would pose a promising research topic.

Chapter 4

ACTUATOR DYNAMICS SUPPRESSION BY GAP CREATION

4.1 INTRODUCTION

Basically the modes of the QDPS with actuator dynamics included (2.1.7) can be divided into three frequency ranges. The first N_1 modes are "Slow Modes", i.e. their frequencies are low compared to the actuators frequency ω_a. The modes that we wish to control are likely to lie within this range only. The next N_2 modes are "Critical Modes" which are vulnerable to instability since their frequencies are of comparable magnitude to ω_a. The last N_3 (such that $N_1+N_2+N_3 = N$, the total number of modes) modes are "Fast Modes" since their frequencies are well above ω_a. The system modal state vector and actuator state vector can thus be partitioned as ;

$$\xi = \begin{bmatrix} \xi_1 \\ \xi_2 \\ \xi_3 \end{bmatrix} \begin{matrix} \}N_1 \\ \}N_2 \\ \}N_3 \end{matrix} \qquad \eta = \begin{bmatrix} \eta_1 \\ \eta_2 \\ \eta_3 \end{bmatrix} \begin{matrix} \}N_1 \\ \}N_2 \\ \}N_3 \end{matrix}$$

It is thus conceivable that if the feedback of the critical modes is suppressed, then the overall system should be stable. One way to achieve this is to design the feedback such that the modal gain matrix B (in (2.1.7)) takes the form

$$B = \begin{array}{c} \overbrace{}^{N_1} \quad \overbrace{}^{N_2} \quad \overbrace{}^{N_3} \\ \left[\begin{array}{c|c|c} B_{11} & 0 & B_{13} \\ \hline B_{21} & 0 & B_{23} \\ \hline B_{31} & 0 & B_{33} \end{array}\right] \end{array} \begin{matrix} \}N_1 \\ \}N_2 \\ \}N_3 \end{matrix} \qquad (4.1.1)$$

Note that, unless $B_{21} = B_{23} = 0$, the gain matrix is non-symmetric.

Intuitively since the scalar gains (diagonal elements of $\mathcal{B}$) for the critical modes ξ_2 are zero, they must be stable to first order perturbations. (In fact, they will be only naturally damped.) A rigorous proof using the K-K lemma is possible, but it will tend to assume an unnecessarily large gap, i.e. an over-restrictive condition. Now that $\mathcal{B}$ is not positive semi-definite, some of the diagonal elements of $\mathcal{B}_{33}$ may become negative but this is not undesirable, as this causes a higher than natural damping for the uncontrolled modes as shown in Chapter 2.

In this chapter we shall consider three different methods to create the "gap" in the modal gain matrix $\mathcal{B}$, as in (4.1.1). The requirements on sensors and actuators and the computational complexity vary; the preferred technique will depend on the particular application.

4.2 GAP CREATION BY COLLOCATED CONTROL

The simplest but somewhat wasteful method is when a large number of collocated sensors and actuators are available. Let N_S and N_A denote the numbers of sensors and actuators respectively, with $N_S = N_A$, $N_A = N_1 + N_2$, we can let

$$N_1 + N_2 \left\{ \left[\begin{array}{c|c} \mathcal{B}_{11} & \mathcal{B}_{12} \\ \hline \mathcal{B}_{21} & \mathcal{B}_{22} \end{array}\right] = \left[\begin{array}{c|c} \begin{matrix} \gamma_1 & & 0 \\ & \gamma_2 & \\ 0 & & \gamma_{N_1} \end{matrix} & \begin{matrix} 0 \\ \\ 0 \end{matrix} \\ \hline \underbrace{\begin{matrix} 0 & \cdots & 0 \end{matrix}}_{N_1} & \underbrace{0}_{N_2} \end{array}\right] \begin{matrix} \} N_1 \\ \} N_2 \end{matrix} \right. \tag{4.2.1}$$

Hence if we partition the modal matrix Φ as

$$\Phi = \underbrace{[\Phi_1}_{N_1} \; \underbrace{\Phi_2}_{N_2} \; \underbrace{\Phi_3]}_{N_3} \tag{4.2.2}$$

then the gain matrix C ($\in \mathbb{R}^{N_1+N_2}$) is given by

$$C = [S\Phi_1 \mid S\Phi_2]^{-T} \left[\begin{array}{c|c} \begin{matrix} \gamma_1 & & \\ & \gamma_2 & \\ & & \ddots \gamma_{N_1} \end{matrix} & 0 \\ \hline 0 & 0 \end{array}\right] [S\Phi_1 \mid S\Phi_2]^{-1} \qquad (4.2.3)$$

assuming that the appropriate non-singularity condition holds. Correspondingly, the modal gain matrix remains symmetric and positive semi-definite and is given by

$$B = \Phi^T S^T C S \Phi = \left[\begin{array}{c|c|c} \begin{matrix} \gamma_1 & & \\ & \ddots & \\ & & \gamma_{N_1} \end{matrix} & 0 & B_{13} \\ \hline 0 & 0 & 0 \\ \hline B_{13}^T & 0 & B_{33} \end{array}\right] \qquad (4.2.4)$$

Note that in this case the modes in ξ_2 are completely decoupled from the modes in ξ_1 and ξ_3 and there is no feedback on each mode in ξ_2 Hence, if the gap is designed appropriately the overall system is guaranteed to be stable. This method nevertheless suffers from the disadvantage that a very large number of sensors and actuators are needed, which may not be permitted in practice.

4.3 GAP CREATION BY THE USE OF Θ_S^{-1} FILTER

In general, sensors are lighter, cheaper and possess much higher bandwidth than actuators; hence, more can be employed. Suppose we have N_S sensors and N_A actuators ($N_S > N_A$) with corresponding location matrices S_S($\in \mathbb{N}^{N_S \times N}$) and S_A($\in \mathbb{N}^{N_A \times N}$), respectively, with $N_A = N_1$ and $N_S - N_A = N_2$ = the number of suppressed modes. Some of the sensors and actuators may still be collocated but since $N_S > N_A$, the modal gain matrix is necessarily nonsymmetric. The motivation for the fancy terminology of "θ_S^{-1} Filter" will become obvious later, as we present the synthesis of the

feedback in the following systematic way:

(i) The state (rate) of the system is picked up by the sensor

$$S_s\dot{y} = S_s\Phi\dot{\xi} = N_S\{[\overbrace{\Theta_S}^{N_S=N_1+N_2} \mid \overbrace{\Theta_3}^{N_3}] \begin{bmatrix} \dot{\xi}_1 \\ \hline \dot{\xi}_2 \\ \hline \dot{\xi}_3 \end{bmatrix} \begin{matrix} \} N_A \\ \} N_2 \\ \} N_3 \end{matrix} \tag{4.3.1}$$

where $$\Theta_S = [\overbrace{S_s\Phi_1}^{N_1=N_A} \mid \overbrace{S_s\Phi_2}^{N_2}] \tag{4.3.2}$$

and $$\Theta_3 = [\overbrace{S_s\Phi_3}^{N_3}] \tag{4.3.3}$$

(ii) The sensor input $S_s\dot{y}$ is pre-multiplied by Θ_S^{-1} to obtain $\hat{\dot{\xi}}(\in \mathbb{R}^{N_S})$

$$\hat{\dot{\xi}} = \Theta_S^{-1}S_s\dot{y} = [\, I_{N_S} \mid \Theta_S^{-1}\Theta_3 \,] \begin{bmatrix} \dot{\xi}_1 \\ \hline \dot{\xi}_2 \\ \hline \dot{\xi}_3 \end{bmatrix}$$

$$= \begin{bmatrix} \dot{\xi}_1 \\ \hline \dot{\xi}_2 \end{bmatrix} + \Theta_S^{-1}\Theta_3\dot{\xi}_3 \tag{4.3.4}$$

(iii) $\hat{\dot{\xi}}$ is pre-multiplied by a control gain matrix $C(\in \mathbb{R}^{N_A \times N_S})$ to obtain the control force $f(\in \mathbb{R}^{N_A})$, where

$$C = \underbrace{[\, C_1}_{N_A} \mid \underbrace{0\,]}_{N_2} \} N_A \tag{4.3.5}$$

such that $$f = C\hat{\dot{\xi}} = C_1\dot{\xi}_1 + C\,\Theta_S^{-1}\Theta_3\dot{\xi}_3 \tag{4.3.6}$$

and we see immediately that the control force is independent of the modes in $\dot{\xi}_2$.

(iv) The modal gain matrix is thus given by

$$\mathcal{B} = \Phi^T S_A^T C \Theta_S^{-1} S_S \Phi$$

$$= \left[\begin{array}{c|c|c} \Theta_{A_1}^T C_1 & 0 & \Theta_{A_1}^T C\, \Theta_S^{-1}\Theta_3 \\ \hline \Theta_{A_2}^T C_2 & 0 & \Theta_{A_2}^T C\, \Theta_S^{-1}\Theta_3 \\ \hline \Theta_{A_3}^T C_3 & 0 & \Theta_{A_3}^T C\, \Theta_S^{-1}\Theta_3 \end{array}\right] \qquad (4.3.7)$$

where $\Theta_A = S_A\Phi = N_1\{[\underbrace{\Theta_{A_1}}_{N_1} | \underbrace{\Theta_{A_2}}_{N_2} | \underbrace{\Theta_{A_3}}_{N_3}]$ (4.3.8)

Hence if the first $N_1 x N_1$ block of $\mathcal{B}$ is prescribed as

$$\mathcal{B}_{11} = \begin{bmatrix} \gamma_1 & & 0 \\ & \ddots & \\ 0 & & \gamma_{N_1} \end{bmatrix} \qquad (4.3.9)$$

then $C_1 = (\Theta_{A_1})^{-T}\, \mathcal{B}_{11}$ (4.3.10)

and the remaining portions of $\mathcal{B}$ are by-products of such a prescription. Note that the synthesis of C (or C_1) and the Θ_S^{-1} filter only requires the knowledge of the first N_S modes and is independent of all higher modes, which are rather uncertain in practice. Computationally, this method requires the inversion of an $N_S x N_S$ matrix (Θ_S) and an $N_A x N_A$ matrix (Θ_{A_1}). When N_S is large, it may be desirable to seek an alternative approach.

4.4 GAP CREATION BY THE USE OF P FILTER

A slightly more complicated gap creation technique is made possible again by using more sensors (N_S) than actuators (N_A); it is called the P filter. The synthesis of the feedback is as follows:

(i) As in the Θ_S^{-1} filter case, the state (rate) of the system is picked up by the sensors

$$S_S\dot{y} = S_S\Phi\dot{\xi} \tag{4.4.1}$$

(ii) An estimated full modal state $\hat{\dot{\xi}} \in \mathbb{R}^N$ is obtained by pre-multiplying the sensor output $S_S\dot{X}$ by an appropriate constant matrix $H(\in \mathbb{R}^{NxN_S})$. The choice of H remains somewhat arbitrary, but we would like $\hat{\dot{\xi}}$ to be as close as possible to the real state $\dot{\xi}$. One way of constructing H is by modal filtering [9], through the use of the Lagrange interpolation formula. The algebra is fairly involved, so we shall include it in Appendix C. Assuming that such a matrix H can be constructed, then

$$\hat{\dot{\xi}} = G\,\dot{\xi} \tag{4.4.2}$$

where
$$G = H\,S_S\Phi = \begin{matrix} \\ N_1 \\ N_2 \\ N_3 \end{matrix}\begin{matrix} \overbrace{\phantom{G_{11}}}^{N_1} & \overbrace{\phantom{G_{12}}}^{N_2} & \overbrace{\phantom{G_{13}}}^{N_3} \end{matrix}\begin{bmatrix} G_{11} & G_{12} & G_{13} \\ G_{21} & G_{22} & G_{23} \\ G_{31} & G_{32} & G_{33} \end{bmatrix} \tag{4.4.3}$$

Thus the purpose of modal filtering is to make G as close to the identity matrix as possible; exact identity is possible only when the same number of sensors as states are used, i.e., $S_S = I_N$ or some permutation of I_N.

(iii) Define the P filter as the N_1xN matrix

$$P = \begin{matrix} \\ N_1 \end{matrix}\begin{matrix} \overbrace{\phantom{I_{N_1}}}^{N_1} & \overbrace{\phantom{-G_{12}G_{22}^{-1}}}^{N_2} & \overbrace{}^{N_3} \end{matrix}\begin{bmatrix} I_{N_1} & -G_{12}G_{22}^{-1} & 0 \end{bmatrix} \tag{4.4.4}$$

so that pre-multiplication of $\dot{\hat{\xi}}$ by P gives

$$P\dot{\hat{\xi}} = P\,G\dot{\xi} = N_1\{[\overbrace{G_{11} - G_{12}G_{22}^{-1}G_{21}}^{N_1}|\overbrace{0}^{N_2}|\overbrace{G_{13} - G_{12}G_{22}^{-1}G_{23}}^{N_3}]\,\dot{\xi} \tag{4.4.5}$$

(iv) The control force $f(\in \mathbb{R}^{N_1})$ is obtained by pre-multiplying $P\dot{\hat{\xi}}$ by $C(\in \mathbb{R}^{N_1 \times N_1})$

$$f = CP\dot{\hat{\xi}} = CPG\dot{\xi} \tag{4.4.6}$$

(v) Finally the modal gain matrix $\mathcal{B}$ is given by

$$\begin{aligned}
\mathcal{B} &= \Phi^T S_A^T CPG \\
&= \begin{bmatrix} \Phi_1^T S_A^T \\ \hline \Phi_2^T S_A^T \\ \hline \Phi_3^T S_A^T \end{bmatrix} [C(G_{11} - G_{12}G_{22}^{-1}G_{21}) \mid 0 \mid C(G_{13} - G_{12}G_{22}^{-1}G_{23})] \\
&= \begin{bmatrix} \Phi_1^T S_A^T\, C(G_{11} - G_{12}G_{22}^{-1}G_{21}) \mid 0 \mid \Phi_1^T S_A^T\, C(G_{13} - G_{12}G_{22}^{-1}G_{23}) \\ \Phi_2^T S_A^T\, C(G_{11} - G_{12}G_{22}^{-1}G_{21}) \mid 0 \mid \Phi_2^T S_A^T\, C(G_{13} - G_{12}G_{22}^{-1}G_{23}) \\ \Phi_3^T S_A^T\, C(G_{11} - G_{12}G_{22}^{-1}G_{21}) \mid 0 \mid \Phi_3^T S_A^T\, C(G_{13} - G_{12}G_{22}^{-1}G_{23}) \end{bmatrix}
\end{aligned} \tag{4.4.7}$$

so that if $\mathcal{B}_{11} = \Phi_1^T S_A^T\, C(G_{11} - G_{12}G_{22}^{-1}G_{21}) = \text{diag}\,(\gamma_i)$ (4.4.8)

then $C = (S_A\Phi_1)^{-T}\mathcal{B}_{11}(G_{11} - G_{12}G_{22}^{-1}G_{21})^{-1}$ (4.4.9)

Note that in practice, we only need to calculate the first $N_S \times N_S$ subblock of G, (i.e. $\begin{bmatrix} G_{11} & G_{12} \\ G_{21} & G_{22} \end{bmatrix}$) which requires knowledge of only the first N_S modes. The rest of G need not be computed and, hence, we need not know anything about the higher modes. Also we have assumed that G_{22} and $G_{11} - G_{12}G_{22}^{-1}G_{21}$ are non-singular. A sufficient and necessary condition

for this is that $G' = \begin{bmatrix} G_{11} & G_{12} \\ G_{21} & G_{22} \end{bmatrix}$ be non-singular since

$$\det G' = \det \begin{bmatrix} G_{11} & G_{12} \\ G_{21} & G_{22} \end{bmatrix} = \det(G_{22}) \det (G_{11} - G_{12}G_{22}^{-1}G_{21}) \neq 0 \quad (4.4.10)$$

This condition can be shown to relate to some controllability and observability conditions . In general, if we have a sufficient number of sensors and actuators well spread out over the system and located away from the nodes of the controlled modes, then the non-singularity of these matrices should be well assured.

In this method, the matrices that need inversion are G_{22}, $(\Phi_1^T S_A^T)$ and $(G_{11} - G_{12}G_{22}^{-1}G_{21})$, of rank $N_S - N_A$ $(=N_2)$, N_A $(=N_1)$ and N_A respectively. In the case when N_S and N_A are both large and $N_S - N_A$ is relatively small, the computational effort required can be substantially less than in the previous case.

Chapter 5

POSITIVE POSITION FEEDBACK CONTROL WITH TUNING FILTERS

5.1 SCALAR THEORY: STABILITY ANALYSIS

In order to understand the mechanics of position feedback, it is constructive to examine first the pertinent scalar system that approximates the dynamics of the i^{th} mode. This mode can be expressed as (with subscripts suppressed from ξ_i, η_i, γ_i)

$$\text{system} \quad \ddot{\xi} + \beta_i\dot{\xi} + \omega_i^2(\xi - \gamma\eta) = 0 \tag{5.1.1}$$

$$\text{actuator} \quad \ddot{\eta} + \beta_a\dot{\eta} + \omega_a^2(\eta - \xi) = 0 \tag{5.1.2}$$

$$\xi,\eta \in \mathbb{R}\,, \quad \gamma > 0$$

The meaning of positive position feedback is obvious from these equations.

Theorem 5.1

The combined system and actuator dynamics of (5.1.1) and (5.1.2) are Liapunov asymptotic stable iff $\gamma < 1$. (Also serves as the stability boundary.)

Proof: The closed loop characteristic equation for (5.1.1) and (5.1.2) is

$$(s^2 + \beta_i s + \omega_i^2)(s^2 + \beta_a s + \omega_a^2) - \gamma\omega_a^2\omega_i^2 = 0 \tag{5.1.3}$$

or $s^4 + (\beta_i + \beta_a)s^3 + (\omega_i^2 + \omega_a^2 + \beta_i\beta_a)s^2 + (\beta_i\omega_a^2 + \beta_a\omega_i^2)s +$

$$+ \omega_i^2\omega_a^2(1 - \gamma) = 0 \tag{5.1.4}$$

A sufficient and necessary condition for stability is that all the principal minors of the corresponding Routh-Hurwitz array be greater

than zero. The principal minors of (5.1.4) can be easily shown to be

$$M_1 = \beta_i + \beta_a$$

$$M_2 = \beta_i\omega_i^2 + \beta_a\omega_a^2 + \beta_a\beta_i(\beta_i + \beta_a)$$

$$M_3 = \beta_i\beta_a\,[(\omega_i^2 - \omega_a^2)^2 + (\beta_i + \beta_a)(\beta_i\omega_a^2 + \beta_a\omega_i^2)] + \gamma(\beta_i + \beta_a)^2\omega_i^2\omega_a^2$$

$$M_4 = \omega_i^2\omega_a^2(1 - \gamma)M_3$$

Thus for positive γ, M_1 , M_2 & M_3 are unconditionally positive. M_4 is positive iff $\gamma < 1$, and the proof is complete. □

It may be interesting to find out how instability would take place if γ exceeds 1. Three possible cases of root-locus diagrams depending on the relative distance of the open loop poles from the real axis are shown in Fig. 5.1. If $\omega_a\sqrt{1 - \zeta_a^2} < \omega_i\sqrt{1 - \zeta_n^2}$, it is the actuator that becomes unstable, whereas if $\omega_a\sqrt{1 - \zeta_a^2} > \omega_i\sqrt{1 - \zeta_n^2}$, then it is the system that becomes unstable. In the critical case where $\omega_a\sqrt{1 - \zeta_a^2} = \omega_i\sqrt{1 - \zeta_n^2}$ the root loci coalesce to form a symmetrical pattern, and either case is possible. Furthermore, the unstable pole always appears as a real root of the characteristic equation (5.1.4). Note in passing that the variable γ in (5.1.1) is a dimensionless variable and the actual gain should be $\omega_i^2\gamma$.

In contrast to the velocity feedback case, the present stability boundary is very simple indeed. Our main concern is : subject to this upper bound on the gain, can we achieve good closed loop damping characteristics?

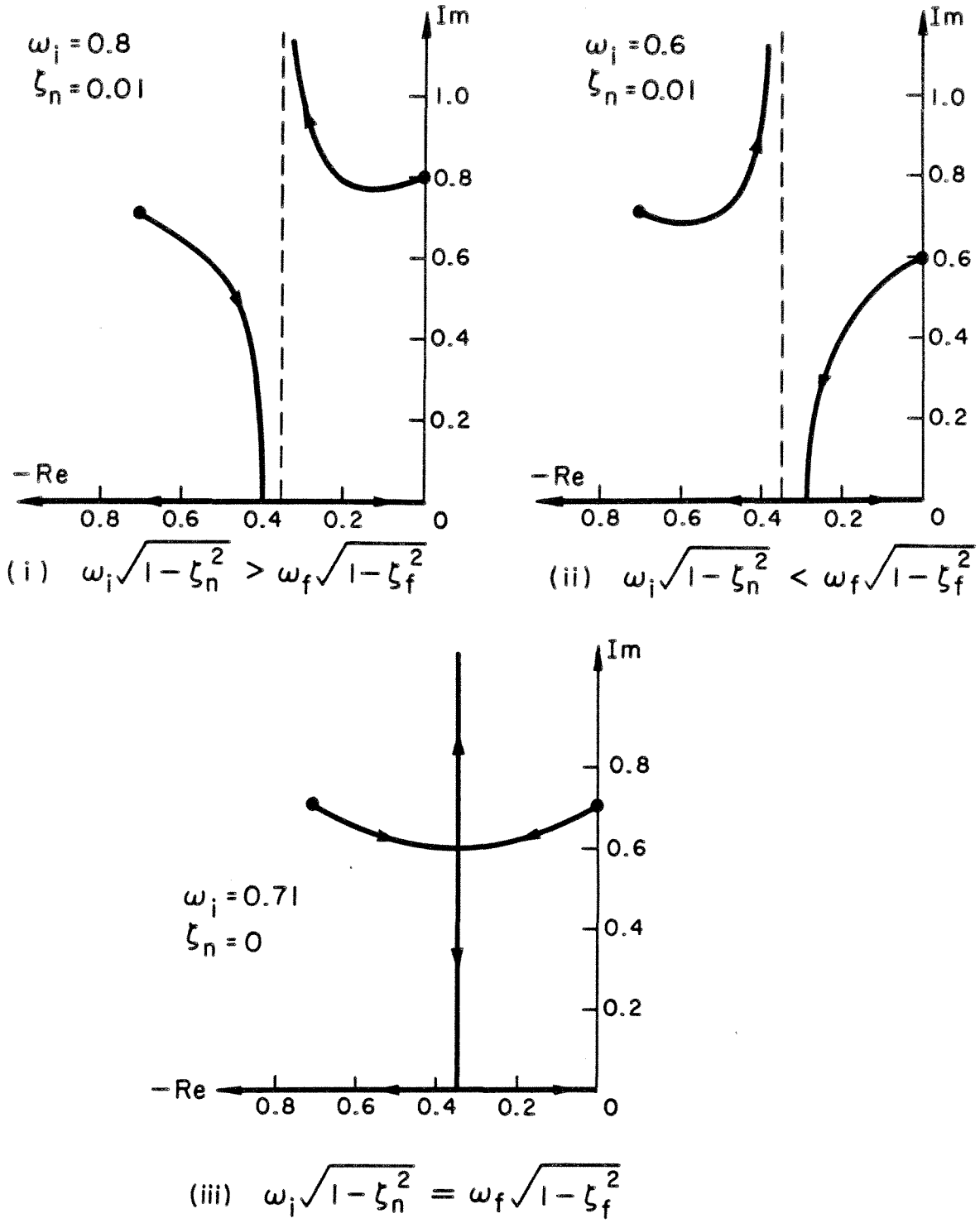

Fig. 5.1 Root Locus Diagram of Scalar Position Feedback System with $\omega_f = 1.0$, $\zeta_f = 0.71$. Note that the subscript f is interchangeable with a.

5.2 CLOSED LOOP DAMPING CHARACTERISTICS OF SCALAR POSITION FEEDBACK CONTROL SYSTEM

To examine the closed loop damping characteristics of the system (5.1.1) and (5.1.2), we compute the roots of its characteristic equation (5.1.4) for fixed γ and plot the negative of the real part of the roots against the frequency ω_i, as shown in Fig. 5.2. The characteristics consist of 2 branches, upper and lower. For sufficiently large γ ($\gtrsim 0.25$), the 2 branches meet at a cusp which we shall examine again later. From Fig.5.1, it is obvious that the upper branch represents the actuator and the lower branch represents the system. For the sake of argument, however, we shall carry out some asymptotic analysis.

For $\omega_i << 1$, (5.1.3) approximately reduces to

$$s^2(s^2 + \beta_a s + \omega_a^2) = 0 \tag{5.2.1}$$

Hence if λ_j, $j = 1,\ldots,4$ are the roots, the plot of $-Re(\lambda_j)$ vs ω_i must necessarily start from $(0,0)$ for the system and $(0,\zeta_a\omega_a)$ for the actuator. On the other hand for $\omega_i >> 1$, (5.1.3) can be approximated by

$$(s^2 + \beta_i s + \omega_i^2(1-\gamma))(s^2 + \beta_a s + \omega_a^2) = 0 \tag{5.2.2}$$

from which we can immediately deduce the asymptotic behaviors

$$\text{for system} \quad \lim_{\omega_i \to \infty} - Re(\lambda_j) = \zeta_n \omega_i \tag{5.2.3}$$

$$\text{for actuator} \quad \lim_{\omega_i \to \infty} - Re(\lambda_j) = \zeta_a \omega_a \tag{5.2.4}$$

Hence, the upper and lower branches approach the asymptote, as shown in Fig. 5.2. From the same figure we note the following:

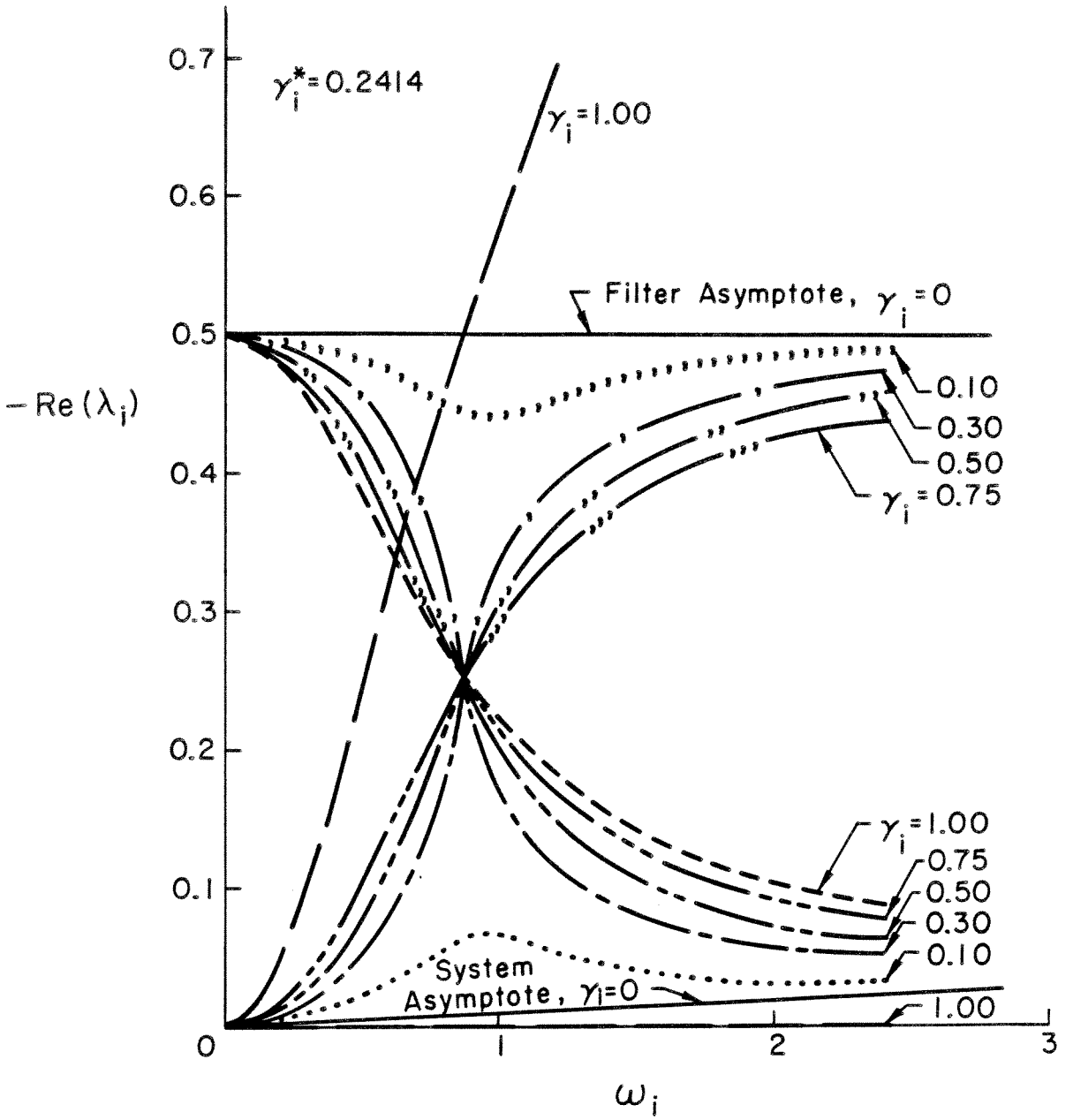

Fig. 5.2 Closed Loop Damping Characteristics

$\zeta_a = 0.5$, $\zeta_n = 0.01$, $\omega_a = 1.0$

(i) For γ lower than a threshold value γ^*(which we will derive in § 5.5)the lower (system) branch exhibits a resonance peak near ω_a and moves to the left as γ increases.

(ii) As γ increases past the threshold value γ^*, the upper and lower branches meet at a cusp; hence, the closed loop damping of the system cannot increase beyond this point. This corresponds to the degenerate situation in Fig. 5.1 (iii). The characteristic to the left of the cusp corresponds to the situation in Fig. 5.1 (ii), and the characteristic to the right of the cusp corresponds to the situation in Fig. 5.1 (i). The frequency at which the cusp occurs can be shown to be

$$\omega_i = \omega_a \frac{\sqrt{1-\zeta_a^2}}{\sqrt{1-\zeta_n^2}} \simeq \omega_a \sqrt{1 - \zeta_a^2} \quad \text{since } \zeta_n^2 << 1 \tag{5.2.5}$$

and the maximum closed loop damping achievable at this cusp is

$$\text{Max } (- \text{Re}(\lambda_i)) = \frac{1}{2} (\zeta_n \omega_i + \zeta_a \omega_a) \tag{5.2.6}$$

We shall defer the derivation of these expressions to § 5.5. It is thus obvious that the best closed loop damping characteristics are achieved in the critical situation (Fig. 5.1 (iii)),when (5.2.5) holds; and maximum closed loop damping (5.2.6) is achieved for all γ exceeding the threshold γ^*, but less than another threshold γ^{**}.

(iii) For $\gamma > \gamma^{**}$ some branches bifurcate into two branches which corresponds to the degeneration into two real roots in the root locus diagram. We should try to avoid this situation by keeping γ low; otherwise,one root will be less stable than the other.

We shall examine the closed loop damping characteristics in detail again in § 5.5 when we attempt to design a procedure for selecting the system parameters.

5.3 MULTIVARIATE THEORY: STABILITY ANALYSIS

Having understood the scalar system, the idea of position feedback can be easily generalized into the multivariate system. The equations governing position feedback (collocated actuators and sensors) control of a QDPS with actuator dynamics are given by

$$M\ddot{y} + D\dot{y} + Ky = S^T C u \tag{5.3.1}$$
$$\ddot{u} + \beta_a \dot{u} + \omega_a^2(u - S y) = 0$$

where $y \in \mathbb{R}^N$ is the system state vector and $u \in \mathbb{R}^{N_A}$ the actuator state vector. The $N_A \times N_A$ gain matrix C is positive definite and can be factorized, using its square root $C^{\frac{1}{2}}$ as follows:

$$C^{T/2}\, C^{1/2} = C \tag{5.3.2}$$

The modal form of the system is obtained by applying the following transformation

$$y = \Phi\xi \tag{5.3.3}$$

$$\eta = \frac{1}{\omega_a} C^{\frac{1}{2}} u \tag{5.3.4}$$

so that

$$\ddot{\xi} + \mathcal{D}\dot{\xi} + \Omega\xi = \omega_a \Phi^T S^T C^{T/2} \eta \tag{5.3.5}$$

$$\ddot{\eta} + \beta_a \dot{\eta} + \omega_a^2 \eta = \omega_a C^{\frac{1}{2}} S\, \Phi\xi \tag{5.3.6}$$

or
$$\begin{bmatrix} \ddot{\xi} \\ \ddot{\eta} \end{bmatrix} + \begin{bmatrix} \mathcal{D} & 0 \\ 0 & \beta_a I_{N_A} \end{bmatrix} \begin{bmatrix} \dot{\xi} \\ \dot{\eta} \end{bmatrix} + \begin{bmatrix} \Omega & -\omega_a \Phi^T S^T C^{T/2} \\ -\omega_a C^{\frac{1}{2}} S\Phi & \omega_a^2 I_{N_A} \end{bmatrix} \begin{bmatrix} \xi \\ \eta \end{bmatrix} = 0 \tag{5.3.7}$$

Theorem 5.2

The combined system and actuator dynamics as represented by (5.3.7) are Liapunov Asymptotic Stable if

$$\Omega - (1+\varepsilon)B \text{ is positive definite} \tag{5.3.8}$$

where ε is some arbitrarily small positive quantity and B is the modal gain matrix given by

$$B = \Phi^T S^T C S \Phi \tag{5.3.9}$$

Proof: Define the Liapunov function V as

$$V = \frac{1}{2}\begin{bmatrix}\dot{\xi}^T & \dot{\eta}^T\end{bmatrix}\begin{bmatrix}\dot{\xi}\\ \dot{\eta}\end{bmatrix} + \frac{1}{2}\begin{bmatrix}\xi^T & \eta^T\end{bmatrix}\begin{bmatrix}\Omega & -\omega_a B^{T/2}\\ -\omega_a B^{\frac{1}{2}} & \omega_a^2 I_{N_A}\end{bmatrix}\begin{bmatrix}\xi\\ \eta\end{bmatrix} \tag{5.3.10}$$

where $$B^{\frac{1}{2}} = C^{\frac{1}{2}} S\Phi \tag{5.3.11}$$

(5.3.10) is equivalent to

$$V = \frac{1}{2}\dot{\xi}^T\dot{\xi} + \frac{1}{2}\dot{\eta}^T\dot{\eta} + \frac{1}{2}\left[\xi^T\Omega\xi + \omega_a^2\eta^T\eta - 2\omega_a\eta^T B^{\frac{1}{2}}\xi\right] \tag{5.3.12}$$

where the last term can be expressed by the Cauchy-Schwartz Inequality as

$$2\omega_a\eta^T B^{\frac{1}{2}}\xi = \frac{2\omega_a}{\sqrt{1+\varepsilon}}\,\eta^T \cdot \sqrt{1+\varepsilon}\, B^{\frac{1}{2}}\xi \;,\quad 0 < \varepsilon << 1$$

$$< \frac{\omega_a^2}{(1+\varepsilon)}\eta^T\eta + (1+\varepsilon)\,\xi^T B\xi \tag{5.3.13}$$

Hence $$V > \frac{1}{2}\dot{\xi}^T\dot{\xi} + \frac{1}{2}\dot{\eta}^T\dot{\eta} + \frac{1}{2}\left(\xi^T(\Omega - (1+\varepsilon)B)\xi + \frac{\omega_a^2\varepsilon}{1+\varepsilon}\eta^T\eta\right) \tag{5.3.14}$$

so that if the assumption (5.3.8) holds, V is positive definite for all non-trivial ξ and η. Differentiating V with respect to t yields

$$\dot{V} = -(\dot{\xi}^T \dot{\eta}^T) \begin{bmatrix} D & 0 \\ 0 & \beta_a I_{N_A} \end{bmatrix} \begin{bmatrix} \dot{\xi} \\ \dot{\eta} \end{bmatrix} \tag{5.3.15}$$

Although $\dot{V}$ in (5.3.15) appears to be only negative semi-definite, it is actually negative definite. $\dot{V} = 0$ if $\begin{bmatrix} \dot{\xi} \\ \dot{\eta} \end{bmatrix} = 0$, but if $\begin{bmatrix} \xi \\ \eta \end{bmatrix} \neq 0$, then $\begin{bmatrix} \ddot{\xi} \\ \ddot{\eta} \end{bmatrix} \neq 0$. Consequently, $\begin{bmatrix} \dot{\xi} \\ \dot{\eta} \end{bmatrix}$ can only be zero momentarily; thus, $\dot{V}$ takes on the value zero only on a set t of measure zero. The proof is thus made complete by invoking the well-known Liapunov theorem. □

Even though Theorem 5.2 is only a sufficient condition, it is minimally restrictive [i.e., close to being sufficient and necessary]. A sufficient and necessary condition can be obtained from the following theorem.

Theorem 5.3

For a second order multivariate dynamical system described by

$$I\ddot{Z} + Q\dot{Z} + PZ = 0 \tag{5.3.16}$$

where Z, Q, P are of appropriate dimension and Q is positive definite, a sufficient and necessary condition for Liapunov asymptotic stability is that

$$P \text{ is positive definite} \tag{5.3.17}$$

Proof: To prove sufficiency, define the following Liapunov function

$$V = \frac{1}{2}(Z^T \dot{Z}^T)\begin{bmatrix} P + \delta Q & \delta I \\ \delta I & I \end{bmatrix}\begin{bmatrix} Z \\ \dot{Z} \end{bmatrix} \tag{5.3.18}$$

$$= \frac{1}{2}[\delta Z^T(Q - \delta I)Z + (\dot{Z} + \delta Z)^T(\dot{Z} + \delta Z) + Z^T P Z] > 0$$

where 2δ = smallest eigenvalue of Q. The time derivatives of V is given by

$$\dot{V} = -\dot{Z}^T[Q - \delta I]\dot{Z} - \delta Z^T P Z \ . \tag{5.3.19}$$

Hence, if P is positive definite, V is strictly less than zero and hence the system is LAS. To prove the reverse [i.e., P nonpositive definite $\Rightarrow$ unstable], we define another indefinite Liapunov function

$$V = Z^T\dot{Z} + \frac{1}{2} Z^T Q Z \lesseqgtr 0 \tag{5.3.20}$$

the time derivative of which is given by

$$\dot{V} = \dot{Z}^T\dot{Z} - Z^T P Z \ . \tag{5.3.21}$$

Define the Hamiltonian H of the system to be

$$H = \dot{Z}^T\dot{Z} + Z^T P Z \tag{5.3.22}$$

so that $$\dot{V} = 2\dot{Z}^T\dot{Z} - H \tag{5.3.23}$$

the time derivative of H is

$$\dot{H} = 2\dot{Z}^T\ddot{Z} + 2Z^T P\dot{Z} = -2\dot{Z}^T Q\dot{Z} \leq 0 \tag{5.3.24}$$

Thus if P is not positive definite, we can always find $Z(0)$ and $\dot{Z}(0)$ such that $H(0)$ in (5.3.22) is negative, and $V(0)$ in (5.3.20) is positive.

Hence $H(t) < 0 \quad \forall \quad t$, and as a result $\dot{V}(t) > 0 \; \forall \; t$, and the system is unstable by the 3rd theorem of Liapunov. □

The following theorem is thus a direct consequence of theorem (5.3).

Theorem 5.4

The system in (5.3.7) is LAS iff the modified stiffness matrix

$$P = \begin{bmatrix} \Omega & -\omega_a \Phi^T S^T C^{T/2} \\ -\omega_a C^{\frac{1}{2}} S \Phi & \omega_a^2 I_{N_A} \end{bmatrix} \text{ is positive definite} \qquad (5.3.25)$$

Note that the sufficient condition for stability (5.3.8) is equivalent to

$$K - (1+\varepsilon)\, S^T C S \quad \text{is positive definite} \; . \qquad (5.3.26)$$

We shall see in the next section that this is difficult to satisfy if high closed loop damping is desired for every controlled model.

5.4 DAMPING ENHANCEMENT WITH THE USE OF TUNING FILTERS

Even though the QDPS with position feedback in (5.3.5) and (5.3.6) is conditionally LAS, it is not likely to have very good closed loop damping characteristics for all the controlled modes. The specification of prescribed damping for the controlled modes is more subtle in this case, since position and not velocity feedback is used. Previously we have found that the added damping due to feedback is only appreciable when the controlled mode frequencies are close to the actuator frequency. For frequencies much higher or lower than ω_a, an undesirably large gain is required to attain the prescribed damping, which is likely to cause instability as a consequence.

This difficulty thus motivates us to use one or more sets of "Tuning Filters." These are basically band-limited electronic filters with dynamics similar to those of the actuators, but with frequencies "tuned" to the controlled mode frequencies, in order to achieve maximum closed loop damping. Assuming that actuator dynamics can be ignored for the moment (we shall show shortly that this is possible by appropriate arrangement) and N_A TF's are available to control N_A modes, then maximal damping effect can be realized if we set the cusp corresponding to each of these TF's to lie right above the corresponding controlled mode frequency.

In general, less than N_A (N_f, say) sets of TF's can also be used to control N_A modes. Each TF is an N_A state second order system with an input from the sensors and an output to the actuators. With the inclusion of these TF's, the complexity of the overall system is increased considerably. In particular, the inclusion of actuator dynamics destroys the symmetry of the system; hence, global stability cannot be proven analytically. To overcome this, we observe that the dynamics of each TF can be arranged to be

$$I_{N_A}(\ddot{Z}_i + 2\zeta_{f_i}\omega_{f_i}\dot{Z}_i + \omega_{f_i}^2 Z_i) = \omega_{f_i} C_i^{\frac{1}{2}} Sy$$

$$i = 1,\ldots,N_f,\ N_f \leq N_A,\ Z_i \in \mathbb{R}^{N_A} \tag{5.4.1}$$

where ζ_{f_i} and ω_{f_i} are the damping ratio and natural frequency of the i^{th} TF and $C_i^{\frac{1}{2}}$ is the square root of the non-negative definite gain matrix for the i^{th} TF. The synthesis of a typical TF is shown by means of a block diagram in Fig. 5.3.

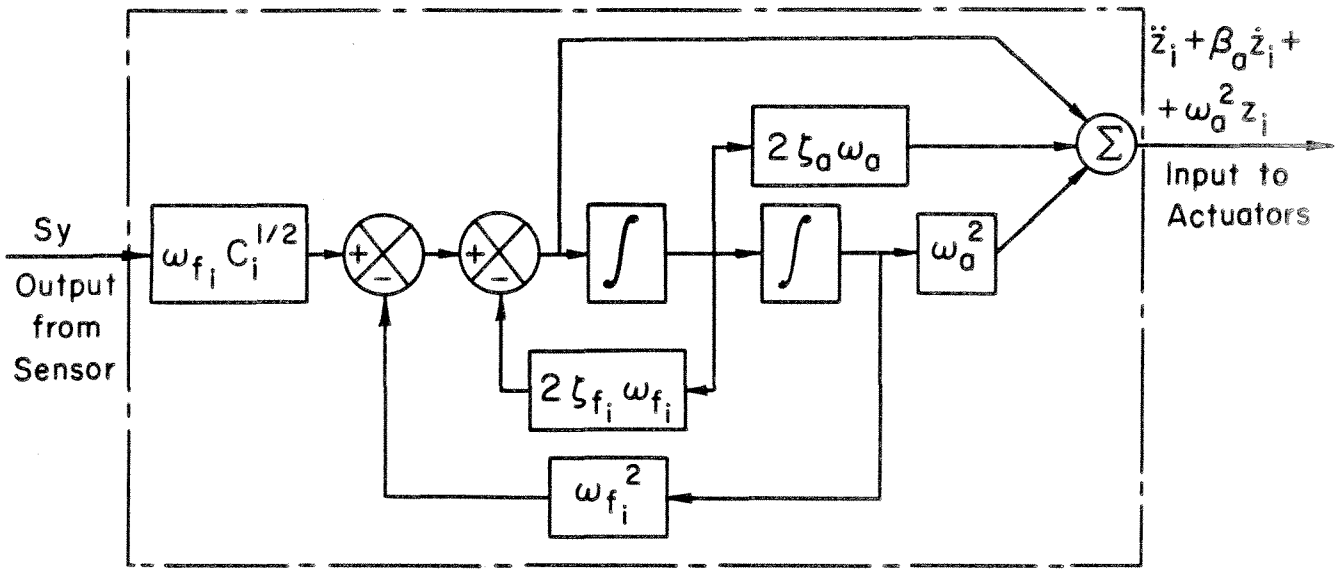

Fig. 5.3 Synthesis of a Tuning Filter

Note that by this synthesis, not only Z_i is available for output, but $\dot{Z}_i$ and $\ddot{Z}_i$ as well; hence, by appropriate arrangement, the signal $\ddot{Z}_i + \beta_a \dot{Z}_i + \omega_a^2 Z_i$ can be made available as input to the actuators. The overall system-filter-actuator dynamics can thus be expressed as

$$\text{System} \qquad M\ddot{y} + D\dot{y} + Ky = S^T u \tag{5.4.2}$$

$$\text{Filters} \qquad I_{N_A}(\ddot{Z}_i + 2\zeta_{f_i}\omega_{f_i}\dot{Z}_i + \omega_{f_i}^2 Z_i) = \omega_{f_i} C_i^{\frac{1}{2}} Sy, \quad i=1\ldots,N_f \tag{5.4.3}$$

$$\text{Actuators} \qquad \ddot{u} + \beta_a \dot{u} + \omega_a^2 u = \sum_{i=1}^{N_f} \omega_{f_i} C_i^{T/2}[\ddot{Z}_i + \beta_a \dot{Z}_i + \omega_a^2 Z_i] \tag{5.4.4}$$

The block diagram representation of these equations is shown in Fig. 5.4.

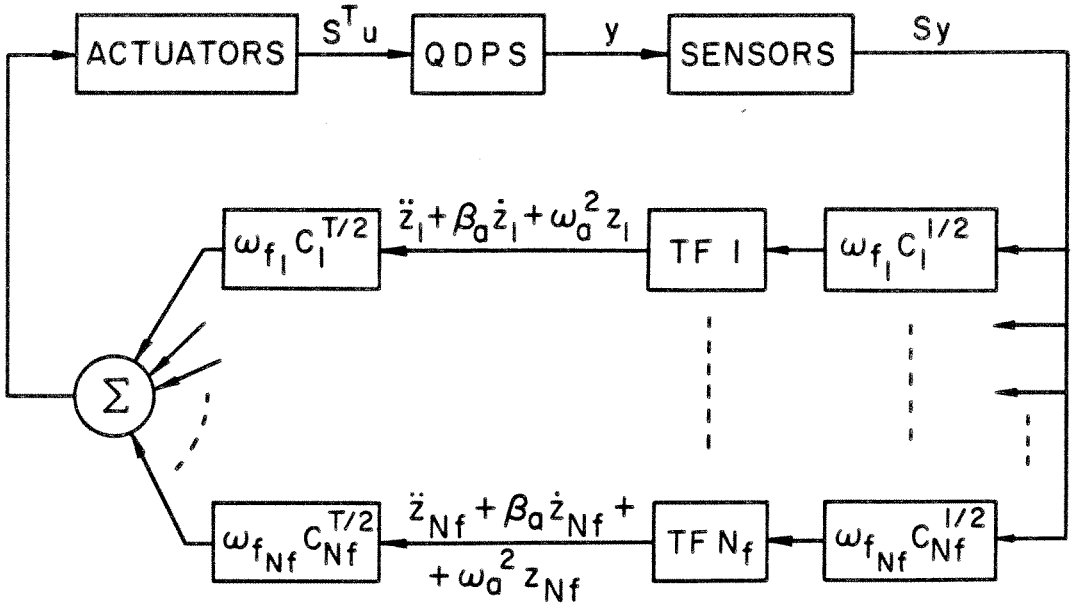

Fig. 5.4 Closed Loop Position Feedback Control System

Now (5.4.4) implies that

$$\text{(i)} \lim_{t\to\infty} u = \sum_{i=1}^{N_f} \omega_{f_i} C_i^{T/2} Z_i \tag{5.4.5}$$

$$\text{(ii) If } u(0) = \dot{u}(0) = Z_i(0) = \dot{Z}_i(0) = 0 \ \forall\ i \tag{5.4.6}$$

$$\text{then } u(t) \equiv \sum_{i=1}^{N_f} \omega_{f_i} C_i^{T/2} Z_i$$

Hence for β_a sufficiently large and initial conditions sufficiently small, u converges rapidly to $\sum_{i=1}^{N_f} \omega_{f_i} C_i^{T/2} Z_i$; and consequently actuator dynamics fall out of the picture completely. The overall system then reduces to the symmetrical form:

$$M\ddot{y} + D\dot{y} + Ky = S^T \sum_{i=1}^{N_f} \omega_{f_i} C_i^{T/2} Z_i \tag{5.4.7}$$

$$I_{N_A}[\ddot{Z}_i + 2\zeta_{f_i}\omega_{f_i}\dot{Z}_i + \omega_{f_i}^2 Z_i] = \omega_{f_i} C_i^{\frac{1}{2}} S y \ , \ i = 1,\ldots,N_f \tag{5.4.8}$$

Applying the appropriate canonical transformation, as defined by (5.3.3), (5.4.7) and (5.4.8) are transformed into

$$I_{N+N_AN_f}\ddot{\rho} + Q\dot{\rho} + P\rho = 0 \tag{5.4.9}$$

where

$$\rho = \begin{bmatrix} \xi \\ Z_1 \\ \vdots \\ Z_{N_f} \end{bmatrix} \in \mathbb{R}^{N+N_AN_f} \tag{5.4.10}$$

$$Q = Q^T = \begin{bmatrix} D & & & 0 \\ & 2\zeta_{f_1}\omega_{f_1} I_{N_A} & & \\ & & \ddots & \\ 0 & & & 2\zeta_{f_{N_f}}\omega_{f_{N_f}} I_{N_A} \end{bmatrix} \in \mathbb{R}^{N+N_AN_f} \tag{5.4.11}$$

$$P = P^T = \left[\begin{array}{c|ccc} \Omega & -E_1^T\omega_{f_1} & \cdots & -E_{N_f}^T\omega_{f_{N_f}} \\ \hline -E_1\omega_{f_1} & \omega_{f_1}^2 I_{N_A} & & 0 \\ \vdots & & \ddots & \\ -E_{N_f}\omega_{N_f} & 0 & & \omega_{f_{N_f}}^2 I_{N_A} \end{array}\right] \in \mathbb{R}^{N+N_A N_f} \tag{5.4.12}$$

$$E_i = C_i^{\frac{1}{2}} S\Phi \tag{5.4.13}$$

$$\text{and} \quad B_i = E_i^{T/2}\, E_i^{\frac{1}{2}} = \Phi^T S^T C_i S\Phi \tag{5.4.14}$$

The stability of the overall system is apparent from the following theorem.

Theorem 5.5

The overall system in (5.4.7) and (5.4.8) is LAS if

$$\Omega - \sum_{i=1}^{N_f} (1 + \varepsilon_i)\, B_i \text{ is positive definite} \tag{5.4.15}$$

where ε_i, $i = 1,\ldots,N_f$ are arbitrarily small positive quantities.

Proof: Define the Liapunov function

$$V = \frac{1}{2}\dot{\rho}^T\dot{\rho} + \frac{1}{2}\rho^T P\rho \tag{5.4.16}$$

$$= \frac{1}{2}\left[\dot{\xi}^T\dot{\xi} + \sum_{i=1}^{N_f}\dot{Z}_i^T\dot{Z}_i\right] + \frac{1}{2}\left[\xi^T\Omega\xi + \sum_{i=1}^{N_f}(\omega_{f_i}^2 Z_i^T Z_i - 2\xi^T E_i^T\omega_{f_i} Z_i)\right]$$

By the Cauchy-Schwartz inequality,

$$V > \frac{1}{2}\left[\dot{\xi}^T\dot{\xi} + \sum_{i=1}^{N_f}\dot{Z}_i^T\dot{Z}_i\right] + \frac{1}{2}\xi^T\left(\Omega - \sum_{i=1}^{N_f}(1+\varepsilon_i)B_i\right)\xi$$

$$+ \frac{1}{2}\sum_{i=1}^{N_f}\omega_{f_i}^2\,\frac{\varepsilon_i}{1+\varepsilon_i}\,Z_i^T Z_i \tag{5.4.17}$$

with first derivative of V is

$$\dot{V} = - \dot{\rho}^T Q \dot{\rho} \leq 0 \qquad (5.4.18)$$

which is negative definite almost everywhere by an argument similar to that in Theorem 5.2. Hence, if the assumption (5.4.15) is satisfied, V is strictly positive for all nontrivial ξ and Z_i with $\dot{V}$ negative almost everywhere (by reasoning similar to that in Theorem 5.2) and the proof is made complete by invoking the Liapunov theorem. □

Note in passing that this sufficient condition for stability is independent of the filter dynamics; hence, if the C_i's are such that

$$K - \sum_{i=1}^{N_f} (1+\varepsilon_i) S^T C_i S \text{ is positive definite} \qquad (5.4.19)$$

then the system is LAS. In practice, the C_i will be dependent on the filter dynamics for greater flexibility in design.

Even though the above condition is minimally restrictive, it is only a sufficient condition. A condition both sufficient and necessary for stability can be easily deduced from Theorem 5.3.

Theorem 5.6

The overall system in (5.4.7) and (5.4.8) is LAS iff the matrix P (as in (5.4.12)) is positive definite.

5.5 A DESIGN PROCEDURE FOR THE TUNING FILTERS AND FEEDBACK GAIN MATRICES

If $N_f = N_A$ then one TF can be used to tune each controlled mode. In practice we only need $N_f < N_A$ TF's so that some TF's will be used to tune more than one mode. The more TF's we use, the better we would expect the performance to be, but the complexity of the overall system would also increase.

As in the velocity feedback case, we shall adopt the technique of approximate pole-placement to prescribe an approximate closed loop damping for the controlled modes. An exact specification of the closed loop damping seems to be a formidable task, but for sufficiently small feedback, the coupling effect from the uncontrolled modes is negligible to first order accuracy, so that, as before, the coupled system can be decoupled into scalar systems. Taking the Laplace transform of (5.4.9), the Laplace transformed state $\hat{\xi}$ is governed by

$$\left((s^2 I_N + \mathcal{D}s + \Omega) - \sum_{i=1}^{N_f} \left(\frac{\omega_{f_i}^2}{s^2 + 2\zeta_{f_i}\omega_{f_i} s + \omega_{f_i}^2} \right) \mathcal{B}_i \right) \hat{\xi} = \begin{array}{l}\text{terms governed by} \\ \text{Initial Conditions}\end{array}$$

We shall first assume the simplest case in which an equal number of filters and actuators are available. Then, by selecting appropriate C_i, $\mathcal{B}_i$ can be constructed as

$$\mathcal{B}_i = \begin{matrix} \\ N_A \end{matrix} \overbrace{\left\{ \begin{bmatrix} \mathcal{B}_{i_{11}} & \mathcal{B}_{i_{12}} \\ \mathcal{B}_{i_{21}} & \mathcal{B}_{i_{22}} \end{bmatrix} \right.}^{N_A} \tag{5.5.1}$$

where only one diagonal entry of $\mathcal{B}_{i_{11}}$ is non-zero, i.e.,

$$(\mathcal{B}_{i_{11}})_{mn} = \delta_{im}\delta_{mn}\gamma_i\omega_i^2 \text{ , or } \mathcal{B}_{i_{11}} = \begin{bmatrix} 0 & & & \\ & \ddots & & \\ & & \omega_i^2\gamma_i & \\ & & & \ddots \\ & & & & 0 \end{bmatrix} \tag{5.5.2}$$

To achieve this, C_i must be

$$C_i = (\Phi_1^T S^T)^{-1} (\mathcal{B}_{i_{11}})(S\Phi_1)^{-1} \tag{5.5.3}$$

where

$$\Phi = [\underbrace{\Phi_1}_{N_A} \mid \underbrace{\Phi_2}_{N-N_A}] \tag{5.5.4}$$

and consequently $B_{i_{12}} = B_{i_{21}}^T$, and $B_{i_{22}}$ appear as by-products, i.e.,

$$B_{i_{12}} = (\Phi_1^T S^T)\, C_i(S\Phi_2) \tag{5.5.5}$$

$$B_{i_{22}} = (\Phi_2^T S^T)\, C_i(S\Phi_2) \tag{5.5.6}$$

The closed loop eigenvalues of the overall system are therefore the roots of the equation

$$\det \left| \begin{array}{c|c} s^2 I_{N_A} + s\mathcal{D}_{11} + \Omega_1 - \left[\dfrac{\omega_i^2 \omega_{f_i}^2 \gamma_i}{s^2 + 2\zeta_{f_i}\omega_{f_i} s + \omega_{f_i}^2} \right] & s\mathcal{D}_{12} - \sum_{i=1}^{N_f} \left(\dfrac{\omega_{f_i}^2 B_{i_{12}}}{s^2 + 2\zeta_{f_i}\omega_{f_i} + \omega_{f_i}^2} \right) \\ \hline s\mathcal{D}_{21} - \sum_{i=1}^{N_f} \left(\dfrac{\omega_{f_i}^2 B_{i_{21}}}{s^2 + 2\zeta_{f_i}\omega_{f_i} s + \omega_{f_i}^2} \right) & s^2 I_{N-N_A} + s\mathcal{D}_{22} + \Omega_2 - \sum_{i=1}^{N_f} \dfrac{\omega_{f_i}^2 B_{i_{22}}}{s^2 + 2\zeta_{f_i}\omega_{f_i} + \omega_{f_i}^2} \end{array} \right| = 0 \tag{5.5.7}$$

where

$$\mathcal{D} = \begin{matrix} \\ N_A \\ \\ \end{matrix} \overbrace{\left[\begin{matrix} \mathcal{D}_{11} & \mathcal{D}_{12} \\ \mathcal{D}_{21} & \mathcal{D}_{22} \end{matrix} \right]}^{N_A} \tag{5.5.8}$$

$$\Omega = \begin{matrix} \\ N_A \\ \\ \end{matrix} \overbrace{\left[\begin{matrix} \Omega_1 & 0 \\ 0 & \Omega_2 \end{matrix} \right]}^{N_A} \tag{5.5.9}$$

Assuming that $\mathcal{D} \sim o(1)$ and $B_i \sim o(1)$, then it is easy to see that the characteristic equation for each of the first N_A controlled modes is approximately

$$(s^2 + \beta_i s + \omega_i^2)\,(s^2 + \beta_{f_i} s + \omega_{f_i}^2) - \omega_i^2 \omega_{f_i}^2 \gamma_i = 0\,, \quad i = 1, \ldots, N_A \tag{5.5.10}$$

where $\beta_{f_i} = 2\zeta_{f_i}\omega_{f_i}$ and $\beta_i = (\mathcal{D})_{ii} = 2\zeta_n\omega_i$ (5.5.11)

which is identical to (5.1.3), except that ω_a & β_a are replaced by ω_{f_i} and β_{f_i},

respectively. Since we have already developed an extensive knowledge of this scalar system, we shall proceed to design each filter so as to prescribe the closed loop damping. Comparing (5.5.10) with the closed loop expression

$$(s^2 + \beta_{p_i} s + \omega_{p_i}^2)(s^2 + \beta_{q_i} s + \omega_{q_i}^2) = 0 \tag{5.5.12}$$

and equating coefficients of s^k, we have

$$s^3 : \beta_i + \beta_{f_i} = \beta_{p_i} + \beta_{q_i} \tag{5.5.13}$$

$$s^2 : \omega_i^2 + \omega_{f_i}^2 + \beta_i\beta_{f_i} = \omega_{p_i}^2 + \omega_{q_i}^2 + \beta_{p_i}\beta_{q_i} \tag{5.5.14}$$

$$s^1 : \omega_i^2\beta_{f_i} + \omega_{f_i}^2\beta_i = \omega_{p_i}^2\beta_{q_i} + \omega_{q_i}^2\beta_{p_i} \tag{5.5.15}$$

$$s^0 : \omega_i^2\omega_{f_i}^2(1 - \gamma_i) = \omega_{p_i}^2\omega_{q_i}^2 \tag{5.5.16}$$

Hence, assuming ω_{p_i} to be the closed loop modal frequency, specifying β_{p_i} will give us four unknowns β_{q_i}, ω_{p_i}, ω_{q_i}, γ_i in the above four simultaneous equations. The solution can be shown to be

$$\beta_{q_i} = \beta_{f_i} + \beta_i - \beta_{p_i} \tag{5.5.17}$$

$$G_{1i} = \omega_i^2 + \omega_{f_i}^2 + \beta_i\beta_{f_i} - \beta_{q_i}\beta_{p_i} \tag{5.5.18}$$

$$G_{2i} = \beta_i\omega_{f_i}^2 + \beta_{f_i}\omega_i^2 \tag{5.5.19}$$

$$\omega_{p_i}^2 = \frac{G_{2i} - \beta_{p_i}G_{1i}}{\beta_{q_i} - \beta_{p_i}} \tag{5.5.20}$$

$$\omega_{q_i}^2 = \frac{G_{2i} - \beta_{q_i}G_{1i}}{\beta_{p_i} - \beta_{q_i}} \tag{5.5.21}$$

$$\gamma_i = 1 - \frac{\omega_{p_i}^2\omega_{q_i}^2}{\omega_i^2\,\omega_{f_i}^2} \tag{5.5.22}$$

Provided that β_{p_i} is sufficiently small, these solutions are expected to be well-behaved (i.e., no complex frequencies or negative damping). Should we wish to specify the closed loop damping ratio ζ_{p_i} instead, where

$$\beta_{p_i} = 2\,\zeta_{p_i}\omega_{p_i} \tag{5.5.23}$$

the resulting simultaneous equations will become very complicated, but the following iterative procedure will enable the solution to be calculated very quickly :

step (i) set $\beta^*_{p_i} = 2\zeta_{p_i}\omega_i$, i.e., approximate ω_{p_i} by ω_i

step (ii) solve for $\beta^*_{q_i}$, $\omega^*_{p_i}$, $\omega^*_{q_i}$, γ^*_i from (5.5.17) to (5.5.22)

step (iii) compute the actual ratio $\zeta^*_{p_i} = \dfrac{\beta^*_{p_i}}{2\omega^*_{p_i}}$

step (iv) if $|\zeta^*_{p_i} - \zeta_{p_i}| < \delta$ to some desired accuracy, STOP.

Otherwise replace $\beta^*_{p_i}$ by $\beta^*_{p_i} = 2\zeta_{p_i}\omega^*_{p_i}$, where $\omega^*_{p_i}$ is the latest approximation to ω_{p_i}, and return to STEP (ii). This procedure is found to converge very rapidly, and in general no more than 2 or 3 iterations are required to obtain accurate solutions. In any case, very accurate solutions are not required, since errors will inherently exist due to the coupling terms having been neglected.

As an illustration, we assume that ω_i corresponds to the first mode of a discrete shear beam of 20 elements, with parameters $\omega_i = 0.2981$, $\zeta_n = 0.01$ (so that $\beta_i = 0.00596$), $\omega_{f_i} = 0.363$, $\zeta_{f_i} = 0.5922$ (so that $\beta_{f_i} = 0.42994$), and ζ_{p_i} prescribed to be 0.3 . The outcome after each iteration is as follows (choose $\delta = 0.001$):

	$\beta^*_{p_i}$	$\beta^*_{q_i}$	$\omega^*_{p_i}$	$\omega^*_{q_i}$	$\zeta^*_{p_i}$	γ^*_i
Iteration 1	0.17886	0.25704	0.30540	0.28970	0.2928	0.3315
Iteration 2	0.18324	0.25266	0.30715	0.28669	0.2977	0.3352
Iteration 3	0.18465	0.25125	0.30863	0.28656	0.2992	0.3367

So far ω_{f_i} and ζ_{f_i} have remained fixed but arbitrary. Our concern is, of course, how to select these parameters so that some optimal criterion can be met. Some objectives of optimality are as follows:

(i) For a given prescribed closed loop damping coefficient (or equivalently, damping ratio), the gain γ_i is to be as small as possible.

(ii) A robust design (in the sense that sensitivity to possible variation in structural properties is reduced to a minimum) is desired. In particular, we do not want a slight variation in modal frequency to result in undesirably large gain.

We shall examine the closed loop damping characteristics as discussed in §5.2 again, bearing in mind this time that adjustable filter dynamics are available to tune each of the controlled modes. In particular, we wish to identify the exact location of the cusp, as shown in Fig. 5.2.

At the cusp, the i^{th} mode and its filter have identical damping, hence $\beta_{p_i} = \beta_{q_i}$ and (5.5.20) and (5.5.21) imply that unless

$$\beta_i\omega_{f_i}^2 + \beta_{f_i}\omega_i^2 = \beta_{p_i}[\omega_i^2 + \omega_{f_i}^2 + \beta_i\beta_{f_i} - \beta_{q_i}\beta_{p_i}] \qquad (5.5.24)$$

the closed loop frequencies ω_{p_i} and ω_{q_i} will be unbounded. (5.5.13) also implies that

$$\beta_{p_i} = \beta_{q_i} = \frac{1}{2}(\beta_i + \beta_{f_i}) \qquad (5.5.25)$$

and hence (5.5.24) is equivalent to a cubic equation in ω_i:

$$\beta_i\omega_{f_i}^2 + \beta_{f_i}\omega_i^2 = \frac{1}{2}(\beta_i + \beta_{f_i})[\omega_i^2 + \omega_{f_i}^2 - \frac{1}{4}(\beta_i - \beta_{f_i})^2] \qquad (5.5.26)$$

The frequency ω_i^* at which the cusp occurs is then the real root of the above cubic. Solution to the cubic looks difficult at first, but we shall guess the following solution which can be verified to satisfy (5.5.26) exactly;

$$\omega_i^* = \frac{\omega_{f_i}\sqrt{1 - \zeta_{f_i}^2}}{\sqrt{1 - \zeta_n^2}}$$

The corresponding maximum closed loop damping is then

$$\beta_{p_i}^* = \omega_{f_i}[\zeta_{f_i} + \zeta_n\sqrt{1 - \zeta_{f_i}^2}]$$

Note that both ω_i^* and $\beta_{p_i}^*$ are independent of γ_i, but in order to reach the cusp, γ_i has to exceed a threshold value γ_i^*. It is easy to see that this is also the γ_i required to reach the coalescent point of Fig. 5.1 (iii), at which $\omega_{p_i}^* = \omega_{q_i}^*$; and hence, (5.5.14) and (5.5.13) imply that

$$\omega_{p_i}^{*2} = \frac{1}{2}[\omega_i^{*2} + \omega_{f_i}^2 - \frac{1}{4}(\beta_i - \beta_{f_i})^2]$$

and consequently, the threshold gain before the cusp is reached is given by

$$\gamma_i^* = 1 - \frac{[\omega_i^{*2} + \omega_{f_i}^2 - \frac{1}{4}(\beta_i - \beta_{f_i})^2]^2}{4\omega_i^{*2}\omega_{f_i}^2}$$

On the one hand, we would like the actual closed loop damping to be as close to the cusp as possible, so that only minimal gain is required. On the other hand, if it lies too close to the cusp, then a slight offset

in the modal frequency will result in an undesirably large gain in the design process, if the same closed loop damping were to be maintained.* Thus, we are faced with a pair of conflicting design criteria, and there exists no definite optimal solution to this situation. A crude rule of thumb is to design ω_{f_i} and ζ_{f_i} such that the system's closed loop damping reaches only 80% of its maximum attainable value (the cusp), so as to strike a compromise between minimal gain and reasonable robustness. As the resonance peak is always slightly to the right of the cusp, we shall also slightly offset the natural modal frequency to the right of the cusp as

$$\omega_i = \frac{1.02\ \omega_{f_i}\sqrt{1-\zeta_{f_i}^2}}{\sqrt{1-\zeta_n^2}} \tag{5.5.27}$$

Having fully understood the overall system and filter behavior and its relation to the design criterion, we are in a position to select the appropriate filter parameters. Since it is desired that the controlled modes all decay at the same rate, we shall set a prescribed damping ratio for the first mode approximately and set the damping of all other controlled modes to be equal to that of the first. An exact prescribed damping for the first mode is quite difficult to obtain; it requires an iterative procedure which cannot be guaranteed to be convergent. We shall only concentrate on the following direct procedure:

---

* Note that this argument is slightly ambiguous because if we were to design the system to be exactly at the cusp, then with the filter parameters fixed and at a given gain, a change in modal frequency will only decrease the closed loop damping but will not cause instability. The meaning of robustness is, hence, twofold here.

Step (i) Decide on the approximate closed loop damping ratio for the first mode ζ_p. Assuming that $\omega_{p_1} \simeq \omega_1$, the closed loop damping for the first mode (and for all controlled modes) is

$$\beta_{p_1} \simeq 2\zeta_p\omega_1 = \beta_{p_i}, \quad i = 2,\ldots,N_A \tag{5.5.28}$$

Step (ii) Set the closed loop damping to be 80% of the maximum attainable value (assuming $\zeta_n << 1$, $\beta_1 << \beta_{f_1}$)

$$\beta_{p_1} = \frac{0.8\ \beta_{f_1}}{2} = 0.8\ \zeta_{f_1}\omega_{f_1} \tag{5.5.29}$$

The resonance peak is placed slightly to the left of ω_1; hence

$$\omega_1 \simeq 1.02\ \omega_{f_1}\sqrt{1 - \zeta_{f_1}^2} + o(\zeta_n^2) \tag{5.5.30}$$

(5.5.28) - (5.5.30) imply that

$$\zeta_p\omega_1 = \frac{0.4\omega_1\zeta_{f_1}}{1.02\sqrt{1-\zeta_{f_1}^2}} \tag{5.5.31}$$

or equivalently

$$\zeta_{f_1} = \left[\frac{(1.02\ \zeta_p)^2}{(1.02\ \zeta_p)^2 + 0.16}\right]^{\frac{1}{2}} \tag{5.5.32}$$

Note that ζ_{f_i} is independent of ω_1, and the corresponding filter frequency is

$$\omega_{f_1} = \frac{\omega_1}{1.02\sqrt{1 - \zeta_{f_1}^2}} \tag{5.5.33}$$

Step (iii) In order that the other controlled modes have a minimal gain (with the 80% allowance), we should set

$$\beta_{p_1} = \beta_{p_i} = 0.8\ \zeta_{f_i}\omega_{f_i}\ ,\ i = 2,\ldots,N_A \tag{5.5.34}$$

and

$$\omega_i = 1.02\ \omega_{f_i}\sqrt{1 - \zeta_{f_i}^2}\ ,\ i = 2,\ldots,N_A \tag{5.5.35}$$

which will give rise to the optimal filter parameters

$$\zeta_{f_i} = \left[\frac{\beta_{p_1}^2}{\left(\frac{0.8}{1.02}\ \omega_i\right)^2 + \beta_{p_1}^2}\right]^{\frac{1}{2}},\ i = 2,\ldots,N_A \tag{5.5.36}$$

and

$$\omega_{f_i} = \frac{\omega_i}{1.02\sqrt{1 - \zeta_{f_i}^2}} \tag{5.5.37}$$

In practice, however, it was found that γ_i, $i = 2,\ldots,N_A$, are usually smaller than γ_1, and this procedure tends to result in an unnecessarily small γ_i, so much so that the stable spillover into the uncontrolled modes tends to be less than if γ_i was larger. For this reason and for convenience of calculation, we simply let $\zeta_{f_i} = \zeta_{f_1}\ \forall_i$ and compute ω_{f_i} as in (5.5.37). This will cause γ_i to increase slightly, yet remain well below the allowable threshold.

Step (iv) Setting $\beta_{p_i} = \beta_{p_1}$, solve for β_{q_i}, ω_{p_i}, ω_{q_i}, and γ_i from (5.5.17) - (5.5.22).

Step (v) The gain matrices C_i are then calculated from γ_i through (5.5.2) and (5.5.3).

That completes our design procedure. Next we shall briefly describe the general case when the number of filters (N_f) is less than

the number of actuators. Despite some additional complexity the same theory still applies. Firstly, the set of N_A controlled frequencies (Λ) are partitioned into N_f sets Λ_i, $i = 1,\ldots,N_f$, each consisting of m_i modes to be tuned by the i^{th} filter, i.e.

$$\Lambda = \{\omega_1 , \omega_2,\ldots, \omega_{N_A}\} = \Lambda_1 \oplus \Lambda_2 \oplus \ldots \oplus \Lambda_{N_f} \tag{5.5.38}$$

where

$$\Lambda_1 = \{\omega_1, \omega_2,\ldots \omega_{m_1}\} \tag{5.5.39}$$

$$\Lambda_{N_f} = \{\omega_{m_1 + \ldots + m_{N_f-1}+1},\ldots, \omega_{N_A}\} \tag{5.5.40}$$

The $B_{l_{11}}$ matrix in (5.5.1) is now modified to be, for example,

$$B_{l_{11}} = \begin{bmatrix} \gamma_1\omega_1^2 & & & & & 0 \\ & \gamma_2\omega_2^2 & & & & \\ & & \ddots & & & \\ & & & \gamma_{m_1}\omega_{m_1}^2 & & \\ & & & & 0 & \\ & & & & & \ddots \\ 0 & & & & & 0 \end{bmatrix} \tag{5.5.41}$$

and in general,

$$B_{f_{11}} = \begin{bmatrix} 0 & & & & & 0 \\ & \ddots & & & & \\ & & * & & & \\ & & & * & & \\ & & & & * & \\ & & & & & \ddots \\ 0 & & & & & 0 \end{bmatrix} \begin{array}{l} \\ \\ \\ \\ \\ \\ \text{correspond to the} \\ i^{th} \text{ subset } \Lambda_i \end{array} \tag{5.5.42}$$

In this case, the determination of the scalar gain γ_i is a lot more difficult, as the resulting set of equations become overdetermined. One heuristic approach when one filter is used to tune 2 modes is to let the 2 modes lie on both sides of the resonance peak such that equal

boosting effect can be realized. In general, as the lower modes tend to be more critical, we would like to use 1 filter for each of the lower modes, and for more than 1 of the higher modes.

5.6 STABLE SPILLOVER INTO THE UNCONTROLLED MODES

Unlike the case of velocity feedback, where spillover from the controlled modes causes the uncontrolled modes to result in lower than natural damping (or even instability), the use of positive position feedback actually causes all modes (including uncontrolled and unmodelled) to result in higher than natural damping.

Theorem 5.7

To first order perturbation, the closed loop damping for all the modes is always greater than or equal to the natural open loop damping.

Proof: To first order perturbation, the closed loop behavior of each mode is determined by the diagonal terms of (5.5.7). The theorem is trivially obvious for the controlled modes but for the m^{th} uncontrolled mode, say, the corresponding characteristic equation is

$$s^2 + \beta_m s + \omega_m^2 - \sum_{j=1}^{N_f} \left(\frac{\omega_{f_j}^2 [\mathcal{B}_{j_{22}}]_{mm}}{s^2+\beta_{f_j} s+\omega_{f_j}^2} \right) = 0 \qquad (5.6.1)$$

where the $[\mathcal{B}_{j_{22}}]_{mm}$ are non-negative quantities. Since the system is linear, the interaction of each of the terms under the summation sign can be superimposed, and hence the damping characteristics of this mode relate to each of the filters as shown in Fig. 5.5 (only a crude picture).

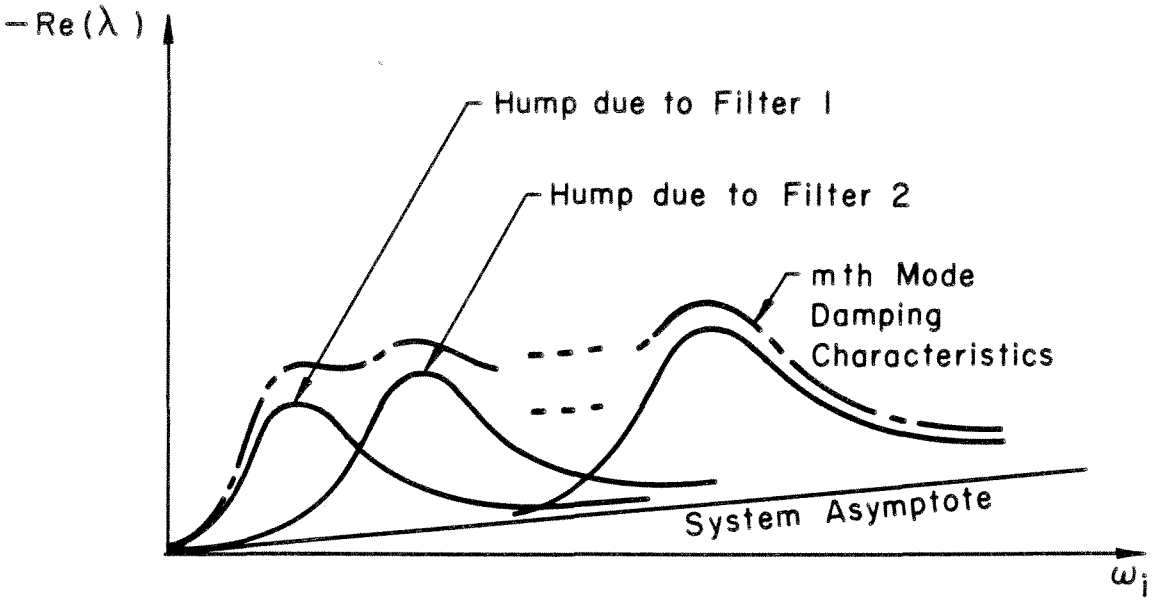

Fig. 5.5 Damping Characteristics for the m^{th} Mode, $m > N_A$.

The characteristics lie above the asymptote representing the natural damping; hence, mode m must have greater than natural closed loop damping. □

We can also prove the following global result :

Theorem 5.8

If the overall system (5.4.9) is stable and $\mathcal{D}$ strictly diagonal, then all the closed loop damping is lower bounded by the minimum open loop damping.

Proof: Consider (5.4.9) and note that the closed loop eigenvalues are those of the stable matrix

$$A = \begin{bmatrix} 0 & I \\ -P & -Q \end{bmatrix} \tag{5.6.2}$$

Consider a specific eigenvalue λ with corresponding eigenvector

$$\mu = \begin{bmatrix} \phi_1 + i\psi_1 \\ \phi_2 + i\psi_2 \end{bmatrix} \tag{5.6.3}$$

By definition $$\phi_2 + i\psi_2 = \lambda(\phi_1 + i\psi_2) \tag{5.6.4}$$

and $$-P(\phi_1 + i\psi_1) - Q(\phi_2 + i\psi_2) = \lambda(\phi_2 + i\psi_2) \tag{5.6.5}$$

Consequently $$\lambda^2(\phi_1 + i\psi_1) + \lambda Q(\phi_1 + i\psi_1) + P(\phi_1 + i\psi_1) = 0 \tag{5.6.6}$$

Premultiplying (5.6.6) by $\phi_1^T - i\psi_1^T = (\phi_1 + i\psi_1)^*$, we have

$$\lambda^2 + \lambda \underbrace{\left[\frac{\phi_1^T Q \phi_1 + \psi_1^T Q \psi_1}{\phi_1^T\phi_1 + \psi_1^T\psi_1}\right]}_{\bar{\beta}} + \underbrace{\left[\frac{\phi_1^T P \phi_1 + \psi_1^T P \psi_1}{\phi_1^T\phi_1 + \psi_1^T\psi_1}\right]}_{\Delta} = 0 \tag{5.6.7}$$

Since from theorem (5.6) P is positive definite, Δ must be positive. The global system is reduced to a scalar characteristic equation with coefficients $\bar{\beta}$ and Δ, where $\bar{\beta}$ can be twice the closed loop damping of any mode depending on the choice of ϕ_1 and ψ_1. By the Rayleigh-Ritz principle

$$\beta = \frac{\phi_1^T Q \phi_1 + \psi_1^T Q \psi_1}{\phi_1^T \phi_1 + \psi_1^T \psi_1} > \text{Min } \{\lambda_j(Q)\} \qquad (5.6.8)$$

Since $\mathcal{D}$ is diagonal, Q is also diagonal; hence, $\lambda_j(Q)$ are simply the diagonal elements of Q which are also twice the open loop damping of the system together with all of its filters. □

The following intuitive theorem can be easily deduced from (5.6.7)

Theorem 5.9

If the overall system were to become unstable due to excessively high gain, the unstable eigenvalue(s) will appear as positive real root(s) of (5.5.7).

Proof: If system is unstable, P is indefinite and Δ in (5.6.7) can take on a negative value, while $\bar{\beta}$ is always positive. Consequently, one root will always be positive, while the other is always negative. □

This fact can also be easily observed from the root locus diagram in Fig. 5.1.

Chapter 6

A QUASI-LINEAR VIBRATION SUPPRESSION TECHNIQUE VIA STIFFNESS MODIFICATION

6.1 ELECTRONIC DAMPING: AN ALTERNATIVE

Throughout this thesis, we have assumed the use of external actuators without questioning their practicality other than the fact that they possess finite bandwidth. In LSS control applications, which we shall concentrate on in this chapter, these actuators are generally the reaction jets. Such a means of imparting control forces onto the space structures has been taken for granted by most researchers, and little attention has been paid to the following facts:

(1) Jet-propulsion type actuators inevitably require propellant such as compressed gas or rocket fuel, which are of limited supply in space. Frequent replenishment of such fuel may prove to be costly.

(2) Repeated use of these actuators causes a decrease in the propellant's mass. In the control of light and flimsy structures, this change in weight distribution may lead to a significant change in the structural configuration, which may subsequently lead to stability problems, if the design is not sufficiently robust.

(3) As these actuators possess finite bandwidth, the interaction with the very large bandwidth system cannot be ignored. The resulting stability problems have been discussed in great detail in Chapter 2 ; hence we shall not elaborate further here.

(4) For vibration suppression of a thin, light-weight and slender surface such as a large solar panel, the surface density is extremely small compared to that of a lumped actuator, which is usually fairly heavy and bulky. Distribution of these actuators will certainly alter the modal structure

significantly, creating difficulty in the a priori design process.

Other minor issues such as the reliability and possible breakdown of these actuators prompt us to consider an alternative control scheme which eliminates the use of conventional actuators altogether. As large solar cells are available, the question is naturally raised regarding the use of this abundant electrical energy for active vibration control. The concept of electronic damping is nothing new and dates back to the fifties where Olson [29] first used it for acoustical noise control. Piezoelectric strain transducers were used to convert electronic control signals into control forces, and conversely, convert strain into electronic signals. This concept remained unpursued for a while until recently when it was applied to the vibration control of optical structures [30] and mechanical structures [31,32]. Control of the latter structures is essentially a disguised form of direct velocity feedback control. Instead of measuring absolute velocity (or displacement) and imparting direct control forces, relative measurements and relative forces are implemented using strain transducers. In the particular cylindrical mast vibration control experiment [31], four transducers are used to control the first two fundamental modes, and spill-over is eliminated by the use of narrow band filters. Chen [33] suggests that if conventional actuators are not suitable to control the out-of-plane motion, then the other alternative is to control the in-plane stiffness using the piezoelectric transducers. However, it must be pointed out that the coupling between in-plane motion and out-of-plane motion is highly nonlinear and complicated [34,35], even in the case of a simple elastic string. It is really more appropriate to talk about, in the mathematical sense, modifying the stiffness matrix resulting from a finite element formulation of the pertinent structure.

In this chapter we shall explore the theory and application of the concept of stiffness modification to the vibration suppression of a multivariate oscillatory system. Despite the relatively simple structure of the control scheme, global stability is always guaranteed by virtue of the positive definite rate of energy decay.

6.2 THE REID'S MODEL

As before, we shall start our investigation with the simplest scalar model first. In actual fact, it is this scalar system—the Reid's spring model[36]—that inspires the whole theory of stiffness modification. The concept of "Linear Hysteresis Damping" had been studied several decades ago in aircraft flutter problems [37]. The Reid's model in particular has a butterfly hysteresis characteristic and was studied in great detail by Caughey and Vijayaraghavan [38]. After appropriate normalization, the equation of motion of a simple harmonic oscillator attached to a "Reid's Spring" is

$$\ddot{y} + y(1+\gamma\,\mathrm{sgn}(y\dot{y})) = 0, \quad 0<\gamma<<1 \tag{6.2.1}$$

here y is the displacement of the oscillator from its equilibrium position and γ a small parameter. One immediately notices that the unit stiffness of the system is modulated by the amount $\gamma\,\mathrm{sgn}(y\dot{y})$. Unlike the Reid's model where γ occurs as a small material constant, the gain γ in the present context is only constrained by the operating range of the piezoelectric transducers, and, hence, need not be small. This system is obviously stable since the total energy of this system

$$E(t) = \frac{1}{2}\dot{y}^2 + \frac{1}{2}y^2 \qquad (6.2.2)$$

has a negative semi-definite* decay rate

$$\dot{E}(t) = -\gamma|y\dot{y}| \leq 0 \qquad (6.2.3)$$

One intuitively reasons that larger γ will result in faster energy decay, but it turns out to be more subtle than that, as dependence on the states y and $\dot{y}$ cannot be ignored in the expression $\dot{E}$. Since the system is piecewise linear nonlinear, we can obtain a closed form solution which differs distinctly in three separate cases, namely $\gamma < 1$, $\gamma = 1$, and $\gamma > 1$. Without loss of generality, we shall assume the initial conditions $y(0) = 0$, $\dot{y}(0) = 1$ and that natural passive damping is negligible. The phase planes for all three cases are shown in Fig. 6.1.

Case (1) $\gamma < 1$

It is trivial to show, by considering each quadrant in the phase plane, that the exact solution is:

Quadrant 1. $y > 0$, $\dot{y} > 0$, $0 \leq t \leq \frac{\pi}{2\sqrt{1+\gamma}}$

$$y(t) = \frac{1}{\sqrt{1+\gamma}} \sin \sqrt{1+\gamma}\, t$$

1st integral is $\dot{y}^2 + (1+\gamma)y^2 = 1$

---

* $\dot{E}$ is actually negative definite almost everywhere, since, unless $y=\dot{y}=0$, either y or $\dot{y}$ can only be momentarily zero; hence, $\dot{E}$ takes on zero value for nonzero $y^2+\dot{y}^2$ only on a set of t of measure zero.

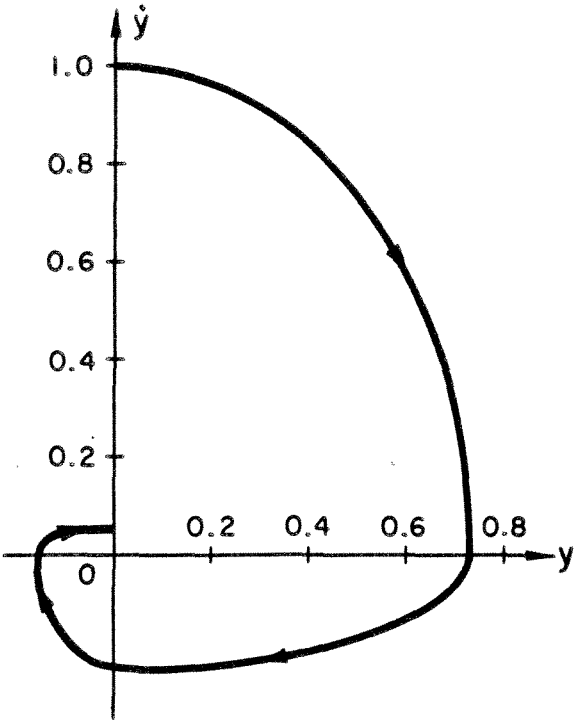

(i) $\gamma = 0.9 < 1$

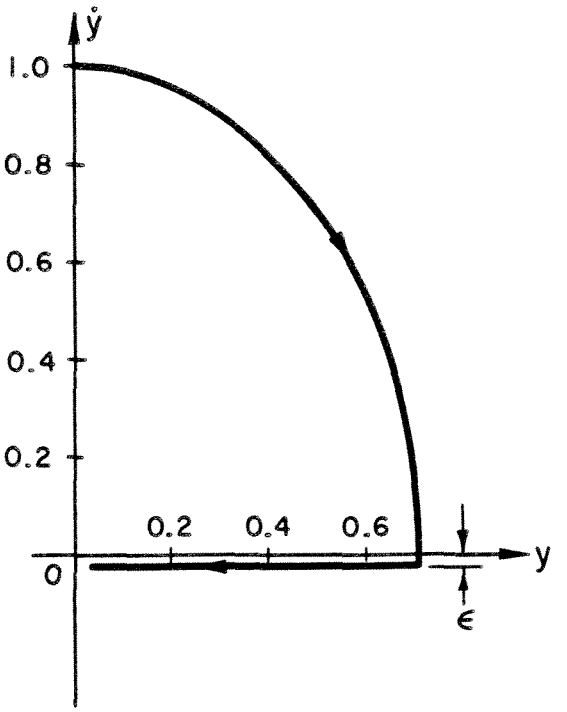

(ii) $\gamma = 1.0$

(iii) $\gamma = 2.0 > 1$

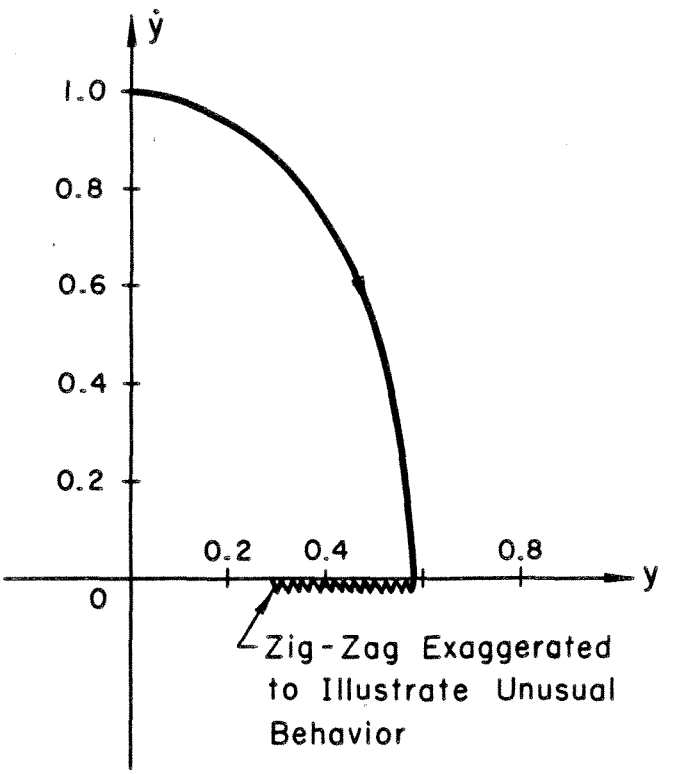

Fig. 6.1 Phase Plane of the Quasi-Linear System

$$\ddot{y} + y\,(1 + \gamma\ \mathrm{sgn}\,(y\dot{y})) = 0$$

Quadrant 2. $y > 0, \quad \dot{y} < 0, \quad \frac{\pi}{2\sqrt{1+\gamma}} \le t \le \frac{\pi}{2\sqrt{1+\gamma}} + \frac{\pi}{2\sqrt{1-\gamma}}$

$$y(t) = \frac{1}{\sqrt{1+\gamma}} \cos\left[\sqrt{1-\gamma}\left(t - \frac{\pi}{\sqrt{1+\gamma}}\right)\right]$$

1^{st} integral is $\dot{y}^2 + (1-\gamma)y^2 = \frac{1-\gamma}{1+\gamma}$

Quadrant 3. $y < 0, \quad \dot{y} < 0, \quad \frac{\pi}{2}\left[\frac{1}{\sqrt{1+\gamma}} + \frac{1}{\sqrt{1-\gamma}}\right] \le t \le \frac{\pi}{\sqrt{1+\gamma}} + \frac{\pi}{2\sqrt{1-\gamma}}$

$$y(t) = \frac{-\sqrt{1-\gamma}}{\sqrt{1+\gamma}} \sin\left[\sqrt{1+\gamma}\left(t - \frac{\pi}{2\sqrt{1+\gamma}} - \frac{\pi}{2\sqrt{1-\gamma}}\right)\right]$$

1st integral is $\dot{y}^2 + (1+\gamma)y^2 = \frac{1-\gamma}{1+\gamma}$

Quadrant 4. $y < 0, \quad \dot{y} > 0, \quad \frac{\pi}{\sqrt{1+\gamma}} + \frac{\pi}{2\sqrt{1-\gamma}} \le t \le \pi\left[\frac{1}{\sqrt{1+\gamma}} + \frac{1}{\sqrt{1-\gamma}}\right]$

$$y(t) = \frac{-\sqrt{1-\gamma}}{1-\gamma} \cos\left[\sqrt{1-\gamma}\left(t - \frac{\pi}{\sqrt{1+\gamma}} - \frac{\pi}{2\sqrt{1-\gamma}}\right)\right]$$

1st integral is $\dot{y}^2 + (1-\gamma)y^2 = \left(\frac{1-\gamma}{1+\gamma}\right)^2$ (6.2.4)

total period for one complete cycle is $T_d = \pi\left[\frac{1}{\sqrt{1+\gamma}} + \frac{1}{\sqrt{1-\gamma}}\right]$ (6.2.5)

and the state at the end of the first cycle is

$$y(T_d) = 0, \quad \dot{y}(T_d) = \frac{1-\gamma}{1+\gamma} \tag{6.2.6}$$

Case (2) $\gamma = 1$

In quadrant 1, the equation of motion is simply

$$\ddot{y} + 2y = 0 \tag{6.2.7}$$

which admits the solution $y = \frac{1}{\sqrt{2}} \sin \sqrt{2}t$ (6.2.8)

with first integral given by $\dot{y}^2 + 2y^2 = 1$ (6.2.9)

However, once the phase-plane trajectory enters the second quadrant, the equation of motion becomes

$$\ddot{y} = 0 \tag{6.2.10}$$

Theoretically, the phase plane trajectory should stop at the point where it crosses the y axis, i.e., at $y = 1/\sqrt{2}$, $\dot{y} = 0$, and remain there henceforth. In practice however there is always some small overshoot $\dot{y} = -\varepsilon$, $0 < \varepsilon << 1$, so that the motion after entering the second quadrant is simply

$$y(t) = -\varepsilon t + 1/\sqrt{2} \tag{6.2.11}$$

For small ε, the decay can be very slow indeed.

Case (3) $\gamma > 1$.

The initial solution in quadrant 1 satisfies a harmonic equation and takes the form

$$y(t) = \frac{1}{\sqrt{1+\gamma}} \sin \sqrt{1+\gamma}\, t \tag{6.2.12}$$

Once the phase plane trajectory enters the 2nd quadrant, the nature of the equation of motion changes completely to

$$\ddot{y} - (\gamma-1)y = 0 \qquad (6.2.13)$$

which admits the hyperbolic solution

$$y(t) = \frac{1}{\sqrt{1+\gamma}} \cos h \sqrt{\gamma-1}\, t - \frac{\varepsilon}{\sqrt{\gamma-1}} \sin h \sqrt{\gamma-1}\, t \qquad (6.2.14)$$

where ε is the small overshoot when the trajectory crosses the y axis. This hyperbolic solution tends to head back up to the first quadrant again and subsequently is pushed back into the 2nd quadrant as an harmonic oscillator, and the process repeats itself. Thus the trajectory zig-zags along the y axis until it slowly finds its way to its stable sink at the origin.

To confirm our theory, the differential equation (6.2.1) is solved numerically using a 5th and 6th order Runge-Kutta-Verner differential equation solver, the time step being adjusted accordingly until satisfactory consistency is achieved. The state history $y(t)$ and energy decay are shown in Fig. 6.2 and Fig. 6.3, respectively, for each of the 3 cases. For all practical purposes, the agreement between theory and simulation is excellent indeed.

It is obvious now that the overall energy dissipation rate in Case (1) is far superior to that of Case (2) or (3). Though the latter two cases have more rapid energy decreases in the first half second, subsequent energy dissipation is very slow indeed. It is thus concluded that the best damping characteristic is achieved when $\gamma < 1$.

It is not clear at this stage what an "optimal" gain is, as the notion of optimality is not well-defined. For example, if one wishes to maximize the percentage energy decay rate per cycle, i.e.,

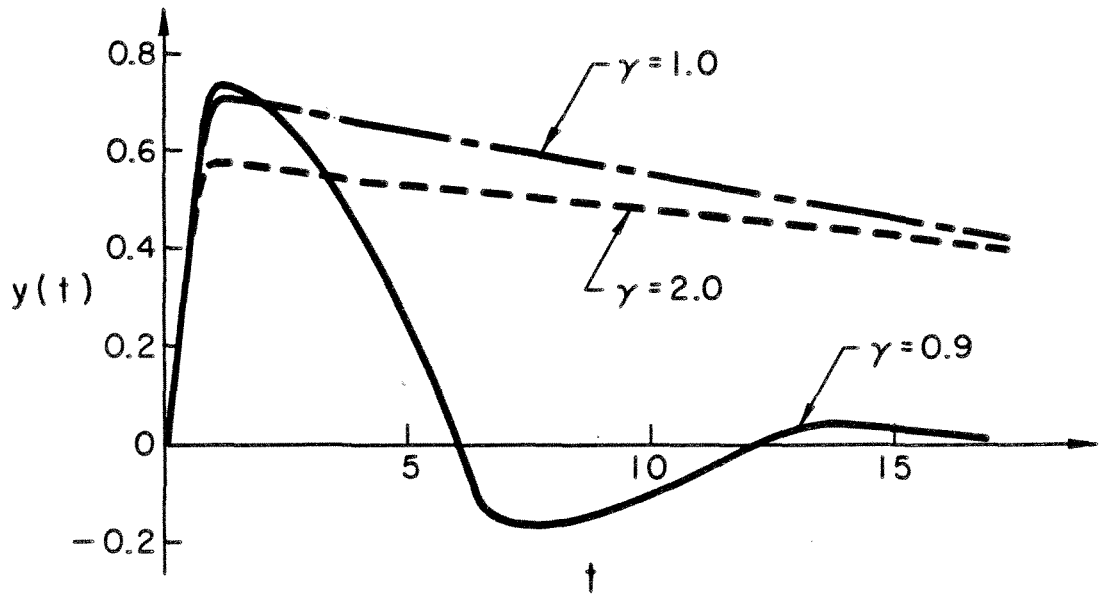

Fig. 6.2 State History for Scalar Quasi-linear System

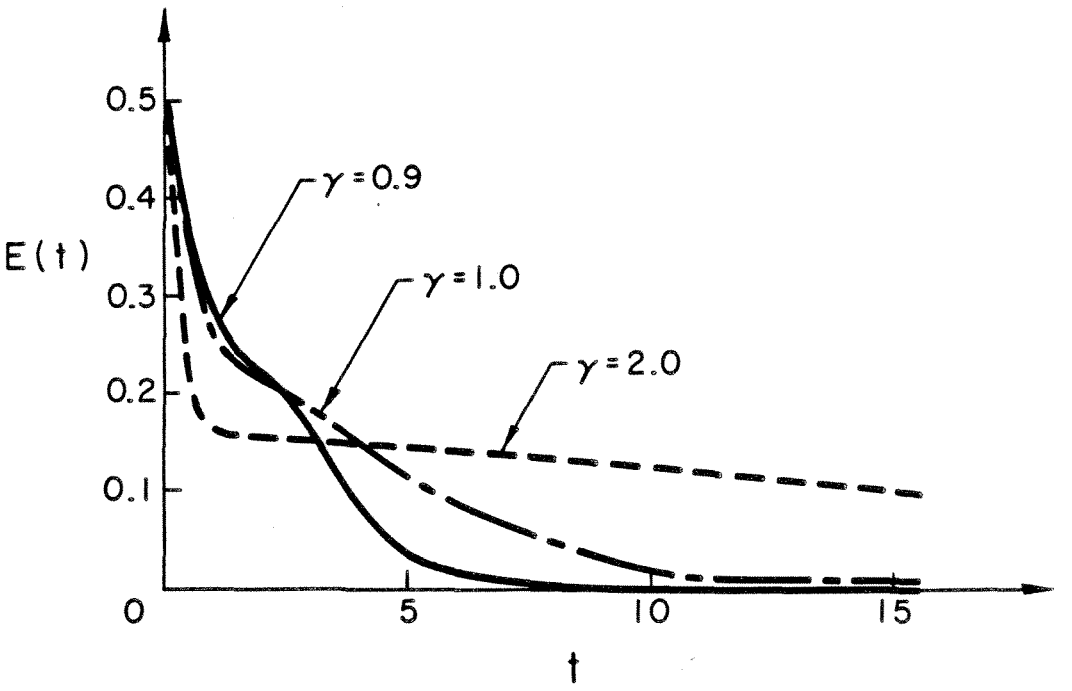

Fig. 6.3 Energy Decay Characteristics of Quasi linear Scalar System

$$\max_{\gamma} R_E = \frac{1-\left(\frac{1-\gamma}{1+\gamma}\right)^2}{\pi\left(\frac{1}{\sqrt{1-\gamma}} + \frac{1}{\sqrt{1+\gamma}}\right)} \tag{6.2.15}$$

then the optimal gain can easily be shown to be 0.53, though this is not the optimal gain if the optimality criterion refers to the percentage decay rate for 2 cycles instead. Alternatively, to maximize the percentage amplitude decay rate in 1 cycle, i.e.,

$$\max_{\gamma} R_A = \frac{1-\left(\frac{1+\gamma}{1+\gamma}\right)}{\pi\left(\frac{1}{\sqrt{1-\gamma}} + \frac{1}{\sqrt{1+\gamma}}\right)} \tag{6.2.16}$$

would require a gain of about 0.66. Infinitely many different criteria can be invented, but it has been found in practice that the energy decay exhibits little difference within the range of $0.5 < \gamma < 0.9$.

Less importantly, one may like to compare the quasi-linear system (6.2.1) with an equivalent linear viscous damped system, and determine some kind of an "Equivalent damping ratio". Some attempts to answer this question in a similar model are made in [33], where an approximate decay envelope $e^{-\zeta t}$ for a linear viscous damped system

$$\ddot{y} + 2\zeta\dot{y} + y = 0 \tag{6.2.17}$$

is computed to bound the state history of the equivalent quasi-linear system (6.2.1). It seems to be such a laborious task to treat a non-crucial issue. In our present theory we are more interested in interpreting the term "Equivalence" in terms of energy decay rate. We simply compare the energy histories of the quasi-linear system (6.2.1) and the linear viscous system (6.2.17), such that the cost function

$$J = \int_0^\infty (E_\gamma(t) - E_\zeta(t))^2 dt \tag{6.2.18}$$

is maximized over all γ, where $E_\gamma(t)$ and $E_\zeta(t)$ are the energy histories of the quasi-linear and the linear viscous system, respectively. For instance, the case of $\gamma \doteq 0.9$ is "equivalent" to a linear damping ratio of about $\zeta = 25\%$.

Another point of mere theoretical interest is that an alternative to our present quasi-linear model is the "quasi-quadratic" model

$$\ddot{y} + y[1 + \gamma(y\dot{y})] = 0 \tag{6.2.19}$$

where the energy decay rate is

$$\dot{E}(t) = -\gamma y^2 \dot{y}^2 \leq 0 \tag{6.2.20}$$

Thus instead of passing the signal through a hard limiter, the signal is used directly to modify the stiffness. A closed form solution to this system does not exist, but for small γ we can obtain a perturbation solution. With the usual initial condition, a zero order solution is given by

$$y(t) = \frac{1}{\sqrt{1 + \frac{\gamma t}{4}}} \sin t \tag{6.2.21}$$

For a large or intermediate value of γ, it can be shown that the amplitude of oscillation will also decay as $O(t^{-\frac{1}{2}})$; hence, for large t and small $\|y\|$, the decay can be very slow indeed. In practice, it is also found that for a comparable energy decay rate, the gain γ required in this case is much higher than in the quasi-linear case, hence rendering it

unattractive. This is also true in the multivariate case, which we shall examine next, even though the detailed mechanism involved is much more complicated then.

6.3. FORMULATION OF THE QUASI-LINEAR MULTIVARIATE CONTROL SYSTEM

The control of QDPS by stiffness modification can be conceived of as a form of direct output feedback control where the control force in (1.1.11) is a non-linear function of the system states. The equation governing such a system is

$$M\ddot{y} + D\dot{y} + Ky = -F(y,\dot{y})y \tag{6.3.1}$$

where $F(y,\dot{y}) \in \mathbb{R}^{NxN}$ is the time varying stiffness modification matrix. There is no unique way of constructing $F(y,\dot{y})$, except that it must render the overall system globally stable. One physically realizable way of constructing $F(y,\dot{y})$ is as follows:

Suppose we have n sets of transducers placed at suitable locations of the structure and suppose these transducers can be conceived of as being attached to adjacent elements in the discrete structure. Collocated with these transducers are n sets of sensors which may also appear in the form of strain transducers. Each transducer simultaneously measures the relative out-of-plane velocity and displacement of the two attached elements. Define the set S of transducer locations as

$$S = \{s_1, s_2, \text{----} s_n\} \subseteq T - \{N\} \tag{6.3.2}$$

where $T = \{1,2,3,\text{----},N\}$ is the set of all (numbered) elements in the discrete finite element model of the structure. For each $s_k \in S$,

there exists a transducer connecting element s_k and element $s_k + 1$. This transducer may be visualized as a (out-of-plane) shear spring of variable stiffness derived from electronic control signals. With such an arrangement, the stiffness modification matrix $F(y,\dot{y})$ in (6.3.1) can be synthesized in two ways. For convenience and obvious physical interpretation, we shall ascribe the names "Global" and "Local" control for these two methods each of which is a generalization of the scalar Reid Model.

Method I—Global Control

Physically, each set of sensors measures the relative displacement and velocity of adjacent elements and multiplies these together with a scalar gain c_k. Then all these products are summed together and transmitted through a hard limiter to form a scalar integer valued signal $v(y,\dot{y})$. This signal, multiplied by the gain c_k, again then determines the stiffness in the k^{th} transducer, which in turn modulates the structural stiffness at its point of actuation. Since the signal $v(y,\dot{y})$ is constructed from global measurements and is common to all transducers, it is thus reasonable to call it "Global" control. Mathematically, this procedure can be formulated in terms of the following equations:

The stiffness modification matrix $F(y,\dot{y})$ is synthesized as

$$F(y,\dot{y}) = v(y,\dot{y}) \sum_{k \in S} c_k Q_k \tag{6.3.3}$$

where $Q_k \in \mathbb{N}^{N \times N}$ has entries given by

$$(Q_k)_{ij} = \begin{cases} 1 & \text{if} \quad i=j=k \quad \text{or} \quad i=j=k+1 \\ -1 & \text{if} \quad i=k,\ j=k+1, \quad \text{or} \quad i=k+1,\ j=k \\ 0 & \text{otherwise} \end{cases} \tag{6.3.4}$$

and $v(y,\dot{y})$ is given by

$$v(y,\dot{y}) = \operatorname{sgn}\{\dot{y}^T[\sum_{k\in S} c_k Q_k]y\} = \operatorname{sgn}\{\sum_{k\in S} c_k(y_k - y_{k+1})(\dot{y}_k - \dot{y}_{k+1})\} \tag{6.3.5}$$

where

$$\operatorname{sgn} w = \begin{cases} 1 & \text{if} \quad w>0 \\ -1 & \text{if} \quad w<0 \\ 0 & \text{if} \quad w=0 \end{cases} \tag{6.3.6}$$

At this stage it is quite unnecessary to study the dynamics of the quasi-linear system in its modal form. Unlike the previous linear techniques, there is not very much we can do about dictating the decay characteristics of, for example, the first n modes. It is easy to see that the feedback system is LAS since the total energy

$$E(t) = \frac{1}{2}\dot{y}^T M\dot{y} + \frac{1}{2} y^T k y \tag{6.3.7}$$

has a positive decay rate

$$\dot{E}(t) = -|\dot{y}^T B y| - \dot{y}^T D\dot{y} < 0 \tag{6.3.8}$$

where

$$B = \sum_{k\in s} c_k Q_k \tag{6.3.9}$$

The presence of natural damping merely increases the rate of energy decay. In the absence of natural damping, $\dot{E}$ seems to be only negative

semi-definite, but it is practically negative definite by the following argument:

$\dot{E} = 0$ iff $By = 0$ or $B\dot{y} = 0$, so we shall examine each case. If $By = 0$ and if B and K have a different null space, then $Ky \neq 0 \Rightarrow \ddot{y} \neq 0 \Rightarrow \dot{y} = 0$ or $By = 0$ only on a set of t of measure zero. Similarly if $B\dot{y} = 0$ but $Ky \neq 0$ or $By \neq 0$ then $\ddot{y} \neq 0 \Rightarrow By = 0$ only on a set of t of measure zero. Thus for non-zero y or $\dot{y}$, $\dot{E}$ is negative definite almost everywhere on t. Hence regarding $E(t)$ as a natural choice of Liapunov function, the closed loop system is LAS by the celebrated Liapunov theory. Note that the matrix B is necessarily singular if fewer transducers than states are used.

Method II—Local Control

In contrast with the case of Global control, the local measurement output from each sensor is directly fed back into its associated transducer, after being multiplied by a positive control gain c_k. The stiffness modification matrix is thus synthesized as

$$F(y,\dot{y}) = \sum_{k \in S} c_k v_k(y,\dot{y}) Q_k \tag{6.3.10}$$

where $v_k(y,\dot{y}) = \text{sgn}\ (\dot{y}^T Q_k y) = \text{sgn}\ [(y_k - y_{k+1})(\dot{y}_k - \dot{y}_{k+1})]$ (6.3.11)

The resulting system is LAS again since the energy decay rate

$$\dot{E}(t) = -\sum_{k \in S} c_k |\dot{y}^T Q_k y| - \dot{y}^T D \dot{y} < 0 \tag{6.3.12}$$

is negative definite, if the c_k's are positive quantities.

For reasons that appear unclear to us, later simulation shows that local control in fact achieves a better energy decay characteristic than global control. Intuitively one may reason that, ignoring the natural damping for the moment, $\dot{E}$ is the sum of n negative definite terms in the local control case, while it consists only of 1 negative definite term in the global case. Certainly this is not the only or most crucial reason. Another possibility is that there exists some kind of multi-dimensional limit cycle in the case of global control, in which the total energy remains very nearly constant once the state is trapped. We shall discuss more about this as we examine the outcome of numerical simulation later.

The design of the gains $\{c_k, k \in S\}$, in both the global and local cases, to achieve "optimal performance" is a very difficult problem indeed. We cannot simply generalize from the scalar theory in view of the complicated nonlinear coupling effects. Furthermore, if a well-defined optimality criterion does exist, it is likely to depend on a large number of factors such as the state initial conditions, the transducer locations and their operating limits, the modal structure of the system, and other factors too numerous to name. So until such time as some ingenious way is available to make sense out of optimality, we shall choose c_k on an arbitrary trial and error basis. Note that one may suspect that the energy decay rate of each mode is dominated by the diagonal elements of the modal gain matrix, as in the case of global control

$$\mathcal{B} = \Phi^T B \Phi \qquad (6.3.13)$$

If n sets of transducers are available, it can be shown that the c_k can be chosen such that the first n diagonal elements of B are prescribed a priori. Such an endeavor, however, proves to be futile, as demonstrated by later numerical simulation.

It must be pointed out that we have assumed that the piezoelectric transducers have no dynamics. This again is not strictly correct, though we would expect these transducer dynamics to be much faster than any reaction jet type external actuators. In the event of improper design, instability due to interaction of transducer dynamics may still arise.

As in the scalar case, some attempts are made to implement the feedback for "quadratic decay," i.e., bypassing the hard limiter with the signal $v(y,\dot{y})$ or $v_k(y,\dot{y})$. It has been found that much higher gains are required to achieve comparable performance, hence rendering it less attractive in practice than the quasi-linear system.

Chapter 7

NUMERICAL SIMULATION OF A SIMPLY SUPPORTED DISCRETE SHEAR BEAM

7.1 PRELIMINARIES

To illustrate the theory and application of various control techniques discussed thus far, we shall consider a simply supported discrete shear beam with N elements which has the following inertia and stiffness matrix:

$$M = m_o I_N \tag{7.1.1}$$

$$K = k_o \begin{bmatrix} 2 & -1 & & & 0 \\ -1 & 2 & -1 & & \\ & -1 & 2 & -1 & \\ & & & \ddots & \\ & 0 & & -1 & 2 \end{bmatrix} \tag{7.1.2}$$

To obtain the frequencies and modal matrix Φ of this system, we note that the equation of motion for the n^{th} element is

$$m_o \ddot{y}_n + 2k_o y_n - k_o y_{n-1} - k_o y_{n+1} = 0, \quad n = 1, \cdots N \tag{7.1.3}$$

To solve for the system of difference-differential equation, we assume a solution of the form

$$y_n = a e^{i(\omega t + n\theta)} + b e^{i(\omega t - n\theta)} \tag{7.1.4}$$

and substitute into (7.1.3) to obtain

$$y_n \left[(-\omega^2 + \frac{2k_o}{m_o}) - \frac{2k_o}{m_o} \cos\theta\right] = 0 \qquad (7.1.5)$$

or

$$\omega^2 = 4(\frac{k_o}{m_o}) \sin^2 \frac{\theta}{2} \qquad (7.1.6)$$

(7.1.4)can be rewritten as

$$y_n = e^{i\omega t}[A \sin n\theta + B \cos n\theta] \qquad (7.1.7)$$

The boundary conditions for a simply supported beam are $y_o = 0$ and $y_{N+1} = 0$ which implies that

$$B \equiv 0 \qquad (7.1.8)$$

and

$$\sin(N+1)\theta = 0 \quad \text{or} \quad \theta_\ell = \frac{\ell\pi}{(N+1)}, \quad \ell=1,2,---,N \qquad (7.1.9)$$

Thus for the ℓ^{th} mode,

$$\omega_\ell = 2\sqrt{\frac{k_o}{m_o}} \sin \frac{\ell\pi}{2(N+1)} \qquad (7.1.10)$$

and hence $\Omega = \text{diag}\ (\omega_\ell^2)$

$$\text{Modal vector} \quad \phi_\ell = \begin{bmatrix} A_\ell \sin \frac{\ell\pi}{(N+1)} \\ A_\ell \sin \frac{2\ell\pi}{(N+1)} \\ \vdots \\ A_\ell \sin \frac{N\ell\pi}{(N+1)} \end{bmatrix} \qquad (7.1.11)$$

It is easy to see that, in order that $\| \phi_\ell \|_2 = 1$,

$$A_\ell = \sqrt{\frac{2}{N+1}}, \quad \forall \ell \tag{7.1.12}$$

Consequently the modal matrix Φ takes the form

$$(\Phi)_{ij} = \sqrt{\frac{2}{N+1}} \sin \frac{ij\pi}{(N+1)}, \quad i,j, = 1,---N \tag{7.1.13}$$

Since the structure of the internal viscous damping D is not clearly known, we shall assume that all modes have the same damping ratio ζ_n and that the modal damping matrix is diagonal and given by

$$(\mathcal{D})_{ij} = 2\zeta_n \omega_i \delta_{ij} \tag{7.1.14}$$

The actual value of ζ_n remains unknown but for most of our simulated example, ζ_n is assumed to be about 1%. In all cases, we shall set the closed loop damping ratio of the first mode to be approximately ζ_p and subsequently set the closed loop damping of all the controlled modes to be approximately equal to that of the first mode. This has the effect of causing all the controlled modes to decay at roughly the same rate.

7.2 COLLOCATED VELOCITY FEEDBACK CONTROL: NO ACTUATOR DYNAMICS

In the absence of actuator dynamics, unconditional global stability is guaranteed for collocated velocity feedback control. Furthermore if N_A pairs of S/A are available, we can approximately assign the closed loop damping for the first N_A modes. To examine the closed loop behavior of the system (2.1.1) we shall calculate all its eigenvalues from its state matrix

$$A = \begin{bmatrix} 0 & I_N \\ -\Omega & -\mathcal{D}-\mathcal{B} \end{bmatrix} \qquad (7.2.1)$$

For illustrative purposes, we let $N = 20$, $N_A = 4$, $\frac{k_o}{m_o} = 4$, $S = \{3,8,13,19\}$ $\zeta_n = 0.01$. Two cases, (i) $\zeta_p = 0.2$, (ii) $\zeta_p = 0.3$ are computed and the outcome of the simulation is shown in Table 7.1. Despite the existence of coupling, the closed loop behavior of the modes agrees very well with scalar theory indeed. More simulations of this sort are considered in [18].

7.3 VELOCITY FEEDBACK WITH ACTUATOR DYNAMICS

To demonstrate the instability caused by actuator dynamics, we shall deliberately choose $\omega_a = 1.0$ to lie between the 3rd and 4th modes. ζ_a is chosen arbitrarily to be about 0.7. The gain matrices are computed as if no actuator dynamics are present. With the rest of the parameters as before, the closed loop eigenvalues of the system (2.1.7)-(2.1.8) are computed from the state matrix

$$A = \begin{bmatrix} 0 & I_N & 0 & 0 \\ -\Omega & -\mathcal{D} & -\mathcal{B} & 0 \\ 0 & 0 & 0 & I_N \\ 0 & \omega_a^2 I_N & -\omega_a^2 I_N & -\beta_a I_N \end{bmatrix} \qquad (7.3.1)$$

The outcome of the simulation for the 2 cases, (i) $\zeta_p = 0.2$ and (ii) $\zeta_p = 0.3$, are shown in Table 7.2.

When the gains are sufficiently low ($\zeta_p = 0.2$), all modes are still stable, though the damping for certain modes becomes very small (e.g., $\zeta_{CL} = 0.01\%$ for the 6th mode). When the gains are raised further ($\zeta_p = 0.3$), the 4th, 5th and 6th modes become unstable. If we plot the scalar gain vs. open loop frequency for these modes on the stability

Mode	Open loop freq. ω_i	(i) $\zeta_p = 0.2$				(ii) $\zeta_p = 0.3$			
		γ_i	ω_{pi}	C-L Damp.	C-L $\zeta(\%)$	γ_i	ω_{pi}	C-L Damp.	C-L $\zeta(\%)$
1	0.299	.1196	0.293	-.0633	21.08	.1794	0.287	-.0944	31.28
2	0.596	.1196	0.596	-.0664	11.06	.1794	0.597	-.0977	16.16
3	0.890	.1196	0.895	-.0692	7.71	.1794	0.902	-.1001	11.03
4	1.179	.1196	1.179	-.0717	6.07	.1794	1.179	-.1020	8.62
5	1.461	.1211	1.461	-.0761	5.20	.1816	1.462	-.1085	7.40
6	1.736	.1744	1.734	-.1081	6.22	.2616	1.732	-.1612	9.27
7	2.000	.1469	1.995	-.0939	4.70	.2203	1.989	-.1307	6.56
8	2.253	.0461	2.250	-.0448	1.99	.0692	2.247	-.0544	2.42
9	2.494	.1433	2.491	-.0981	3.94	.2150	2.488	-.1376	5.52
10	2.721	.0875	2.720	-.0710	2.61	.1312	2.722	-.0932	3.42
11	2.932	.0830	2.929	-.0713	2.43	.1245	2.924	-.0931	3.18
12	3.127	.0891	3.128	-.0763	2.44	.1336	3.129	-.0996	3.18
13	3.305	.0490	3.309	-.0556	1.68	.0735	3.314	-.0635	1.92
14	3.464	.1628	3.474	-.1271	3.66	.2442	3.485	-.2215	6.35
15	3.604	.1468	3.586	-.1138	3.17	.2202	3.551	-.1309	3.68
16	3.723	.1134	3.718	-.0969	2.60	.1702	3.708	-.1272	3.43
17	3.822	.2003	3.803	-.1366	3.59	.3004	3.779	-.1824	4.82
18	3.900	.1130	3.873	-.0845	2.18	.1696	3.853	-.0880	2.28
19	3.955	.0995	3.937	-.0870	2.21	.1493	3.914	-.1012	2.59
20	3.989	.1040	3.973	-.0823	2.07	.1560	3.963	-.0962	2.43

Table 7.1 Collocated Velocity Feedback Control : No Actuator Dynamics

$\zeta_n = 0.01$, $S = \{3,8,13,19\}$

Mode	(i) $\zeta_p = 0.2$				(ii) $\zeta_p = 0.3$			
	γ_i	ω_{pi}	C-L Damp.	C-L ζ(%)	γ_i	ω_{pi}	C-L Damp.	C-L ζ(%)
1	.1196	0.326	-.0671	20.16	.1794	0.345	-.1105	30.51
2	.1196	0.646	-.0366	5.66	.1794	0.673	-.0468	6.94
3	.1196	0.933	-.0128	1.37	.1794	0.951	-.0127	1.33
4	.1196	1.212	-.0030	0.25	.1794	1.227	+.0016	*-0.13
5	.1211	1.483	-.0022	0.15	.1816	1.494	+.0035	*-0.24
6	.1744	1.756	-.0001	0.01	.2616	1.766	+.0079	*-0.45
7	.1469	2.012	-.0068	0.34	.2203	2.018	-.0003	0.02
8	.0461	2.256	-.0154	0.84	.0692	2.257	-.0169	0.75
9	.1433	2.500	-.0154	0.62	.2150	2.503	-.0107	0.43
10	.0875	2.724	-.0221	0.81	.1312	2.725	-.0196	0.72
11	.0830	2.934	-.0250	0.85	.1245	2.935	-.0229	0.78
12	.0891	3.129	-.0272	0.87	.1336	3.130	-.0252	0.80
13	.0490	3.306	-.0310	0.94	.0735	3.306	-.0301	0.91
14	.1628	3.467	-.0284	0.82	.2442	3.468	-.0254	0.73
15	.1468	3.606	-.0308	0.85	.2202	3.607	-.0281	0.78
16	.1134	3.725	-.0334	0.90	.1702	3.726	-.0351	0.85
17	.2003	3.825	-.0318	0.83	.3004	3.826	-.0285	0.75
18	.1130	3.901	-.0354	0.91	.1696	3.901	-.0336	0.86
19	.0995	3.956	-.0365	0.92	.1493	3.957	-.0350	0.88
20	.1040	3.990	-.0368	0.92	.1560	3.990	-.0351	0.88
Actuators		.5981	-.6644	77.32		0.518	-.6367	77.55
		.5632	-.7218	78.84		0.476	-.7310	83.78
		.5960	-.7095	76.57		0.534	-.7208	80.33
		.6546	-.7173	77.87		0.625	-.7263	75.78

Table 7.2 Velocity Feedback with Actuator Dynamics

$\omega_a = 1.0$, $\zeta_a = 0.7$, $\zeta_n = 0.01$, $S = \{3,8,13,19\}$

* Unstable Modes

boundary picture Fig 2.2, we find that they all lie in the unstable region. In fact, if we do likewise for each of the 20 modes, we can also predict their relative stability margins approximately. Thus, our scalar theory discussed in Chapter 2 seems to be well justified.

To examine the effect of ill-located S/A, we shall consider the stable case $\zeta_p = 0.2$ with actuator dynamics (Table 7.2(i)) and alter the S/A location to $s = \{4,10,11,13\}$. It was found that the scalar gains went wild (Table 7.3(i)). In this case perturbation theory does not apply since the gains are not small and we cannot use scalar theory to predict stability, nevertheless the 7th and 20th modes are found to be unstable. To explain this phenomenon, we observe that two of the S/A pairs are adjacent to each other; careful examination of the Φ matrix indicates that this has the effect of causing $(s\Phi_1)$ to be nearly singular, which in turn causes some of the elements of C to become very large since C is constructed from

$$C = (s\Phi_1)^{-T} \begin{bmatrix} \gamma_1 & & \\ & \ddots & \\ & & \gamma_{N_A} \end{bmatrix} (s\Phi_1)^{-1} \qquad (7.3.2)$$

To avoid this sort of singular condition is not difficult. In principle, we can use integer programming to work out an optimal S/A location matrix, or can even minimize the scalar gain γ_i for modes near or within the critical range. This is, however, more easily said than done and is not very practical either. In reality Φ is not known exactly and is affected by the S/A distribution as well; hence, any such design procedure will be necessarily iterative. By experimenting with various S/A locations, we found that in general if we spread out the S/A uniformly over the structure,

Mode	(i) ζ_p = 0.2, ζ_n = 0.01 S = {4,10,11,13}				(ii) ζ_p = 0.2, ζ_n = 0.005 S ={3,8,13,19}			
	γ_i	ω_{pi}	C-L Damp.	C-L (%)	γ_i	ω_{pi}	C-L Damp.	C-L ζ(%)
1	.1196	0.325	-.0514	15.62	.1196	0.326	-.0652	19.61
2	.1196	0.635	-.0289	4.54	.1196	0.646	-.0333	5.16
3	.1196	0.925	-.0126	1.36	.1196	0.933	-.0083	0.89
4	.1196	1.204	-.0060	0.50	.1196	1.212	+.0028	*-0.23
5	.9496	1.500	-.0043	0.29	.1211	1.483	+.0049	*-0.33
6	.8248	1.760	-.0087	0.49	.1744	1.756	+.0084	*-0.48
7	2.3800	2.054	+.0050	*-0.24	.1469	2.012	+.0031	*-0.15
8	3.4810	2.306	-.0125	0.54	.0461	2.256	-.0076	0.34
9	2.1120	2.523	-.0121	0.48	.1433	2.500	-.0030	0.12
10	9.1940	2.821	-.0168	0.60	.0875	2.724	-.0086	0.31
11	1.0270	2.945	-.0230	0.78	.0830	2.934	-.0104	0.35
12	14.6680	3.267	-.0158	0.48	.0891	3.129	-.0116	0.37
13	.1815	3.308	-.0270	0.82	.0490	3.306	-.0145	0.44
14	15.3790	3.593	-.0275	0.76	.1628	3.467	-.0111	0.32
15	.2623	3.611	-.0289	0.80	.1468	3.606	-.0128	0.35
16	13.4120	3.814	-.0344	0.90	.1134	3.725	-.0148	0.40
17	.6965	3.842	-.0298	0.77	.2003	3.825	-.0127	0.33
18	10.3850	3.954	-.0368	0.93	.1130	3.901	-.0159	0.41
19	.2857	3.965	-.0345	0.87	.0995	3.956	-.0168	0.42
20	7.5600	4.664	+1.3140	*-27.12	.1040	3.990	-.0168	0.42
		0.000	-0.0978	100.00		0.598	-.6664	74.32
			-4.1200	100.00				
		0.545	-0.7320	80.19		0.564	-.7216	78.80
		0.632	-0.6723	72.85		0.597	-.7095	76.54
		0.622	-0.7094	75.20		0.655	-.7172	73.84

Table 7.3 Velocity Feedback with Actuator Dynamics: Effect of S/A Location and Natural Damping. ω_a = 1.0, ζ_a = 0.7

* Unstable Modes

the resulting scalar gains will be of uniform order, hence avoiding any singularity condition. In the absence of a more sophisticated strategy for optimal S/A location, this will serve as a reasonably good rule of thumb.

Next we would like to illustrate the intimate dependence on the system's natural damping. The same case as in Table 7.2(i) is considered again; this time ζ_n is reduced to 0.005. The previously stable structure now has four unstable modes (see Table 7.3(ii)). This illustrates an important fact: since ζ_n is rather uncertain in practice, the stability boundary is not well-defined beforehand either; as a result, we cannot simply ascertain stability by choosing ω_a to be far away from the controlled mode frequency, thus raising the stability boundary. This also points out the fact that velocity feedback is not a very robust control scheme, since stability is highly dependent on an uncertain parameter. Even though ζ_n is small, it is usually nonzero; otherwise, all modes of $\omega_i > \omega_a$ will be unstable if their scalar gains γ_i are positive.

7.4 VELOCITY FEEDBACK WITH GENERALIZED LEAD COMPENSATION

To demonstrate the feasibility of using the generalized lead compensation technique for overcoming instability, we shall compute the closed loop eigenvalues of the system (3.2.4)-(3.2.6) from the state matrix (dimension $2N + 3N_A) \times (2N + 3N_A)$)

$$A = \begin{bmatrix} 0 & I_N & 0 & 0 & 0 \\ -\Omega & -\mathcal{D} & -\Phi^T s^T c & 0 & 0 \\ 0 & 0 & 0 & I_{NA} & 0 \\ \frac{\omega_a^2}{T_1} s\Phi & \frac{\omega_a^2 T_2}{T_1} s\Phi & -\omega_a^2 I_{N_A} & -\beta_a I_{N_A} & -\frac{\omega_a^2}{T_1} I_{N_A} \\ \frac{1}{T_1} s\Phi & \frac{T_2}{T_1} s\Phi & 0 & 0 & -\frac{1}{T_1} I_{N_A} \end{bmatrix} \qquad (7.4.1)$$

As the critical frequency range starts from $\omega_i \simeq \omega_a = 1.0$, we shall choose $T_2 = 1.0$ so as to increase the phase of the relevant Bode Plot in this range. The choice of T_1 must be such that the resulting phase increase can reverse the sign of the phase margin for the unstable modes. The unstable case of Table 7.2(ii) is considered again, this time with added lead compensation. Two cases ($T_1 = 0.1, 0.2$) are computed, and the outcomes are shown in Table 7.4. It is obvious that smaller T_1 tends to stabilize the system more; but even though T_1 in the 2 cases differs by a factor of 2, there is not a good deal of difference in the closed loop performance in the two cases.

7.5 ACTUATOR DYNAMICS SUPPRESSION BY GAP CREATION

Of the three gap creation techniques proposed in Chapter 4, we shall only consider the first technique, namely by collocated control, since the other two basically follow the same principle. We reconsider the unstable system in Table 7.2(ii) and note that the 4^{th}, 5^{th} and 6^{th} modes are unstable. Hence if we use 6 pairs of S/A so as to suppress these 3 modes, we should expect a stable closed loop system. This is

	(i) T_1= 0.1, T_2= 1.0, ζ_p= 0.3				(ii) T_1= 0.2, T_2= 1.0, ζ_p= 0.3			
Mode	γ_i	C-L Freq.	C-L Damp.	C-L ζ(%)	γ_i	C-L Freq.	C-L Damp.	C-L ζ(%)
1	.1794	0.299	-.1092	34.31	.1794	0.303	-.1111	34.45
2	.1794	0.653	-.1034	15.63	.1794	0.660	-.0978	14.65
3	.1794	0.962	-.0574	5.95	.1794	0.964	-.0505	5.23
4	.1794	1.251	-.0451	3.60	.1794	1.252	-.0359	2.86
5	.1816	1.524	-.0315	2.07	.1816	1.523	-.0226	1.46
6	.2616	1.812	-.0280	1.54	.2616	1.809	-.0164	0.91
7	.2203	2.059	-.0240	1.17	.2203	2.055	-.0136	0.66
8	.0692	2.271	-.0228	1.00	.0692	2.269	-.0190	0.84
9	.2150	2.538	-.0229	0.90	.2150	2.533	-.0143	0.57
10	.1312	2.745	-.0251	0.91	.1312	2.742	-.0202	0.74
11	.1245	2.954	-.0265	0.90	.1245	2.950	-.0221	0.75
12	.1336	3.148	-.0281	0.89	.1336	3.144	-.0239	0.76
13	.0735	3.315	-.0314	0.95	.0735	3.313	-.0294	0.89
14	.2442	3.496	-.0285	0.81	.2442	3.490	-.0220	0.63
15	.2202	3.634	-.0292	0.80	.2202	3.627	-.0231	0.64
16	.1702	3.745	-.0321	0.86	.1702	3.740	-.0277	0.74
17	.3004	3.861	-.0277	0.72	.3004	3.851	-.0202	0.53
18	.1696	3.923	-.0315	0.80	.1696	3.916	-.0271	0.69
19	.1493	3.974	-.0338	0.85	.1493	3.969	-.0302	0.76
20	.1560	4.009	-.0329	0.82	.1560	4.003	-.0293	0.73
Actuators		0.690	-.5635	63.25		0.676	-.5572	63.58
		0.658	-.6507	70.32		0.651	-.6530	70.82
		0.597	-.5859	70.03		0.585	-.5892	70.94
		0.621	-.5758	67.98		0.604	-.5799	69.25
Filters			-10.123				-5.202	
			-10.085				-5.141	
			-10.047				-5.079	
			-10.081				-5.135	

Table 7.4 Velocity Feedback with Generalized Lead Compensation

ω_a= 1.0, ζ_a= 0.7, ζ_n= 0.01, N_A= 4, S= {3,8,13,19}

indeed so and the outcome is shown in Table 7.5 By virtue of the gap, the previously unstable modes now reduce to only naturally damped.

7.6 POSITIVE POSITION FEEDBACK CONTROL WITH TUNING FILTERS

With filter parameters designed according to the procedure described in Chapter 5, the closed loop eigenvalues of the system (5.4.9) are computed from the state matrix (dimension $2(N+N_AN_f)\times 2(N+N_AN_f)$)

$$A = \begin{bmatrix} \overbrace{\mathbf{O}}^{N+N_AN_f} & & & & I_{N+N_AN_f} \\ \Omega & -E_1^T\omega_{f_1} & \cdots & -E_{N_f}^T\omega_{f_{N_f}} & \mathcal{D} & 0 \\ -E_1\omega_{f_1} & \omega_{f_1}^2 I_{N_A} & & & & 2\zeta_f\omega_{f_1} I_{N_A} \\ \vdots & & \ddots & & & \ddots \\ -E_{N_f}\omega_{f_{N_f}} & & & \omega_{f_{N_f}}^2 I_{N_A} & 0 & 2\zeta_f\omega_{f_{N_f}} I_{N_A} \end{bmatrix} \quad (7.6.1)$$

where E_i are as defined in (5.4.13). As a check of the sufficient and necessary condition for stability in theorem 5.6, the eigenvalues of the matrix P (in (5.4.12)) are also computed.

When a full complement of filters is available (i.e., $N_A = N_f$) the closed loop damping performance for the 3 cases computed: ζ_p=0.3,0.4,0.5, is very good indeed (see Table 7.6). We can achieve closed loop damping as high as $\zeta_p = 50\%$ for the first mode (it is expected that ζ_p can even be considerably higher than this) without causing instability or undesirable situations. The closed loop damping ratio for the first mode

Mode	$N_A = 6$, $N_c = 3$, $S = \{2,5,8,11,15,18\}$ $\zeta_n = 0.01$, $\omega_a = 1.0$, $\zeta_a = 0.7$			
	γ_i	C-L Freq.	C-L Damping	C-L $\zeta(\%)$
1	.1794	0.341	-.1130	31.46
2	.1794	0.678	-.0525	7.72
3	.1794	0.959	-.0129	1.34
4	.0000	1.179	-.0118	1.00
5	.0000	1.461	-.0146	1.00
6	.0000	1.735	-.0174	1.00
7	.0312	2.002	-.0173	0.86
8	.0021	2.253	-.0224	0.99
9	.0433	2.496	-.0221	0.89
10	.1071	2.724	-.0210	0.77
11	.1071	2.935	-.0239	0.81
12	.1690	3.131	-.0235	0.75
13	.0680	3.306	-.0302	0.91
14	.1419	3.466	-.0293	0.84
15	.1636	3.606	-.0301	0.83
16	.1718	3.726	-.0314	0.84
17	.0627	3.823	-.0362	0.95
18	.0226	3.900	-.0383	0.98
19	.0321	3.956	-.0386	0.98
20	.0729	3.989	-.0377	0.94
Actuator		0.714	-.7000	70.00
		0.714	-.7000	70.00
		0.714	-.7000	70.00
		0.565	-.6090	73.33
		0.561	-.6700	76.68
		0.592	-.7110	76.82

Table 7.5 Velocity Feedback with Gap to Suppress Actuator Dynamics

	(i)			(ii)			(iii)		
	ζ_p=0.30 ζ_f=0.6076			ζ_p=0.40 ζ_f=0.7141			ζ_p=0.50 ζ_f=0.7869		
	$\lambda_j(P) > 0\ \forall_j$			$\lambda_j(P) > 0\ \forall_j$			$\lambda_j(P) > 0\ \forall_j$		
	γ_1=0.3430 ω_{f_1}=0.369 γ_2=0.2288 ω_{f_2}=0.736 γ_3=0.1639 ω_{f_3}=1.099 γ_4=0.1255 ω_{f_4}=1.455			γ_1=0.4773 ω_{f_1}=0.419 γ_2=0.3338 ω_{f_2}=0.835 γ_3=0.2456 ω_{f_3}=1.246 γ_4=0.1917 ω_{f_4}=1.651			γ_1=0.5843 ω_{f_1}=0.475 γ_2=0.4289 ω_{f_2}=0.947 γ_3=0.3235 ω_{f_3}=1.414 γ_4=0.2566 ω_{f_4}=1.873		
Mode	C-L Freq.	C-L Damp.	C-L ζ(%)	C-L Freq.	C-L Damp.	C-L ζ(%)	C-L Freq.	C-L Damp.	C-L ζ(%)
1	0.296	-.0875	28.389	0.286	-.1172	37.846	0.275	-.1473	47.230
2	0.584	-.0931	15.742	0.573	-.1298	22.091	0.560	-.1722	29.397
3	0.883	-.0964	10.854	0.878	-.1389	15.629	0.876	-.1926	21.467
4	1.158	-.0918	7.898	1.138	-.1255	10.959	1.111	-.1627	14.495
5	1.473	-.0365	2.478	1.472	-.0528	3.583	1.467	-.0711	4.838
6	1.742	-.0220	1.263	1.745	-.0272	1.557	1.747	-.0341	1.953
7	2.001	-.0218	1.091	2.002	-.0234	1.171	2.002	-.0254	1.268
8	2.255	-.0242	1.072	2.256	-.0261	1.155	2.257	-.0286	1.267
9	2.495	-.0260	1.042	2.496	-.0272	1.090	2.496	-.0288	1.155
10	2.722	-.0279	1.024	2.723	-.0287	1.055	2.724	-.0301	1.103
11	2.934	-.0302	1.030	2.935	-.0314	1.071	2.936	-.0333	1.134
12	3.131	-.0336	1.073	3.133	-.0366	1.167	3.134	-.0409	1.304
13	3.306	-.0334	1.010	3.306	-.0339	1.025	3.307	-.0347	1.049
14	3.465	-.0350	1.011	3.466	-.0356	1.028	3.467	-.0366	1.056
15	3.604	-.0364	1.010	3.605	-.0369	1.023	3.606	-.0376	1.044
16	3.725	-.0377	1.013	3.726	-.0384	1.032	3.727	-.0396	1.063
17	3.823	-.0387	1.013	3.824	-.0395	1.032	3.825	-.0407	1.063
18	3.901	-.0394	1.010	3.901	-.0400	1.025	3.902	-.0410	1.051
19	3.956	-.0398	1.006	3.956	-.0401	1.014	3.957	-.0406	1.026
20	3.990	-.0403	1.010	3.990	-.0409	1.026	3.991	-.0420	1.052
Filters									
1	0.249	-.1396	48.850	0.217	-.1848	64.871	0.163	-.2306	81.626
2	0.508	-.3565	57.470	0.431	-.4668	73.485	0.266	-.5927	91.255
3	0.746	-.5523	59.500	0.631	-.7064	74.562	0.422	-.8189	88.895
4	1.093	-.7972	58.920	1.040	-1.051	71.058	0.966	-1.298	80.230

Table 7.6 Positive Position Feedback Control with Tuning Filters

N_A=N_F= 4, ζ_n= 0.01, S= {3,8,13,19}

turns out to be within 6% of the actual prescribed value. This error is mainly attributed to the presence of off-diagonal couplings. (By ignoring the coupling terms, the closed loop damping ratios for the first mode in each of the 3 cases are 0.2903, 0.3914, 0.4971 whereas actually they are 0.2839, 0.3785, 0.4723 respectively.) As predicted from theory, the uncontrolled modes all result in higher than natural closed loop damping.

If fewer filters than controlled modes are used, the technique still applies though the performance deteriorates. This is expected since we are using less resources to do more work. If we assumed that $N_A = 4$ and $N_f = 2$, so that one filter is used to tune the first and second mode and the other used to tune the 3rd and 4th, and filter parameters are selected more-or-less by intuition, the outcome for $\zeta_p = 0.3$ is as shown in Table 7.7 (i). Note that the scalar gains are now considerably higher than before, and one of the filter modes actually degenerates into 2 real roots, one of which is only marginally stable. Also the importance of fine tuning the filters is clearly demonstrated in Table 7.7 (ii), where the first filter frequency is slightly altered from 0.5 to 0.48. As a result one filter mode becomes unstable. Note that even though all the γ_i are less than unity, one eigen value of P has become negative hence indicating instability. Furthermore, note that the allowable ζ_p is much more restricted in this case and the prescribed value is not quite the same as the actual value [compare the values of 58.33 and 52.72 with the prescribed value of 0.3]. This can be attributed to the decrease in closed loop frequency of the first mode from its open loop frequency.

(i)				(ii)		
ω_{f1} =0.50 ω_{f2} =1.10 $\lambda_j(P) > 0\ \forall_j$ γ_1 =0.6861 γ_2 =0.6793 γ_3 =0.1621 γ_4 =0.1620				ω_{f1} =0.48 ω_{f2} =1.10 1 e.v. of P is negative γ_1 =0.6322 γ_2 =0.8739 γ_3 =0.1621 γ_4 =0.1620		
MODE	C-L Freq.	C-L Damp.	C-L ζ(%)	C-L Freq.	C-L Damp.	C-L ζ(%)
1	0.135	-.0967	58.330	0.155	-.0961	52.720
2	0.679	-.0787	11.520	0.694	-.0778	11.150
3	0.882	-.0968	10.910	0.882	-.0968	10.910
4	1.204	-.0873	7.232	1.204	-.0873	7.232
5	1.474	-.0364	2.467	1.474	-.0363	2.466
6	1.744	-.0216	1.239	1.745	-.0219	1.255
7	2.003	-.0214	1.070	2.003	-.0214	1.069
8	2.255	-.0240	1.064	2.255	-.0240	1.064
9	2.496	-.0257	1.030	2.496	-.0257	1.030
10	2.722	-.0278	1.022	2.722	-.0278	1.022
11	2.934	-.0303	1.028	2.934	-.0302	1.028
12	3.130	-.0325	1.039	3.130	-.0325	1.039
13	3.306	-.0334	1.010	3.306	-.0334	1.010
14	3.465	-.0350	1.010	3.465	-.0350	1.010
15	3.605	-.0363	1.006	3.605	-.0363	1.006
16	3.725	-.0377	1.012	3.725	-.0377	1.012
17	3.823	-.0386	1.009	3.823	-.0386	1.009
18	3.901	-.0393	1.009	3.901	-.0393	1.009
19	3.956	-.0397	1.004	3.956	-.0397	1.004
20	3.990	-.0401	1.006	3.990	-.0402	1.006
Filters						
1	0.429	-.2061	43.300	0.412	-.1945	42.730
2	0.000	-.3867	100.00	0.000	+.0427	*-100.0
	0.000	-.0619	100.00	0.000	-.4691	100.0
3	0.753	-.5482	58.880	0.753	-.5481	58.880
4	0.766	-.5767	60.170	0.766	-.5767	60.170

Table 7.7 Position Feedback: Effect of Fine Tuning

N_A= 4, N_F= 2, ζ_p= 0.3, ζ_f= 0.6, ζ_n= 0.01, S= {3,8,13,19}

* Unstable Mode

7.7 STABILIZATION BY QUASI-LINEAR STIFFNESS MODIFICATION

Unlike all previous cases, where linearity permits the evaluation of system's eigenvalues, the present technique is nonlinear, and hence the damping characteristics of the modes can only be studied by direct integration of the equations of motion. It is convenient to examine the system in the modal space; hence, the differential equations to be integrated are

$$\frac{d}{dt}\xi = \dot{\xi} \tag{7.7.1}$$

$$\frac{d}{dt}\dot{\xi} = -\mathcal{D}\dot{\xi} - \Omega\xi - \hat{F}(\xi\dot{\xi})\xi \tag{7.7.2}$$

$$\text{where } \hat{F}(\xi,\dot{\xi}) = \text{sgn}\left(\dot{\xi}^T\Phi^T\left(\sum_{k\in S} c_k Q_k\right)\Phi\xi\right)\sum_{k\in S}\left(c_k\Phi^T Q_k\Phi\right) \tag{7.7.3}$$

in the case of "Global" control and

$$F(\xi,\dot{\xi}) = \sum_{k\in S}\left(\text{sgn}(\dot{\xi}^T\Phi^T Q_k\Phi\xi)c_k\Phi^T Q_k\Phi\right) \tag{7.7.4}$$

in the case of "Local" control.

In order to highlight the non-linear damping, the natural viscous damping is assumed zero [ie. $\mathcal{D} = 0$]. Since we have not come up with an optimal way of determining the scalar gain c_k, $k = 1,---n$, we shall compute with various values of c_k and present the best case only. The equations (7.7.1) and (7.7.2) are solved using a 5th and 6th order Runge-Kutta-Verner differential equation subroutine, and due to the restricted capacity of this subroutine, we shall only consider an $N = 5$

elements example. The other system parameters chosen for simulation are $n = 2$, $S = \{1,3\}$, (i.e., 2 transducers are placed across the 1st and 2nd, and the 3rd and 4th elements). $\frac{k_o}{m_o} = 1.0$ (and hence the 5 modal frequencies are respectively 0.5176, 1.000, 1.4142, 1.7321, 1.9319). The initial conditions are chosen such that all 5 modes are excited initially and each is given unit initial velocity. A representative case for each of "Global" control and "Local" control is presented in Fig. 7.1 to Fig. 7.6 where the energy (total and individual), modal displacement and physical displacement are plotted as a function of time. We shall summarize our experimental findings in the following points.

(1) In the "Local" control case (Fig. 7.4-7.6), the energy decay characteristics are very good indeed; total energy is reduced to about 2% of its initial energy after 20s. Although energy of individual modes fluctuates, the total energy decreases monotonically. It is also observed that the higher order modes generally decay faster than the lower order modes which is consistent with intuition.

(2) In the "Global" control case, the total energy decay is good up to about 20s. From then on it follows a flat plateau where there is very little appreciable decrease in energy. The main bulk of the total energy is contributed by the first mode.

(3) The choice of transducer location plays an important role in determining the energy decay characteristics, but is unfortunately dependent on the initial conditions of the system. For example, if S were chosen to be $\{1,4\}$, then the 1st mode is found to be better controlled but the 2nd mode is not controlled at all; as a result the 2nd mode's energy remains constant! This is easily explained as the pairs of

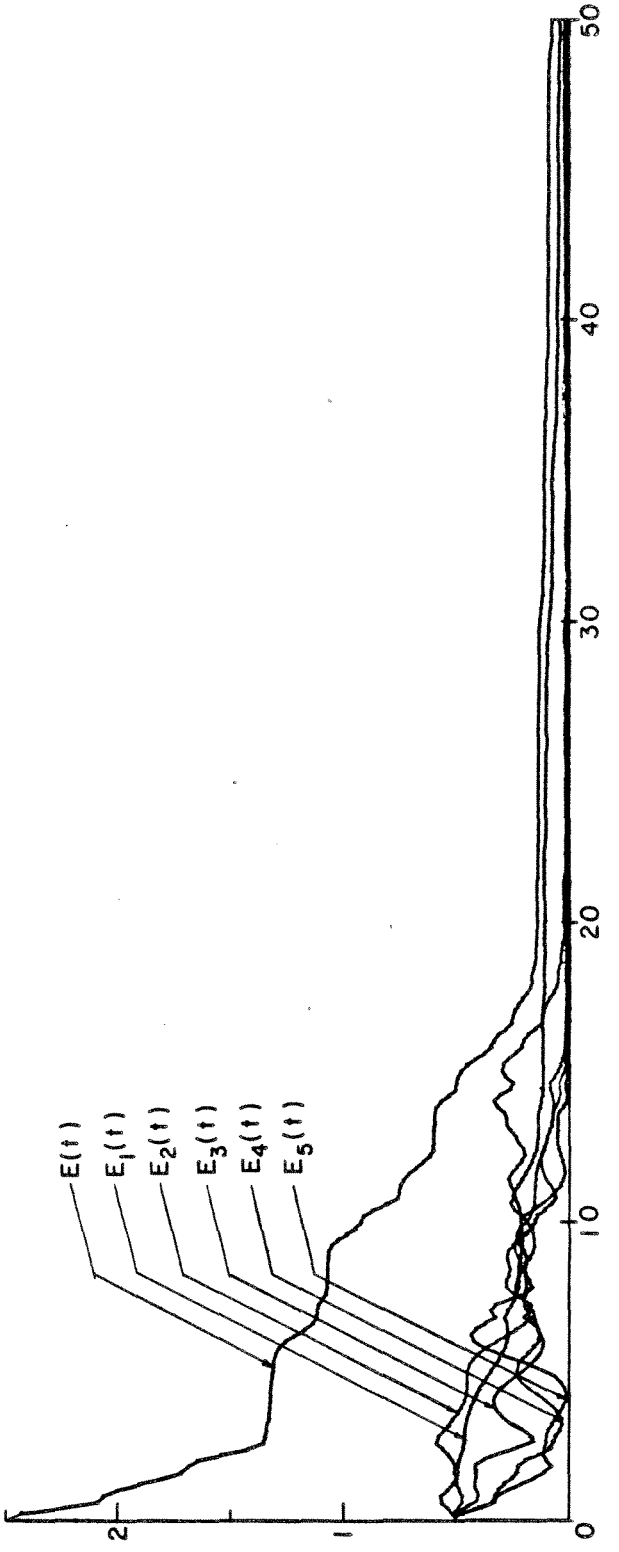

Fig. 7.1 Energy History for "Global" Control, $c_1 = c_2 = 1.2$

$$E_i(t) = \frac{1}{2}(\dot{\xi}_i^2 + (\omega_i \xi_i)^2), \quad E(t) = \sum_{i=1}^{N} E_i(t)$$

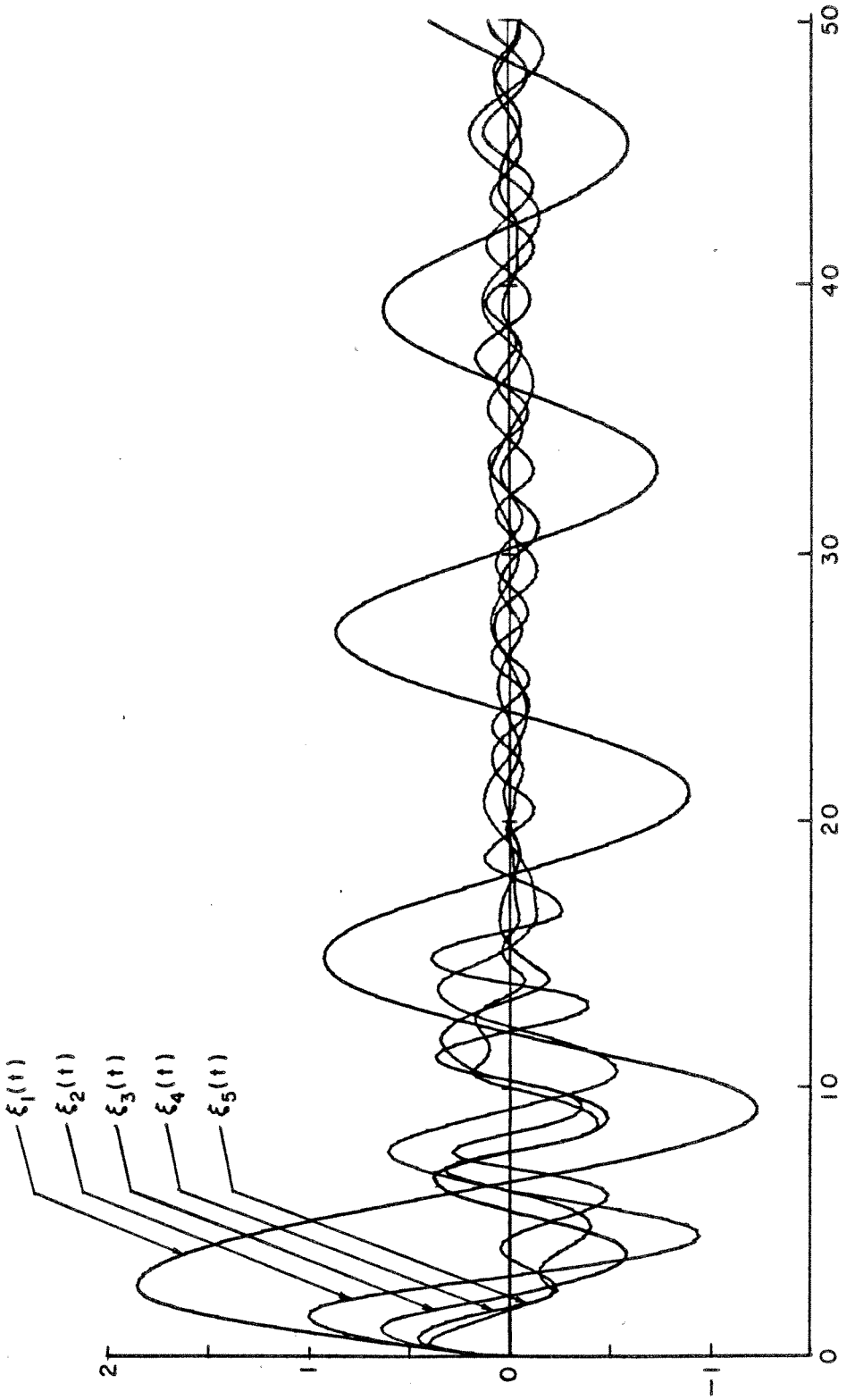

Fig. 7.2 Modal State History for "Global" Control, $c_1 = c_2 = 0.9$

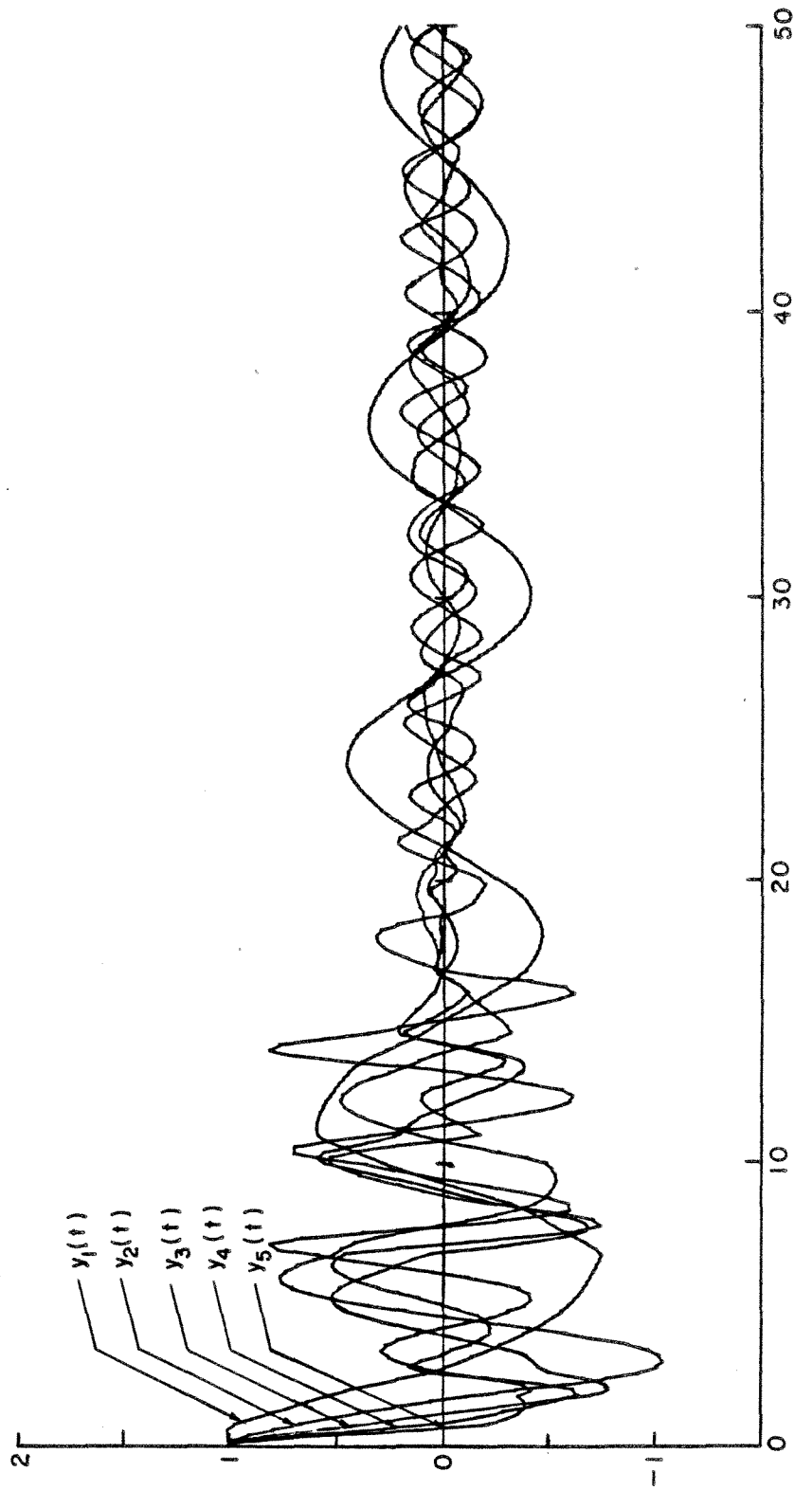

Fig. 7.3 State History for "Global" Control, $c_1 = c_2 = 0.9$

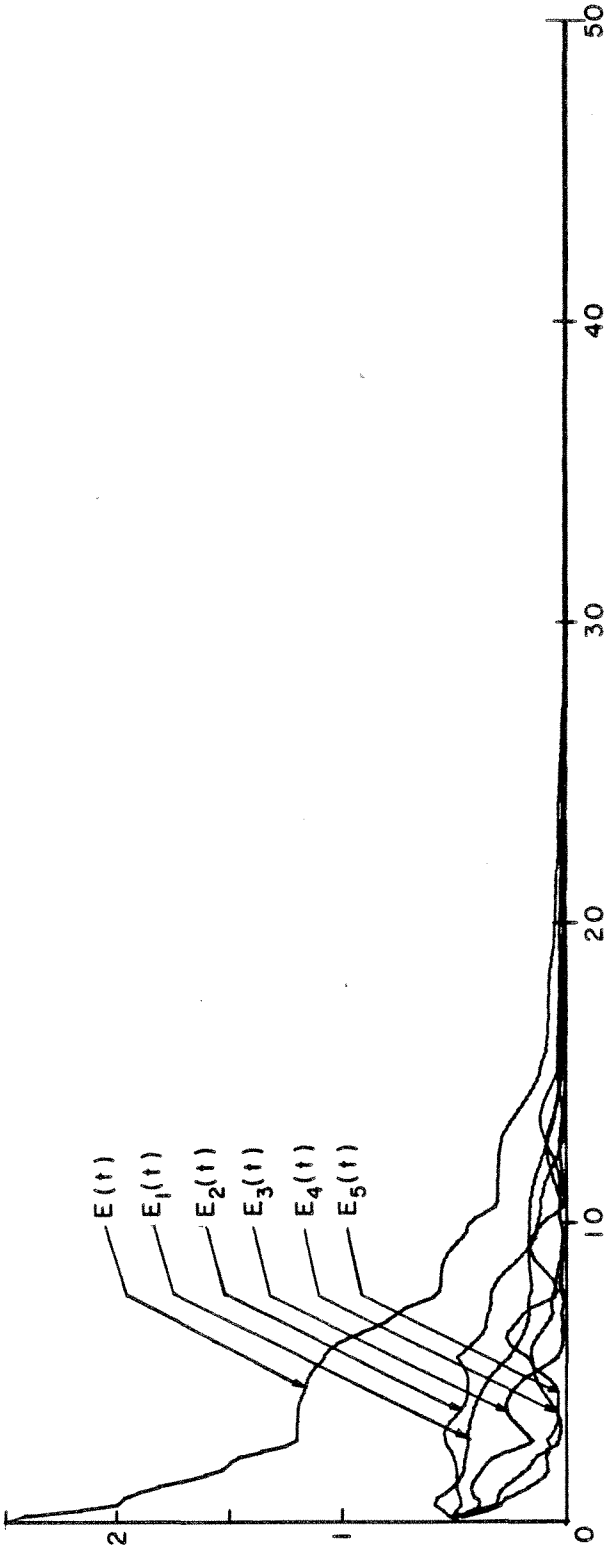

Fig. 7.4 Energy History for "Local" Control, $c_1 = c_2 = 0.9$

$$E_i(t) = \frac{1}{2}\left(\dot{\xi}_i^2 + (\omega_i \xi_i)^2\right), \quad E(t) = \sum_{i=1}^{N} E_i(t)$$

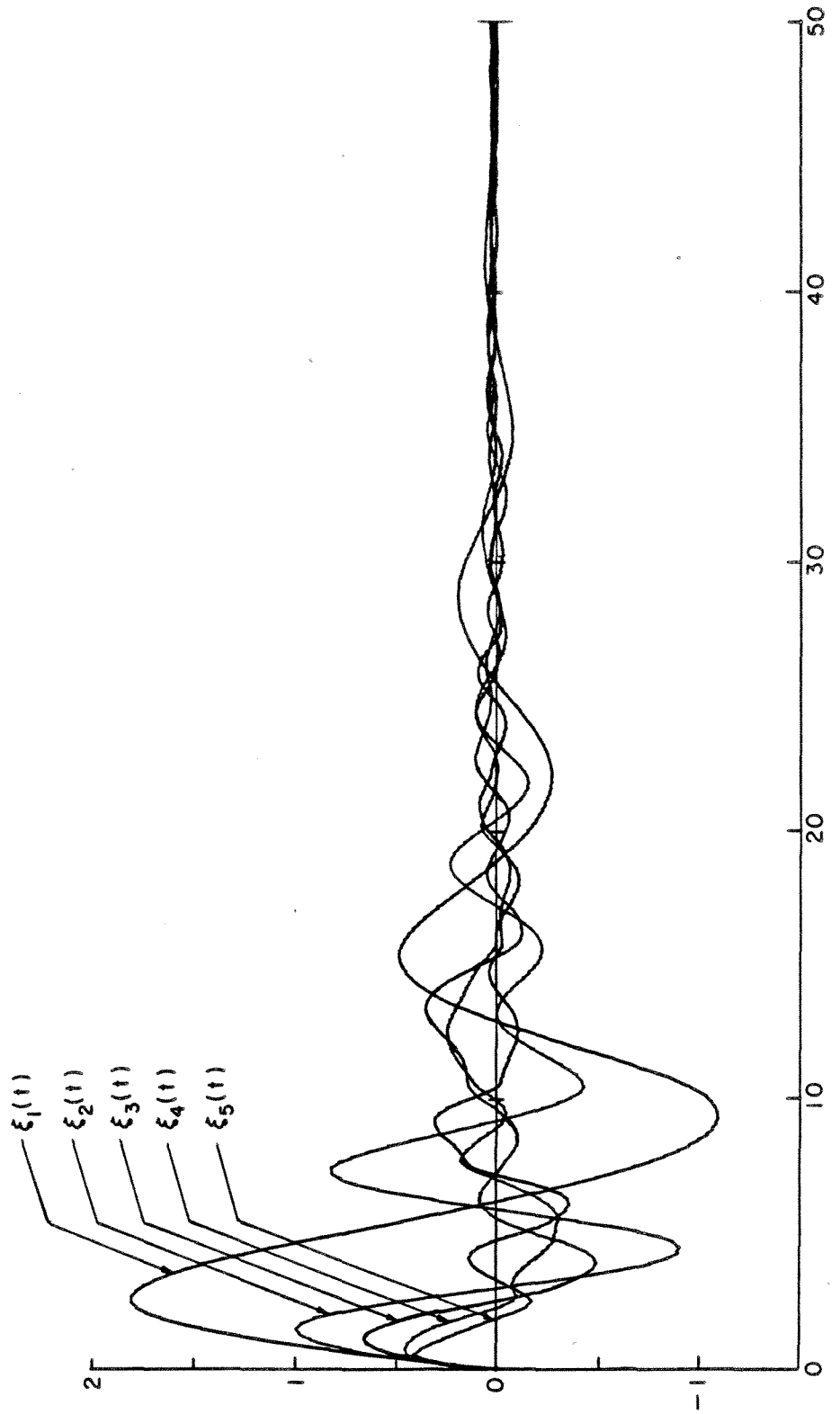

Fig. 7.5 Modal State History for "Local" Control, $c_1 = c_2 = 1.2$

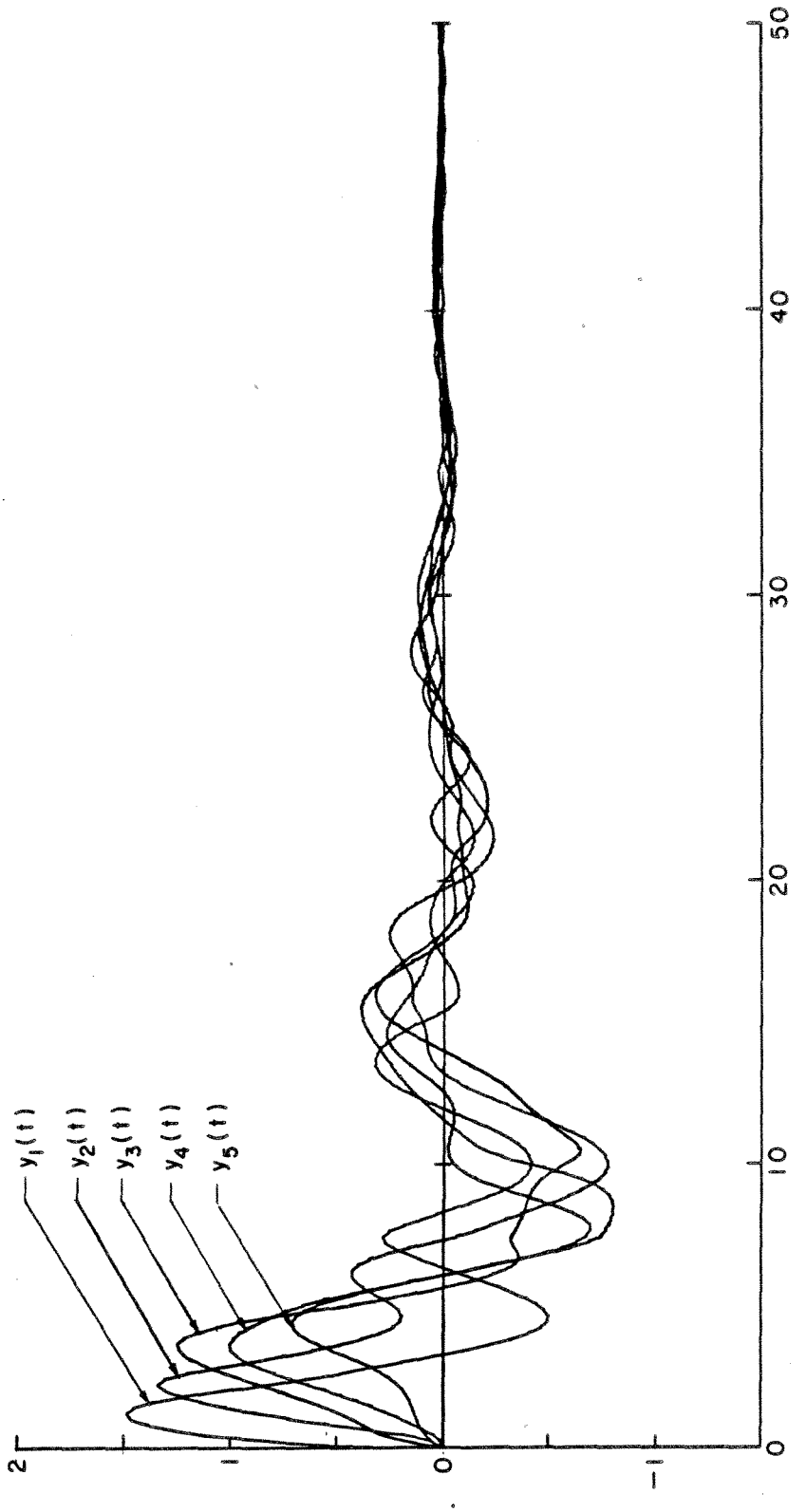

Fig. 7.6 State History for "Local" Control, $c_1 = c_2 = 1.2$

elements (1,2) and (4,5) have zero relative displacement in the 2nd mode; hence, the transducer across them cannot exhibit any control over them. In order to minimize control effort, the transducer should be placed near the node (where the slope is the greatest) of the modes which are more likely excited.

In comparison, the existence of an energy plateau in the "Global" control indicates that "Local" control is really the better of the two; it also has the added advantage that it is easier to implement physically.

CHAPTER 8

CONCLUDING REMARKS

> Neither seeking nor avoiding mathematical exercitation, we enter into problems solely with a view to possible usefulness for physical science.
>
> Lord Kelvin and Peter Guthrie Tait
> "Treatise in Natural Philosophy" Part III.

8.1 ACKNOWLEDGEMENT OF PREVIOUS RESEARCH WORKS

It was directed to our attention that certain works, not widely available, [39]-[42] contain some overlap with materials considered in this report. Since this notice came at a rather late date we regretably have not been able to include these works in our literature survey. Nevertheless, despite different approaches, these works turn out to be supportive and consistent with our present work. In particular, when the number of inputs and outputs are small, the concept of roll-off in the frequency domain analysis of Greene and Stein [39] [40] allows more sophisticated compensation networks to alleviate instability in the case of velocity feedback control. We wish to point out that the generalized lead compensation technique discussed in Chapter 3 is just one special case of these compensation techniques.

8.2 AN OVERVIEW OF DIRECT OUTPUT FEEDBACK CONTROL TECHNIQUES

In retrospect, the technique of direct velocity feedback is simple and efficient to use only when the actuator dynamics is infinitely fast. With finite actuator dynamics however, complications arise and unless

appropriately designed, certain uncontrolled modes are likely to become unstable. The stability of other modes are also strongly dependent on the natural damping of the structures, which unfortunately remains rather uncertain in practice. Two methods, namely, generalized lead compensation and gap creation are proposed as possible solutions to overcome these potential instabilities. Even though we have not been able to derive necessary and sufficient conditions for stability, our numerical simulation shows that these methods are indeed feasible under appropriate design conditions.

Under the assumption that the rigid body modes can be decoupled from the vibrational modes, the use of positive position feedback proves to be another useful technique. Note that this assumption is necessary since otherwise the rigid body modes are likely to be destabilized by the use of positive position feedback. Additional features in the form of tuning filters are included in the feedback to enhance the closed loop damping of the controlled modes. Position feedback is concluded to be the potentially more important one of the two DOFB techniques primarily because, firstly, necessary and sufficient conditions for stability can be derived and are easily satisfied; and secondly, it is far less dependent on the uncertain natural damping of the structure. Other factors, such as the fact that the maximum attainable closed loop damping can exceed what is normally required for vibration suppression purposes; that uncontrolled and unmodelled modes result in higher than natural damping, and that accurate prescription of the controlled modes closed loop damping is possible, render it an attractive technique to use. Intuitively, position feedback is also attractive because of the fact

that position feedback basically retains the "symmetry" of the overall system. In multidimensional control this property is very important, as powerful analytical tools have been developed for symmetric systems but not for non-symmetric systems, which occur in the case of velocity feedback.

In the event that conventional external actuation is not feasible, a possible alternative is internal or relative actuation, which we treated only superficially in Chapter 6. Of course, this can be implemented as a direct output feedback control but we choose to examine the use of a quasi-linear stiffness modification technique. As the systems are now non-linear and multi-dimensional, detailed rigorous analytical treatment has not been touched upon, but from numerical simulation we have found that, in some cases at least, this is indeed a simple, efficient and stable method. Two different stiffness modification schemes were proposed, and it was found that the "Local" control approach is better than the "Global" control approach.

8.3 DIRECTIONS FOR FURTHER RESEARCH

There remain a multitude of unanswered questions and unsolved problems in the control of QDPS. We shall list just a few below.

(1) A necessary and sufficient condition for any control system to be stable is that all the eigenvalues of the closed loop system have negative real part However, without resorting to brute force computation of eigenvalues, we have not been able to establish any useful form of global stability theorem, either sufficient, necessary or both, for the velocity feedback system. Conceptually this is not a trivial problem as there is no inherent symmetry involved. Extremely

restrictive sufficient conditions for stability may be obtained by means of a vector Liapunov function [28]. Other sophisticated techniques, for instance, the generalized Nyquist stability criterion and multivariate root loci concept [43] [44], are available in the literature, but these are extremely complex to use and applicable only to low order multivariate systems with a single parameter. Hence, they are unsuitable for our present application. What is really needed is a general stability criterion for a non-symmetric multivariate system.

(2) There exists plenty of room for future research in the generalized lead compensation technique discussed in Chapter 3. In particular, the frequency domain method of Green and Stein [39] [40] should be extended to the case of multiple-input multiple-output systems. Also, the parameters T_1 and T_2 in the lead network may conceivably be generalized into matrices to improve the overall performance.

(3) The design procedure for position feedback is far from perfect, in particular, when there are fewer filters than controlled modes. Some considerations regarding the optimal number of filters are also desirable.

(4) Throughout this report, the issue of robustness has not been discussed rigorously. An extensive study of the problem of robustness will not be trivial but would surely be valuable.

(5) An optimal design for the set of feedback gains in the quasi-linear stiffness modification technique also deserves some attention, though again this is not a trivial problem. The non-linearity and high order of the system have given rise to a number of elusive but interesting phenomena. For example, the existence of a plateau in the energy decay history of the "Global" control case suggests the possibility

of a multi-dimensional limit cycle. This is expected to be related to some controllability conditions, but the details of the mechanics are not clear at this time.

Other efforts, such as a detailed examination of the inter-dependence of the transducer locations and the controllability of various modes and the interaction of the transducer dynamics with the non-linear system are also worthwhile.

This report is theoretical, and all theories rely heavily on certain basic assumptions. In the present problem, for example, if there exists an unmodelled system pole in the position feedback case, then it is quite possible that instability may result and dependence on inherent natural damping may become prominent again.

In conclusion, it must be stressed that the problem of active control of QDPS is by no means straightforward. No one can boldly claim certainty in his theory. In particular, in the application to LSS, there have been no experiments carried out in gravity-free conditions to verify any of these theories. Such experiments will continue to be expensive and difficult to perform; but they may be required before the theories are ever put into practice. The multitude of ground experiments carried out recently (see, e.g., [45] [46]) must be regarded with some caution, as their resemblance to actual space structure is arguable.

Appendix A DERIVATION OF ASYMPTOTIC FORMULAE FOR STABILITY BOUNDARY

Assuming that $\zeta_n << 1$ or that terms in $O(\zeta_n^2)$ are negligible, let $R = \frac{\omega_i}{\omega_a}$ and rewrite (2.3.8) as

$$\frac{\gamma}{\omega_a} = 4\zeta_n\zeta_a(\zeta_n R + \zeta_a)\, R + (\zeta_a - \zeta_n R)(1 - R^2) + (\zeta_n R + \zeta_a)\sqrt{(1 - R^2)^2 + 8\zeta_n\zeta_a R\,(1 + R^2)}$$

For $R < 1$, and $O(1 - R^2) >> O(\zeta_n)$

$$\begin{aligned}\frac{\gamma}{\omega_a} &= 4\zeta_n\zeta_a(\zeta_n R + \zeta_a)R + (\zeta_a - \zeta_n R)(1 - R^2) \\ &\quad + (\zeta_n R + \zeta_a)(1 - R^2) + (\zeta_n R + \zeta_a)\frac{4\zeta_n\zeta_a R(1+R^2)}{1-R^2} + O(\zeta_n^2) \\ &= 2\zeta_a(1 - R^2) + 4\zeta_n\zeta_a R(\zeta_n R + \zeta_a)\left[1 + \frac{1+R^2}{1-R^2}\right] + O(\zeta_n^2) \\ &= 2\zeta_a(1 - R^2) + \frac{8\zeta_n\zeta_a^2 R}{1-R^2} + O(\zeta_n^2)\end{aligned}$$

If we assume $\zeta_n << 1$, then

$$R = \sqrt{1 - \frac{\gamma}{2\zeta_a\omega_a}}$$

$$\text{or} \quad \omega_i^*(\gamma) = \omega_a\sqrt{1 - \frac{\gamma}{2\zeta_a\omega_a}} \qquad R < 1 \qquad \square$$

For $R >> 1$, and $O(R^2 - 1) >> O(\zeta_n)$

$$\begin{aligned}\frac{\gamma}{\omega_a} &= 4\zeta_n\zeta_a(\zeta_n R + \zeta_a)R + (\zeta_a - \zeta_n R)(1 - R^2) \\ &\quad + (\zeta_n R + \zeta_a)(R^2 - 1)\left[1 + \frac{8\zeta_n\zeta_a R(1 + R^2)}{(R^2 - 1)^2}\right]^{1/2} \\ &= 4\zeta_n\zeta_a R(\zeta_n R + \zeta_a)\left[1 + \frac{R^2 + 1}{R^2 - 1}\right] + 2\zeta_n R(R^2 - 1) \\ &= 2\zeta_n R^3 + 2\zeta_n R[4\zeta_a^2 - 1] + O(\tfrac{1}{R}) + O(\zeta_n^2)\end{aligned}$$

so that

$$\left(R + \frac{4\zeta_a^2 - 1}{3R}\right)^3 = \frac{\gamma}{2\zeta_n\omega_a} + O\left(\frac{1}{R}\right) + O(\zeta_n^2)$$

$$R + \frac{4\zeta_a^2 - 1}{3}\,\frac{1}{R} = \left(\frac{\gamma}{2\zeta_n\omega_a}\right)^{\frac{1}{3}}$$

and hence

$$R = \frac{1}{2}\left(\frac{\gamma}{2\zeta_n\omega_a}\right)^{\frac{1}{3}}\left\{1 + \sqrt{1 - \frac{4(4\zeta_a^2-1)}{3}\left(\frac{2\zeta_n\omega_a}{\gamma}\right)^{2/3}}\right\}.$$

or

$$\omega_1^{**}(\gamma) = \frac{\omega_a}{2}\left(\frac{\gamma}{2\zeta_n\omega_a}\right)^{\frac{1}{3}}\left[1 + \sqrt{1 - \frac{4(4\zeta_a^2-1)}{3}\left(\frac{2\zeta_n\omega_a}{\gamma}\right)^{2/3}}\right], R >> 1.$$

□

Appendix B STABILITY ANALYSIS OF A SCALAR LEAD COMPENSATED SYSTEM

The closed loop characteristic equation for the system (3.1.7) - (3.1.9) is

$$f(s) = (s^2 + \beta_i s + \omega_i^2)(s^2 + \beta_a s + \omega_a^2)(T_1 s + 1) + \gamma_i \omega_a^2 s(T_2 s + 1) = 0 \tag{B.1}$$

Setting $s = i\omega$, the real and imaginary parts of $f(s)$ are

$$\text{Re } f(i\omega) = [T_1(\beta_i + \beta_a) + 1]\omega^4 - [T_1(\beta_i\omega_a^2 + \beta_a\omega_i^2) + \omega_i^2 + \omega_a^2 + \beta_i\beta_a + \gamma_i\omega_a^2 T_2]\omega^2 + \omega_i^2\omega_a^2 \tag{B.2}$$

$$\text{Im } f(i\omega) = T_1\omega^5 - [T_1(\omega_i^2 + \omega_a^2 + \beta_i\beta_a) + (\beta_i + \beta_a)]\,\omega^3 + [T_1\omega_i^2\omega_a^2 + \beta_i\omega_a^2 + \beta_a\omega_i^2 + \gamma_i\omega_a^2]\,\omega \tag{B.3}$$

The 4 possible Nyquist diagrams for this characteristic equation are shown in Fig. B1. The stability of the system is determined by the cross-over of the Nyquist plot with the real axis. Denoting the first and second cross-overs on the real axis as Δ_1 and Δ_2, respectively, then the system is stable iff $\Delta_1 < 0$ and $\Delta_2 > 0$. If there is no cross-over, as in case four, the system is unstable, so a sufficient condition for instability (or a necessary condition for stability in reverse) is

$$B^2 < 4\,AC \tag{B.4}$$

where

$$A = T_1$$
$$B = T_1(\omega_i^2 + \omega_a^2 + \beta_i\beta_a) + (\beta_i + \beta_a) \tag{B.5}$$
$$C = T_1\,\omega_i^2\omega_a^2 + \beta_i\omega_a^2 + \beta_a\omega_i^2 + \gamma_i\omega_a^2$$

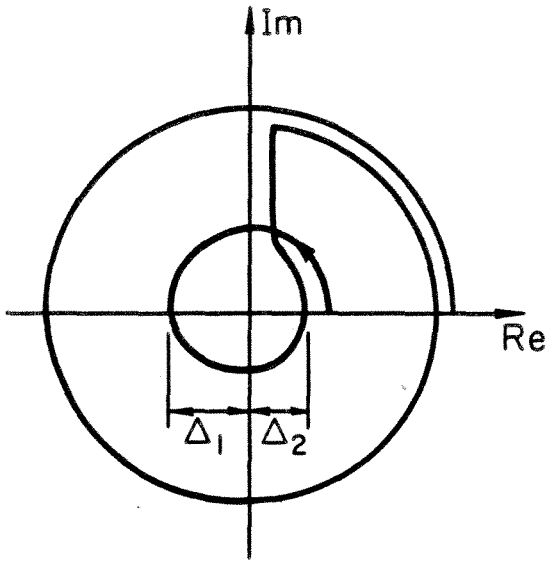

Case 1, $\Delta_1 < 0$, $\Delta_2 > 0$
STABLE

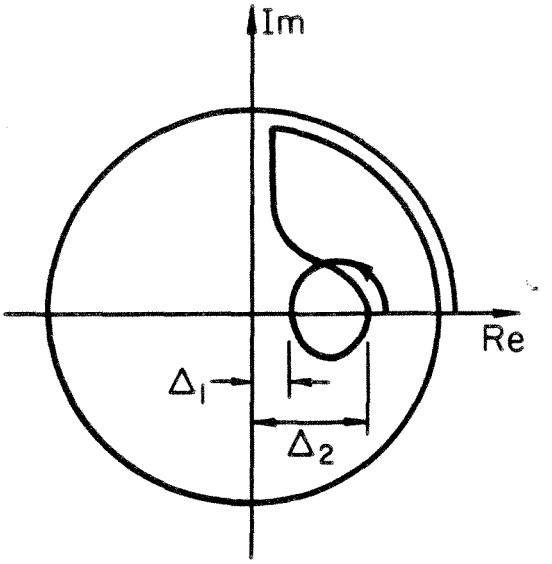

Case 2, $\Delta_1 > 0$, $\Delta_2 > 0$
UNSTABLE

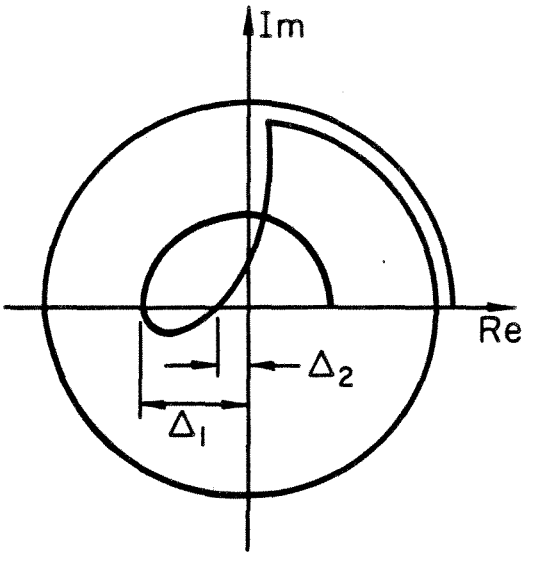

Case 3, $\Delta_1 < 0$, $\Delta_2 < 0$
UNSTABLE

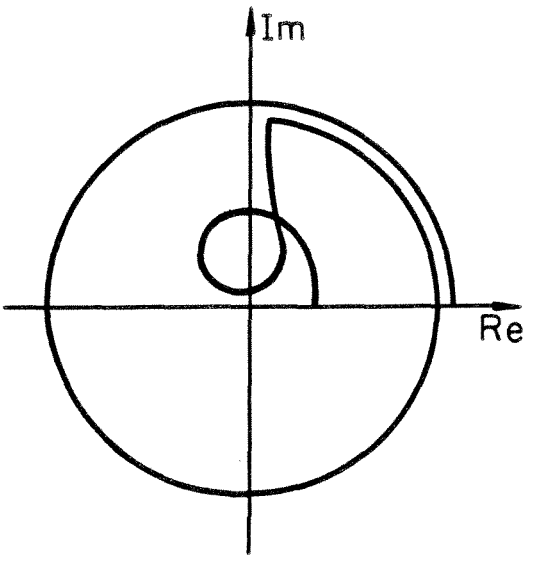

Case 4, NO CROSS OVER
UNSTABLE

Fig. B.1 Nyquist Diagram for Lead Compensated System

Substituting (B.5) into (B.4) and after some algebra, the sufficient condition for instability is

$$\gamma_i > \frac{1}{4T_1\omega_a^2}\Big([T_1\omega_a^2 - \beta_i]^2 + [T_1\omega_i^2 - \beta_a]^2 + T_1^2\beta_i^2\beta_a^2 + 2T_1^2\beta_i\beta_a(\omega_i^2 + \omega_a^2) + 2T_1(\omega_i^2\beta_i + \omega_a^2\beta_a) - 2T_1^2\omega_i^2\omega_a^2 + 2\beta_i\beta_a[1 + T_1\beta_i + T_1\beta_a]\Big) \tag{B.6}$$

From observing Fig. B.1, a sufficient and necessary condition for stability (stability boundary) is obviously

$$\Delta^* = \Delta_1\Delta_2 < 0 \tag{B.7}$$

More specifically,

$$Re\ f(\omega^*) \cdot Re\ f(\omega^{**}) < 0 \Leftrightarrow \text{STABLE} \tag{B.8}$$

where $Re\ f(\omega)$ is given by (B.2) and

$$\omega^*, \omega^{**} = \frac{B \mp \sqrt{B^2 - 4AC}}{2A}$$

where A,B,C are defined in (B.5) .

The conditions for stability (or instability) given by (B.6) & (B.8) are nevertheless messy expressions, and involve more than one adjustable parameter, (γ_i, T_1, and T_2) and hence are not likely to be very useful.

Appendix C MODAL FILTERING BY LAGRANGE INTERPOLATION

Without loss of generality, consider the physical state $y(x_i,t)$ of a chain of N point masses distributed in the open interval (0,1) of the real line at $S = \{x_1,x_2,\ldots,x_N\}$, with homogeneous boundary conditions at $x_0 = 0$ and $x_{N+1} = 1.0$. Suppose we have N_s sensors distributed at

$$S_s = \left\{ \bar{x}_1, \bar{x}_2, \ldots \bar{x}_{N_s} \right\} \subseteq S , \quad N_s \leq N , \tag{C.1}$$

and $\bar{x}_0=0, \bar{x}_{N_s+1} = 1.0$. The modal state of the system $\xi \in \mathbb{R}^N$ is given by

$$\xi(t) = \Phi^T y(t), \qquad y(t) = \begin{bmatrix} y(x_1,t) \\ y(x_2,t) \\ \vdots \\ y(x_N,t) \end{bmatrix} \tag{C.2}$$

where Φ is the modal matrix of the system. Assuming that the sensors can measure accurately with no dynamics for all frequencies, theidea of modal filtering is to construct a full state estimate of the modal state ξ by a reduced order measurement of

$$\bar{y}(t) = S_s y(t) = \begin{bmatrix} y(\bar{x}_1,t) \\ y(\bar{x}_2,t) \\ \vdots \\ y(\bar{x}_{N_s},t) \end{bmatrix} \tag{C.3}$$

where S_s is the N_sxN sensor location matrix defined by (C.1). Unless a full complement of sensors is used, the full state $y(t)$ is unknown but an estimate

$$\hat{y}(t) = \begin{bmatrix} \hat{y}(x_1,t) \\ \vdots \\ \hat{y}(x_N,t) \end{bmatrix} \tag{C.4}$$

can be constructed by interpolating the sensor measurement $\bar{y}(t)$ by the use of the Lagrange interpolation formula

$$\hat{y}(x,t) = \sum_{j=1}^{N_s} \ell_j(x) y(\bar{x}_j, t) \tag{C.5}$$

where

$$\ell_j(x) = \frac{(x-\bar{x}_0)(x-\bar{x}_1) \ldots (x-\bar{x}_{j-1})(x-\bar{x}_{j+1}) \ldots (x-\bar{x}_{N_s+1})}{(\bar{x}_j-\bar{x}_0)(\bar{x}_j-\bar{x}_1)\ldots(\bar{x}_j-\bar{x}_{j-1})(\bar{x}_j-\bar{x}_{j+1})\ldots(\bar{x}_j-\bar{x}_{N_s+1})} \tag{C.6}$$

or $$\ell_j(x) = a_{0j} + a_{1j}x + \ldots + a_{N_s+1}\, x^{N_s+1} \tag{C.7}$$

An explicit formula to generate these coefficients a_{ij} in terms of $\{\bar{x}_0, \bar{x}_1, \ldots \bar{x}_{N_s+1}\}$ can be found in [47]. Consequently

$$\hat{y}(x,t) = \left(\sum_{j=1}^{N_s} a_{0j} y(\bar{x}_j,t)\right) + \left(\sum_{j=1}^{N_s} a_{1j} y(\bar{x}_j,t)\right)x + \ldots$$

$$+ \left(\sum_{j=1}^{N_s} a_{N_s+1,j}\, y(\bar{x}_j,t)\right)x^{N_s+1}$$

$$= \alpha_0 + \alpha_1 x + \ldots + \alpha_{N_s+1} x^{N_s+1} \tag{C.8}$$

and hence

$$\hat{y}(t) = \Gamma A \bar{y}(t) = \Gamma A S_s\, y(t) \tag{C.9}$$

where

$$\Gamma = \begin{bmatrix} 1 & x_1 & \ldots & x_1^{N_s+1} \\ 1 & x_2 & \ldots & x_2^{N_s+1} \\ \vdots & \vdots & & \vdots \\ 1 & x_N & & x_N^{N_s+1} \end{bmatrix} \tag{C.10}$$

and

$$A = \begin{bmatrix} a_{01} & a_{02} \cdots & a_{0,N_s} \\ \vdots & & \vdots \\ a_{N_s+1,1} & \cdots & a_{N_s+1,N_s} \end{bmatrix} \tag{C.11}$$

The estimated modal state $\hat{\xi}(t)$ is then obtained from the estimated state $\hat{y}(t)$ by modal filtering

$$\hat{\xi}(t) = \Phi^T \hat{y} = \Phi^T \Gamma A S_s \Phi \xi(t) \tag{C.12}$$

Finally the matrices G and H as required in Chapter 4 are given by

$$G = \Phi^T \Gamma A S_s \Phi \tag{C.13}$$

and

$$H = \Phi^T \Gamma A \tag{C.14}$$

REFERENCES

[1] HUGHES, P.C., "Passive Dissipation of Energy in Large Space Structures," J. Guidance & Control, Vol. 13, No. 4, pp. 380-382, 1980.

[2] LIONS, J.L., "Optimal Control of Systems Governed by Partial Differential Equations," Springer Verlag, N.Y. 1971.

[3] AHMED, N.U. and TEO, K.L., "Optimal Control of Distributed Parameter Systems," North Holland Publication, 1981.

[4] BUTKOUSKII, A.G., "Theory of Optimal Control of Distributed Parameter Systems," American Elsevier, 1965.

[5] HUGHES, P.C., "Space Structure Vibration Modes: How many exist? Which ones are important?," presented at the Workshop on Application of Distributed System Theory to the Control of Large Space Structures," Jet Propulsion Laboratory, Pasadena, CA, July 14-16, 1982.

[6] BALAS, M.J., "Trends in Large Space Structure Control Theory: Fondest Hopes, Wildest Dreams," IEEE Trans. Auto. Control AC-27, No. 3, pp. 522-535, 1982.

[7] MEIROVITCH, L., BARUH, H. and ÖZ, H., "A Comparison of Control Techniques for Large Flexible Systems," AAS/AIAA Astrodynamics Specialists Conference, Lake Tahoe, Nev., Aug. 1981, (paper 81-195).

[8] BALAS, M.J., "Active Control of Flexible Structures," J. Optimization Theory and Applications, Vol. 25, pp. 415-436, July 1978.

[9] MEIROVITCH, L. and BARUH, H., "Control of Self-Adjoint Distributed Parameter Systems," J. Guidance, Control, and Dynamics, Vol. 5, No. 1, pp. 60-66, 1982,

[10] SCHAECHTER, D.B., "Optimal Local Control of Flexible Structures," J. Guidance and Control, Vol. 4, No. 1, pp. 22-26, 1981.

[11] BREAKWELL, J.A., "Optimal Feedback Slewing of Flexible Spacecraft ," J. Guidance and Control, Vol. 4, No. 5, pp. 472-479, 1981.

[12] MEIROVITCH, L. and OZ, H. "Optimal Modal Space Control of Flexible Gyroscopic Systems," J. Guidance and Control, Vol. 3, No. 3, pp. 218-226, 1980.

[13] SCHAECHTER, D.B., "Hardware Demonstration of Flexible Beam Control," J. Guidance, Control and Dynamics, Vol. 5, No. 1, pp. 48-53, 1982.

[14] SESAK, J.R., LIKINS, P.W. and CORADETTI, T., "Flexible Spacecraft Control by Model Error Sensitivity Suppression," J. Astronautical Sciences, Vol. XXVII, No. 2, pp. 131-156, 1979.

[15] SKELTON, R.E. and LIKINS, P.W., "Orthogonal Filters for Model Error Compensation in the Control of Non-rigid Spacecraft," J. Guidance and Control, Vol. 1, No. 1, pp. 41-49, 1978.

[16] BALAS, M.J., "Direct Output Feedback Control of Large Space Structures," J. Astronautical Sciences, Vol. XXVII, No. 2, pp. 157-180, 1979.

[17] BALAS, M.J., "Direct Velocity Feedback Control of Large Space Structures," J. Guidance and Control, Vol. 2, No. 3, pp. 252-253, 1979.

[18] CHEN, C.L., "Direct Output Feedback Control of Large Flexible Spacecraft ," Dynamic Lab. Report DYNL-82-1, California Institute of Technology, 1982.

[19] AUBRUN, J.N., "Theory of the Control of Structures by Low Authority Controllers," J. Guidance and Control, Vol. 3, No. 5, pp. 444-451, 1980.

[20] WONHAM, W.M., "On Pole Assignment in Multi-Input Controllable Linear Systems," IEEE Trans. Auto. Control, Vol. AC-12, No.6, pp. 660-665, 1967.

[21] CAUGHEY, T.K., and GOH, C.J., "Vibration suppression in Large Space Structures," presented at the Workshop on Application of Distributed System Theory to the Control of Large Space Structures, Jet Propulsion Laboratory, Pasadena, CA, July 14-16, 1982.

[22] CAUGHEY, T.K., GOH, C.J., and CHEN, C.L., "On Stability Problem Caused by Finite Actuator Dynamics in the Collocated Control of Large Space Structures," in preparation.

[23] CAUGHEY, T.K., and GOH, C.J., "The Use of Position Feedback Control in the Vibration Suppression of Large Space Structures," in preparation.

[24] CAUGHEY, T.K. and GOH, C.J., "A Quasi Linear Large Space Structures Vibration Suppression Technique via Stiffness Modification," in preparation.

[25] BALAS, M.J., "Observer Stabilization of Singularly Perturbed Systems," J. Guidance and Control, Vol. 1, No.1, pp. 93-95, 1978.

[26] KLIMUSHCHEV, A.L. AND KRASOVSKII, N.N., "Ravnomernaia Asimptoticheskaia Ustoichivost' Sistem Differentsial' Nykh Uravnenii S Malym Parametrom pri Proizbodnykh," Prikladnaia Matematika I Mekhanika, Vol. 25, No. 4, pp. 680-690, 1961.

[27] Šiljak, D.D., "Large Scale Dynamic Systems: Stability and Structure," N.Y., North Holland, 1978.

[28] BAILEY, F.N., "The Application of Liapunov's Second Method to Interconnected Systems," SIAM, J. Control, Vol. 3, No. 3, pp.443-462, 1966.

[29] OLSON, H.F., "Electronic Control of Noise, Vibration and Reverberation," J. Acoustical Society of America, Vol. 28, No. 5, pp. 966-972, 1956.

[30] FORWARD, R.L., "Electronic Damping of Vibration in Optical Structures," Applied Optics, Vol. 18, pp. 690-697, 1979.

[31] FORWARD, R.L., "Electronic Damping of Orthogonal Bending Modes in a Cylindrical Mast - Experiment," J. Spacecraft and Rockets, Vol. 18, No. 1, pp. 11-17, 1981.

[32] SWIGERT, C.J., and FORWARD, R.L., "Electronic Damping of Orthogonal Bending Modes in a Cylindrical Mast - Theory," J. Spacecraft and Rockets, Vol. 18, No.1, pp. 5-10, 1981.

[33] CHEN, J.C., "Response of Large Space Structures with Stiffness Control," Unpublished Internal Report, JPL,Pasadena, CA, 1982.

[34] CAUGHEY, T.K. "Large Amplitude Whirling of an Elastic String - A Non-Linear Eigen-Value Problem," SIAM. J. Applied Math., Vol. 18, No. 1, pp. 210-237, 1970.

[35] CARRIER, G.F., "On the Non-Linear Vibration Problem of the Elastic String," Quarterly of Applied Mathematics, Vol. 7, pp. 97-101, 1949.

[36] REID, T.J., "Free Vibration Hysteretic Damping," J. Royal Aeronautical Society, Vol. 69, pp. 283, 1956.

[37] DUNCAN, W.J., and LYON, H.M., "Calculated Flexual-Torsional Flutter Characteristics of Some Typical Cantilever Wings," R & M, pp. 1782, 1937.

[38] CAUGHEY, T.K. and VIJAYARAGHAVAN, A., "Free and Forced Oscillation of a Dynamic System with Linear Hysteretic Damping (Non-Linear Theory)," Int. J. Non-Linear Mechanics, vol. 5, pp. 533-555,1970.

[39] GREENE, C.S. and STEIN, G., "Control of Large Space Structures," Honeywell Interoffice Correspondence MR12554, April, 1979.

[40] GREENE, C.S. and STEIN, G., "Control of Large Space Structures, an Update," Honeywell Interoffice Correspomdence MR12576, Jan.,1980.

[41] GUPTA, N.K., LYONS, M.G., AUBRUN, J.N. and MARGULIES, G., "Modeling, Control abd System Indentification for Flexible Structures," To appear in Spacecraft Guidance and Control, Advisory Group for Aerospace Research and Developement, France, 1981.

[42] AUBRUN, J.N. and MARGULIES, G., "Low-Authority Control Synthesis for Large Space Structures," NASA Contractor Report NAS1-14887-TASK 11, May, 1982.

[43] MACFARLANE, A.G.J. and POSTLETHWAITE, I., "The Generalised Nyquist Stability Criterion and Multivariate Root Loci.," Int. J. Control, Vol. 25, pp. 81-127,1977.

[44] MOSSAHEB, S., "A Nyquist Type Stability Criterion for Linear Multivariable Delayed Systems," Int. J. Control, Vol 32, No.5, pp. 821-847,1980.

[45] BREAKWELL, J.A., "Experiment in Control of Flexible Structures," presented at the Workshop on Application of Distributed System Theory to the Control of Large Space Structures, Jet Propulsion Laboratory, Pasadena, CA, 1982.

[46] EIDRED, D. and SCHAECHTER, D.B., "Hardware Verification of Distributed / Adaptive Control," Ibid.,1982.

[47] DEMODOVICH, B.P. and MARON, I.A., "Computational Mathematics," MIR Publishers, Moscow, 1981.